

Review

Zeolite-supported silver as antimicrobial agents

Prabir Dutta^{a,*}, Bo Wang^{a,b}^a Department of Chemistry and Biochemistry, The Ohio State University, Columbus, OH, United States^b ZeoVation, Inc, 1275 Kinnear Road, Columbus, OH, United States

ARTICLE INFO

Article history:

Received 7 August 2018

Accepted 23 December 2018

Available online 8 January 2019

ABSTRACT

Use of silver for medical and water purification dates back to thousands of years. During 18th to early 20th century, silver was used for wound management. With the advent of organic antimicrobials, the use of silver faded. Recently, the interest in silver as broad-spectrum antimicrobial has emerged because of the increase in antibiotic resistance. Silver also exhibits inhibitory effects towards fungi and viruses. Currently, silver's antimicrobial effect is exploited in a very diverse set of applications ranging from simple consumer goods to complex medical devices. How and in what form silver is introduced in these applications varies widely. The activity as well as release of silver from these products is environment-dependent and not reported in literature, driven possibly by proprietary needs. Zeolites are a novel platform for storage and release of silver. Since the aluminosilicate framework of the zeolite is negatively charged, silver ions can be readily incorporated by ion-exchange. Nanoparticles of silver anchored on zeolite can also be prepared by simple reduction. Commercial sources of silver ion-exchanged zeolite are available. There have been several recent reviews of antimicrobial properties of silver, and a few of these discuss zeolites, but there has never been a comprehensive review of silver zeolites. This review article fills that void, and covers the research in this subject area over the past two decades. Research in silver zeolites cover use of many different zeolite frameworks, and the applications are driven by incorporating silver zeolite into polymers, textiles, metal coatings. Research on dental/medical materials as well as environmental/consumer products are also prevalent. All these topics are covered in the review. In addition, an exhaustive table with chronological detail of silver/zeolites for quick reference is also provided. A critical assessment of the literature and future possibilities with silver/zeolite conclude this review article.

© 2018 Elsevier B.V. All rights reserved.

Contents

1. Introduction	2
2. Mechanism of silver antimicrobial activity	3
2.1. Silver ions	3
2.2. Silver nanoparticles (AgNP)	3
3. Brief introduction to zeolites	4
3.1. Siting of cations	5
4. Silver-zeolite powder antimicrobial activity	5
4.1. Natural zeolites	5
4.1.1. Clinoptilolite	5
4.1.2. Chabazite	6
4.2. Synthetic zeolites	6
4.2.1. Low Si/Al zeolites	6
4.2.2. High Si/Al zeolites	9
4.2.3. Zeolite membranes	11
5. Zeolite-silver supported on matrices and their antimicrobial activity	11
5.1. Zeolite/polymer composites	11

* Corresponding author.

E-mail address: dutta.1@osu.edu (P. Dutta).

5.1.1.	Synthetic polymers	11
5.1.2.	Biopolymers	13
5.2.	Zeolite/textile composites	14
5.2.1.	Cellulose	14
5.2.2.	Cotton	14
5.3.	Zeolite/metal coatings	14
5.3.1.	Stainless steel	14
5.3.2.	Titanium alloys	15
5.4.	Dental materials	15
5.5.	Environmental/consumer materials	16
5.5.1.	Odor prevention	16
5.5.2.	Ventilation/air conditioning	16
5.5.3.	Metal door handles	16
5.5.4.	Cement/concrete	16
5.5.5.	Paper	17
5.5.6.	Food-related	17
6.	Environmental, toxicity and regulatory issues	17
6.1.	Environmental concerns with silver colloids	17
6.2.	Silver zeolite interactions with eukaryotic cells	18
6.3.	Animal studies with silver colloids	18
6.4.	Regulatory issues	23
7.	Assessment of the literature	24
8.	Future trends	24
	References	25

1. Introduction

Silver, in its metallic form, as salts and more recently as nanoparticles is used in diverse set of applications, ranging from consumer goods to medical devices. Health related use of silver dates back to antiquity, with reports of silver use for water purification dating back to 1000 BCE. Silver for wound management was practiced in the 18th century, and the US FDA allowed its use for wound management in the 1920s [1,2].

In recent times, the increasing resistance to antibiotics has renewed interest in silver as a broad-spectrum antimicrobial with low human toxicity [3,4]. In addition, silver also exhibits inhibitory effects towards growth of fungi and viruses. The forms of silver used include silver salts, silver nanoparticles and metallic silver.

Silver finds use in cosmetics, detergents, dietary supplements, cutting boards, clothes, socks, shoes, cell phones, keyboards, children's toys, food containers, dentures, medical devices such as catheters, wound dressing, paints, coatings and water purifiers [5].

The concentrations of silver in drinking water and foods are regulated in many countries. European Food Safety Agency has

allowed a legal limit of 50 ppb of release Ag^+ ions into food, whereas, FDA has approved silver zeolite in food contact surfaces at levels of <5% [6,7].

Considering the diversity of applications, the methodology of introduction of silver into these products varies widely, and is application-specific. Supports for silver can be fibers, textiles, metals, polymers, and the processing conditions depends on both the support and the type of silver (salts, metal, nanoparticle) being incorporated. Mechanical properties of silver-support composites are relevant for practical use. The amount of silver and the temporal characteristics of the release of silver vary widely depending on the material and the exposed environment. Unfortunately, these characteristics of release are not known for many products.

From a silver storage and release perspective, zeolites provide a unique platform. Zeolites with aluminosilicate framework function as ion-exchange agents and varying amounts of Ag^+ can be stored in the framework [8]. The release characteristics depend on the zeolite, as well as on the ionic strength of the surrounding medium [9]. These features of controlled storage and release has motivated many studies of Ag^+ -containing zeolites. In addition, silver nanoparticles (AgNP) can also be generated within and on the surface of zeolite, with the zeolite as anchor [10,11]. There are commercial sources of silver ion-exchanged zeolites, e.g. Zeomic, Novaron, AgION, some of these products are available since 1980.

There are several reviews on silver as antimicrobial agents that discuss zeolites, but no comprehensive and critical reviews on silver zeolite literature are available [12–24]. This review attempts to fill that void.

The structure of the review is as follows, the first two sections briefly review the mechanism of how Ag^+ and AgNP manifest their activity. Next is a discussion of the structural features of zeolite relevant for storage and release of silver. The fourth section, which forms the bulk of the review, summarizes the silver zeolite literature over the past two decades. Organization of this section is done by studies on zeolite powders, followed by zeolites on supports, including membranes, polymers, coatings, dental, and environmental/food applications. The fifth section is a discussion of the regulatory and toxicity issues around silver. This is followed by a critical assessment of the silver zeolite literature, followed by a final section on the future of silver zeolites as antimicrobial agents.

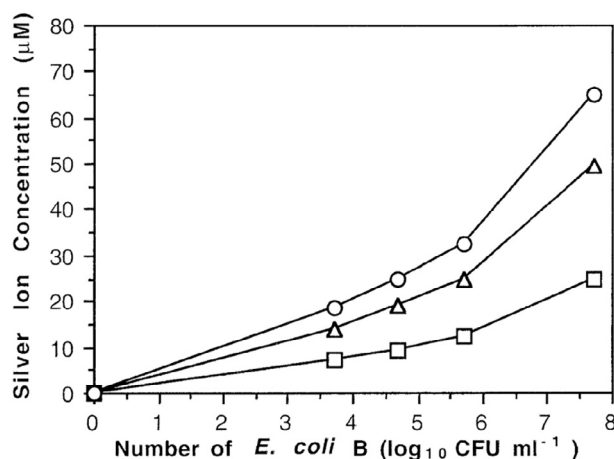


Fig. 1. Influence of inoculum size of *E. coli* B on the MBC (\circ), the CIC (Δ), and the MIC (\square) of the silver ion (adapted from Ref. [3]).

A table presents a chronological view of the literature over the past twenty years.

2. Mechanism of silver antimicrobial activity

Several recent review articles discuss the mechanisms of antimicrobial activity of Ag^+ and AgNP [12–24]. We, therefore, just highlight the most important modes of action, because of their relevance to the activity of silver zeolite.

2.1. Silver ions

The potency of Ag^+ to kill bacteria is demonstrated in Fig. 1. The initial inhibitory concentration (IIC) causes slow growth, complete inhibitory concentration (CIC) causes no growth and minimum bactericidal concentration (MBC) causes irrevocable cell death of *E. coli* B (ATCC 23848 wild type) [3]. For bacteria at an inoculum size of 10^4 – 10^5 CFU/ml, IIC = 9.45 μM , CIC = 18.90 μM and MBC = 24 μM , demonstrating bactericidal action at micromolar concentrations. In general, Gram-positive bacteria (e.g. *S. aureus*) is more resistant than Gram-negative bacteria (*E. coli*), due to the thicker peptidoglycan layer.

What does Ag^+ do? Ag^+ has a strong propensity to form complexes with ligands containing S, N and O [25]. Thus, biologically relevant species, such as thiols, carboxylic acids, phosphates, amines will act as ligands for silver ion. In addition, Ag^+ can also compete with the native binding metals in enzymes, particularly the iron-sulfur clusters of bacterial enzymes involved in amino acid synthesis and with DNA bases [4,26]. Thus, there are many points of attack on the cell, within the cell as well as cell surface, and this multi-pronged effect of Ag^+ is responsible for antimicrobial activity.

The interference of silver ions at micromolar concentrations with cell function is evident in inhibition of both phosphate uptake and exchange, as well as causing the efflux of succinate, glutamine and proline in *E. coli*. Inclusion of uncouplers such as N-ethylmaleimide stopped the phosphate efflux, but Ag^+ still inhibited exchange of phosphate, suggesting that Ag^+ is involved in interaction with the cell at multiple sites [27].

Silver ions also disrupt the proton gradients across membranes necessary for metabolic activity [28–30]. Collapse of the proton gradient increases cell respiration, and becomes uncoupled from ATP-dependent process. SERS suggests that Ag^+ is binding to flavo-proteins, possibly the cysteine residues of NADH dehydrogenases involved in the proton pumping [29].

Ag^+ also inhibits energy-dependent Na^+ transport by binding with the Na^+ -translocating NADH: ubiquinone oxidoreductase, as demonstrated in *Bacillus* sp. strain FTU and *Vibrio alginolyticus* [31]. In *Vibrio cholera*, where the oxidoreductase is not essential, submicromolar concentration of Ag^+ cause cell death by massive proton leakage through the cell membrane. Very low concentrations of Ag^+ (1×10^{-8} M) can suppress respiration-supported uphill Na^+ transport of certain bacteria, e.g. *Bacillus* FTU by binding to NADH-quinone reductase. For bacteria in which the Na^+ cycle is relevant e.g. *Vibrio cholerae*, *Vibrio parahaemolyticus*, *Klebsiella pneumoniae*, *Vibrio parahaemolyticus*, *Klebsiella pneumoniae*, and *Salmonella typhimurium*, Ag^+ is bactericidal at very low concentrations. Ag^+ activity is not necessarily arising from binding to a specific target, but nonspecific binding to membrane proteins and/or the phospholipid bilayer.

Another mechanism proposed for antimicrobial activity of silver involves the formation of reactive oxygen species, though the literature is conflicted on this issue [32,33].

Electron microscopy studies of Gram-negative *Escherichia coli* (*E. coli*, ATCC 23282) and Gram-positive *Staphylococcus aureus*

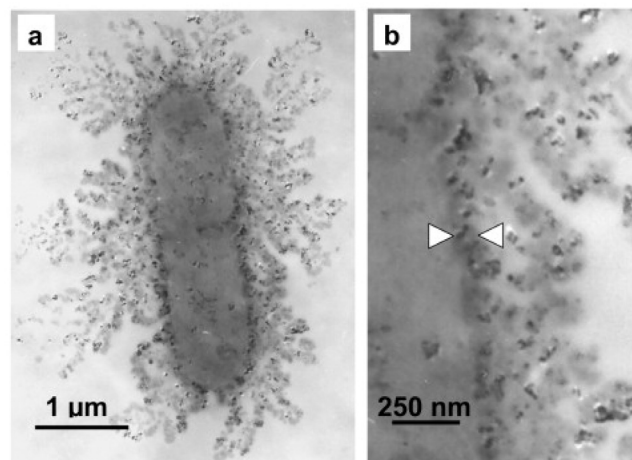


Fig. 2. Transmission electron micrograph of *E. coli* cell treated with $50 \mu\text{g cm}^{-3}$ of silver nanoparticles in liquid LB medium for 1 h (a) and enlarged view of the membrane of this cell (b). (Adapted from Ref. [91]).

(*S. aureus*, ATCC 35696) upon exposure to 10 $\mu\text{g/ml}$ of AgNO_3 provides insight into the morphological changes brought on by Ag^+ . Upon Ag^+ exposure, the DNA appears to be aggregated in the center of the cell. Similar morphological changes were observed in *S. aureus*. Ag^+ containing granules have been found in vacuole and cell walls [34]. In another electron microscopy study, either localized or complete separation of the cell membrane from the cell wall upon treatment with Ag^+ was observed [4].

Species that can compete/bind with Ag^+ binding also influence its activity. The inhibitory effect of Ag^+ on growth of *E. coli* is moderated in the presence of Cu^{2+} , suggesting that Ag^+ and Cu^{2+} are competing for the same sites, and high concentrations of Cu^{2+} can have protective effects [26]. Compounds containing thiol groups, such as cysteine and glutathione when added to the growth medium also neutralized the silver activity against growth of *Pseudomonas aeruginosa*, due to the thiols chelating the Ag^+ [25]. In complex broth samples, biological species present in broth such as proteins, amino acids peptides can bind released Ag^+ . Also, broths contain chloride ions that can precipitate Ag^+ , but at high Cl^- concentrations will form soluble AgCl_x^{y-} species. Silver however is often precipitated in real world environment streams, e.g. it was effectively absent in waste water in sewage treatment plants, due to the precipitation of highly insoluble and stable Ag_2S [35].

2.2. Silver nanoparticles (AgNP)

There is considerable research activity focused on AgNP as antimicrobial agents. The AgNP are typically generated by reduction of dissolved Ag^+ , typically in an aqueous solution. Diverse group of reducing agents are used. Chemical reducing agents are typically NaBH_4 , citrate, hydrazine, ascorbate, polyoxometalate, Tollens agent, polysaccharides and polyphenols [36–46]. Proteins, amino acids, vitamins, plant extracts, as well as microorganisms are used to make AgNP [40,47–59]. Irradiation of silver salts by electromagnetic and microwave radiation to produce AgNP is reported [58,60–67]. Other methods include solvated metal atom dispersion, where the nanoparticles form via aggregation of atoms upon solvent removal [68,69].

The nanoparticles made by these diverse methods differ in size, morphology and surface groups. Considering this heterogeneity, it is not surprising that there is wide variation in the antimicrobial activity of AgNP.

How do AgNP exhibit their activity? There is evidence that AgNP oxidatively dissolves to form Ag^+ , which acts by pathways listed above. Bulk silver metal also acts by dissolution, though at a different rate than nanoparticles. However, there is also indication that direct interaction of AgNP with bacteria can take place and internalization of AgNP by bacteria has also been noted. We summarize these possible pathways.

For AgNP to dissolve to form Ag^+ ions will require an oxidizing agent [70]. The most plausible agent is oxygen from air [71]. Support for this hypothesis comes from several observations [72]. Silver NP prepared under anaerobic conditions does not exhibit antimicrobial activity. However, if such particles are oxidized, the activity is restored [73,74]. Longer storage of AgNP in aerated environments gradually increases their activity. AgNP that are in contact with cell surfaces or internalized can also be oxidized by H_2O_2 e.g. in mitochondria of eukaryotic cells.

Surface ligands added for particle size control, and other adsorbed species on the AgNP will also influence dissolution [75–78]. Chemisorbed Ag^+ ions on the surfaces of AgNP incorporated during synthesis can also be released into the medium [79,80], and it has been calculated that a ~ 5 nm Ag nanoparticle can adsorb $20 \mu\text{g}$ of Ag^+ /mg Ag [20]. Another line of support for Ag^+ involvement is that anions that promote precipitation as silver salts, such as Cl^- , S^{2-} can produce an insoluble passivation layer on the NP, and decrease antibacterial activity of AgNP [81–84].

Morphological characteristics of the AgNP also have a significant impact on their antimicrobial activity. With similar surface ligands, smaller particles tend to be more active [85]. Correlations between Ag^+ released into solution with smaller size and increased antimicrobial activity has been demonstrated [86]. Shape of the AgNP also has an influence, with antimicrobial activity following the order: nanoprisms > nanorods > nanospheres. This effect was explained as due to increasing exposure of [111] facets, which promote dissolution. Increased dissolution can be the result of Ag coordination, altered ligand binding and differences in formation/stability of Ag_2O layers [87–90].

AgNP exhibit additional effects, besides just releasing Ag^+ . They can bind to cell surface and form pits. AgNP with a mean particle size of ~ 12 nm were prepared by reduction of Ag^+ with ascorbic acid in the presence of a high molecular weight sodium salt of naphthalene sulfonate formaldehyde condensate. Electron microscopy (Fig. 2) shows that the AgNP accumulated in the membrane, and small fraction penetrated into the cells [91]. “Pits” are also observed on the cell surfaces. In the liquid medium, the dead cell debris can trap the AgNP and remove them from the medium, and the bacteria can resume growth.

Using EPR spectroscopy, the formation of free radicals when AgNP contacts cell surfaces has been noted. AgNP can be a source of concentrated Ag^+ release, once it is within the bacteria [92]. Mechanical abrasion effects can also occur upon contact of AgNP with bacterial surfaces [93].

Surface charge of NP also influence their activity, primarily because bacterial surfaces carry negative charges. Positively charged chitosan supported AgNP exhibited higher antimicrobial activity since the chitosan can bind to negatively charged bacteria, allowing the attached AgNP to promote bacterial death (chitosan itself has antimicrobial properties) [94]. Positively charged polyethyleneimine coated AgNP were found to have higher toxicity [95]. Caution needs to be exercised since the charge of the particle as-prepared can be altered in the media due to ligand replacement or adsorption of proteins to form a corona [96]. For example, negatively charged AgNP have also been found to be strongly associated with the bacterial surface [91].

Another unique feature of NP is that they can diffuse through biofilms, whereas Ag^+ binds to the diverse sites, such as thiols, amines and carboxylates, impeding motion. Thus, for ~ 2 nm

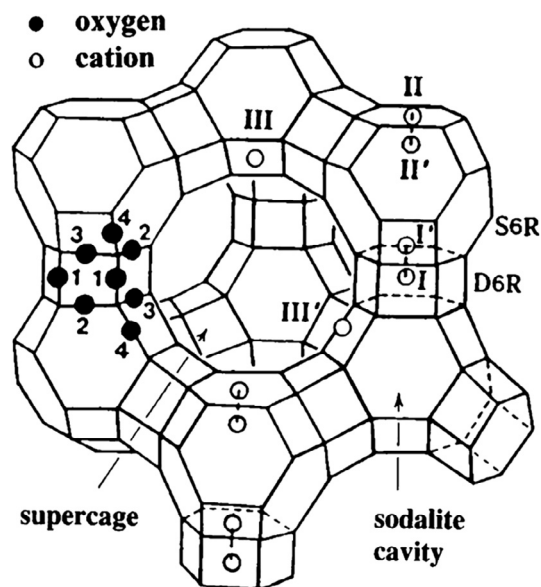


Fig. 3. Schematic of the framework structure of faujasitic zeolites (zeolites X and Y). Each line segment is a T-O-T bridge with oxygen atom in the center. The nonequivalent oxygen atoms are indicated by the numbers 1–4 representing O (1)–O(4). Silicon and aluminum atoms make up the T atoms, are present in the tetrahedral intersections, and Al-O-Al bonding is not allowed (Lowenstein's rule). Extra framework cation positions are labeled with Roman numerals.

negatively charged AgNP, only a 14% reduction in diffusion coefficient was noted in a biofilm, whereas for Ag^+ , mass transport is limited until all the possible binding sites are saturated. AgNP (20 nm) were found to penetrate a $40 \mu\text{m}$ *E. coli* film within 1 h [97–99].

3. Brief introduction to zeolites

Zeolites are microporous crystalline aluminosilicates of composition $\text{M}_{n/m}^{m+} \text{Si}_{1-n}\text{Al}_n\text{O}_2 \cdot x\text{H}_2\text{O}$, with the framework made up of interconnected TO_4 (T = Si, Al) tetrahedra [8,9]. Introduction of Al^{3+} into the structure results in a negatively charged framework, with extra-framework ion-exchangeable M^{m+} providing charge neutrality. The Si/Al ratio of the framework can vary from 1 to ∞ . With increasing Si/Al ratio, there are fewer ion-exchanging M^{m+} in the zeolite. The most recent Atlas of Zeolite Framework

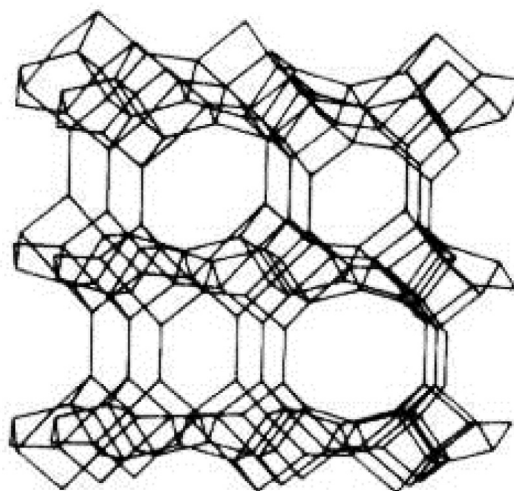


Fig. 4. Schematic structure of clinoptilolite.

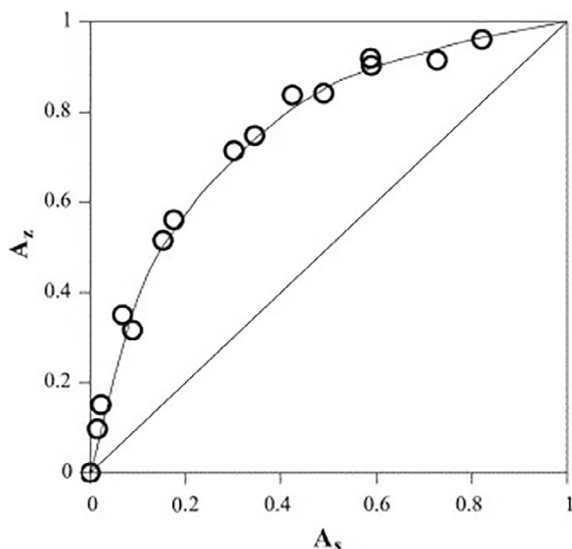


Fig. 5. Ag^+ – Na^+ exchange isotherm of clinoptilolite at 25 °C (adapted from Ref. [106]).

Types lists 133 structures, all with distinct topologies, and characterized by different pore structures, and crystal morphology [100].

Some zeolites are found in nature, and 40 different frameworks are known [8,9]. Typically, zeolites are synthesized under hydrothermal condition in the laboratory. High porosity zeolites are metastable structures. Of particular relevance to silver zeolites is the ion-exchange process of replacing the cations in the as-synthesized zeolite with Ag^+ . Ion exchange isotherms provide information about the thermodynamic selectivity of particular cations for the framework. Faujasitic zeolites (zeolite X and Y) are studied commonly for silver antimicrobials. Ion-exchange isotherms at low loadings suggest selectivity of $\text{Ag} \gg \text{Tl} > \text{Cs} > \text{Rb} > \text{K} > \text{Na} > \text{Li}$ [8]. The selectivity for the natural zeolite clinoptilolite is quite distinct from zeolite A or X/Y and follows the sequence $\text{K} > \text{NH}_4 > \text{Ag} \geq \text{Pb} > \text{Na} > \text{Ca} > \text{Li}$ [101]. The ion-release characteristics will vary with the framework and the types of ions in the surrounding e.g. in a K^+ – rich broth, Ag^+ will be more readily released from clinoptilolite as compared to zeolite A or zeolite X/Y [101].

Silver ions are polarized by the strong electric fields within the framework, and results in strong attraction between Ag^+ and the zeolite framework. This tight binding of Ag^+ by the framework also implies that the release of Ag^+ by the framework will require higher ionic strength solutions. In general, all zeolites show high selectivity for Ag^+ , and with increasing Si/Al ratio for a particular framework, the selectivity towards Ag^+ tends to be higher [102].

Besides the framework structure and Si/Al ratio of the zeolite determining Ag^+ uptake and release, there are several other zeolite

features that are relevant for antimicrobial activity. Zeolite morphologies can vary from rods to spheres, which will alter the extent of bacteria-zeolite contact [8,9]. Zeolites can also be synthesized with particle sizes varying from nanometers to microns [103]. With the smaller zeolite crystals, there is the potential for uptake of the zeolite particle by the bacteria. Nanozeolites have the potential advantage of faster ion exchange and ion release because of shorter diffusion lengths. This could be relevant for applications that require a quick antimicrobial effect. Release characteristics of the Ag^+ from the zeolite will be altered with amorphization of the surface and is dependent on sample preparation.

3.1. Siting of cations

The extraframework cations in the zeolite are distributed over specific crystallographic sites. The positions of the cations are best determined by single crystal X-ray crystallography. Below we discuss antimicrobial activity of zeolite frameworks, and the siting of Ag^+ in all of these structures has not yet been reported. Much work, however, has been done with faujasitic zeolites regarding Ag^+ siting and we summarize this work. Zeolites X and Y represent the faujasitic structure with typical compositions of $\text{Na}_{86}\text{Al}_{86}\text{Si}_{106}\text{O}_{384} \cdot 264\text{H}_2\text{O}$ and $\text{Na}_{56}\text{Al}_{56}\text{Si}_{136}\text{O}_{384} \cdot 250\text{H}_2\text{O}$, respectively. As synthesized, the framework is filled with water, which can be completely removed at high temperatures. The framework variation between zeolite X and Y is only in the Si/Al ratio. The cations are located at specific crystallographic sites identified as sites I, I', II and II', III and III', as indicated in Fig. 3. Single crystal structure of completely exchanged Ag^+ -zeolite X has been reported in the literature [104,105]. Of the 92 Ag^+ , 16 fill site I, 16 at site I', 32 fill site II, and 28 occupy four different III' sites [104,105].

4. Silver-zeolite powder antimicrobial activity

The following is a review of the silver-zeolite literature since 2000. The sections that make up this part includes natural zeolites, low Si/Al zeolites, high Si/Al zeolites, zeolite membranes, zeolite/polymer composites, zeolite/textile composites, zeolite coatings, zeolite in medical/dental and in environmental/consumer applications.

4.1. Natural zeolites

4.1.1. Clinoptilolite

The structure of this framework is shown in Fig. 4.

Top et al. studied Ag^+ , Zn^{2+} and Cu^{2+} exchanged clinoptilolite. Samples were prepared by ion-exchange and antibacterial activities towards *P. aeruginosa* and *E. coli* was investigated using the agar disk diffusion method [106]. Ion-exchange isotherms showed

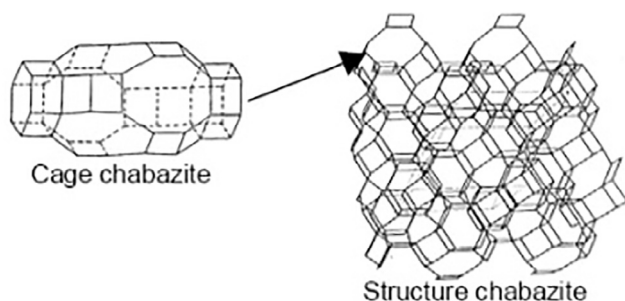


Fig. 6. The structure of chabazite.

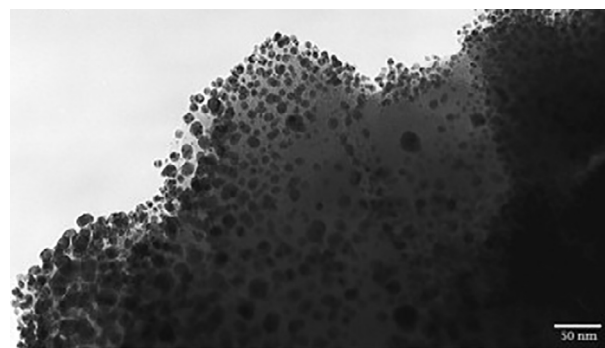


Fig. 7. TEM images of the silver-supported chabazite sample (adapted from Ref. [109]).

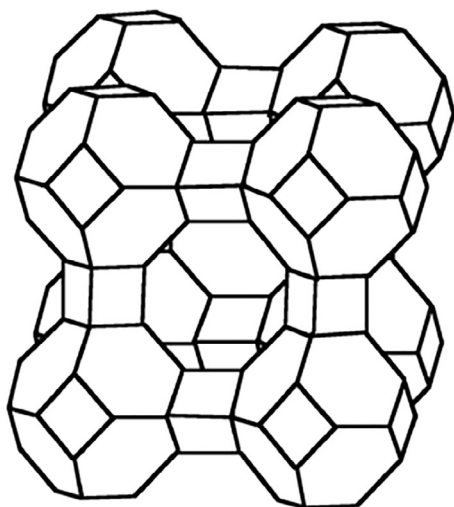


Fig. 8. The structure of zeolite A.

considerable selectivity of Ag^+ over Na^+ , and complete replacement of Na^+ was noted, as shown in Fig. 5. For Zn^{2+} and Cu^{2+} , there was slight preference over Na^+ for clinoptilolite, but only at low concentrations. About 50% exchange of the Na^+ by the divalent ions was observed. Ag^+ -clinoptilolite showed the best antibacterial activity, but the activity did not scale with the amount of Ag^+ in the zeolite. Formation of metallic Ag at the higher concentrations of Ag^+ exchange, as well as loss in porosity was proposed as the reason for lower activity at high Ag^+ loading in the zeolite.

Akhigbe et al. ion-exchanged clinoptilolite with Ag^+ (4.34 wt%) and examined the antimicrobial activity towards *E. coli* [107]. With a zeolite concentration of 2 mg/ml, 10 \log_{10} reduction was noted within 30 min (Ag^+ release during this period was 0.76 $\mu\text{g}/\text{ml}$, and accounts for 0.9 wt% of Ag in zeolite). Part of this enhanced activity could be due to osmotic shock, since these experiments were done in water. In the presence Pb^{2+} , Cd^{2+} and Zn^{2+} in solution, the activity of the Ag^+ -zeolite was enhanced (15 min for 10 \log_{10}), since these metal ions increased the Ag^+ exchange out of the zeolite into solution (e.g. 1.05 $\mu\text{g}/\text{ml}$ of Ag^+ for Pb^{2+} as compared to 0.4 $\mu\text{g}/\text{ml}$ without Pb^{2+} in 15 min). The role of ion-exchange kinetics in influencing antimicrobial activity for zeolite with multiple ions was evident from this study.

Guerra et al. prepared AgNP on clinoptilolite surface and tested it against *E. coli* and *Salmonella typhi* [108]. Nanoparticles on the zeolite surface were generated by reduction of Ag^+ exchanged zeolite with H_2 at elevated temperatures. Particle size of the Ag NP ranged from 0.9 to 7.4 nm. With the highest loaded Ag sample (4 wt%), 1.7 mg/ml of AgNP-zeolite produced a 2 \log_{10} decrease for *E. coli* (~starting with 200 CFU/ml) within an hour. *Salmonella* required a larger amount of sample (6.7 mg/ml) for complete killing of the bacteria.

4.1.2. Chabazite

The structure of chabazite is shown in Fig. 6.

Flores-Lopez et al. generated AgNP on surface of chabazite by reducing Ag^+ -exchanged zeolite with thermal annealing in air [109]. The loading of Ag was ~19 wt%, and AgNP were evident on the zeolite surface (Fig. 7). Six bacterial strains, *S. epidermidis* (ATCC 12228), *S. aureus* (ATCC 25923), *Salmonella typhimurium* (ATCC 14028), *E. coli* (ATCC 25922), *Shigella flexneri* (ATCC 12022) and *P. aeruginosa* (ATCC 27853) were examined. Using 10^5 CFU/ml of bacteria, and zeolite loadings of 0.001, 0.1 and 1 wt% (10 $\mu\text{g}/\text{ml}$ to 10 mg/ml) in a saline solution, the killing of bacteria was complete in 48 h, except for *S. aureus*. At 0.00001 wt% (0.1 $\mu\text{g}/\text{ml}$) zeolite,

only *S. epidermidis* was completely killed, whereas a low number of counts was noted with the other bacteria.

Summary of this section is:

- Natural zeolites can accommodate Ag^+ and AgNP.
- High loading of Ag^+ can lead to formation of metallic Ag.
- Ions in the medium influences antimicrobial activity of silver zeolite by influencing ion-exchange kinetics.

4.2. Synthetic zeolites

4.2.1. Low Si/Al zeolites

4.2.1.1. Zeolite A. The structure of zeolite A is shown in Fig. 8. Many studies are reported with this zeolite, possibly because commercial forms of the Ag^+ exchanged version of this zeolite are available.

Kawahara et al. investigated the antibacterial activity of a commercial sample of Ag^+ -zeolite A (Zeomic, 2.5 wt% Ag) towards 14 distinct oral bacteria under anaerobic conditions [110]. In all cases, Ag^+ -A exhibited antimicrobial activity with Minimum Inhibitory Concentration (MIC) varying from 256 to 2048 $\mu\text{g}/\text{ml}$ (corresponds to 4.8–38.4 $\mu\text{g}/\text{ml}$ of Ag^+ , using 10^7 cells/ml). Seventy-five percent of the Ag^+ present in the zeolite was released into broth via ion-exchange within 30 min of exposure. Gram-negative bacteria were more susceptible than Gram-positive bacteria with lower MIC values. The important conclusion of this paper was that silver zeolites can kill oral bacteria under anaerobic conditions.

Matsumura et al. studied the antimicrobial properties of a commercial sample of Ag^+ -zeolite A (2.5 wt% silver, Zeomic) with *E. coli* strain OW6 (Pro⁻) and CSH7 (*lacY rspL thi*) and its catalase-deficient mutant UM1. In 20 μM potassium phosphate or 20 μM HEPES-NaOH buffers, the Ag^+ -zeolite exhibited bactericidal activity [111]. The concentration units in the paper were not consistent (mg/l and mg/ml used interchangeably) so it is unclear what concentrations were actually used. The survival rate decreased non-linearly with time, being slow initially. This aspect is possibly a reflection of the ion-exchange dynamics. This study also noted that under anaerobic conditions, more cells are viable. It was proposed that the presence of oxygen could lead to ROS formation, due to Ag^+ -mediated inhibition of respiratory enzymes. Close proximity of the zeolite and bacteria promoted the antibacterial effect, possibly due to higher concentration of Ag^+ that are ion-exchanged out of the zeolite around the bacteria. The source of cations (possibly Na^+ , K^+) that can exchange out the Ag^+ can come from the buffer or from the bacteria.

Zhang et al. prepared Ag^+ ion-exchanged zeolite A under microwave radiation and found it to be more active [112]. The antimicrobial activity towards *E. coli* (ATCC 10231), *B. subtilis* (ATCC 6633) and *S. aureus* (ATCC 27154) was examined. Towards all three bacteria, the MIC of the microwave prepared sample was 50 $\mu\text{g}/\text{ml}$, and 100 $\mu\text{g}/\text{ml}$ for the conventional ion-exchanged Ag^+ -A. The higher activity with the microwave prepared sample is possibly a reflection of the higher level of Ag^+ loading (factor of 2) in the zeolite.

Krishnani et al. examined the antimicrobial activity of Ag^+ -exchanged zeolite A (39.4 wt% Ag) towards *E. coli*, *Vibrio harveyi*, *V. cholerae* and *V. parahaemolyticus* [113]. The MIC for *E. coli* and *V. harveyi* was 40 $\mu\text{g}/\text{ml}$, whereas for *V. cholerae* and *V. parahaemolyticus*, MIC was higher at 50 and 60 $\mu\text{g}/\text{ml}$, respectively (all after 48 h of contact, 10^9 CFU/ml). *V. cholerae* and *V. parahaemolyticus* have thicker cell walls and thus needed higher levels of Ag^+ -zeolite. The presence of ammonia increased the antimicrobial activity of the Ag^+ zeolite and was attributed to the toxicity of NH_3 .

Kaali et al. studied the ion-exchange isotherms of single, binary and ternary mixtures of Ag^+ , Cu^{2+} and Zn^{2+} with zeolite A (Zeomic) [114]. Ag^+ exhibits almost 100% of the theoretical exchange,

indicating clear preference of zeolite A towards Ag^+ over Na^+ Even in the binary and ternary systems, Ag^+ content of the zeolite was significantly higher than Cu^{2+} and Zn^{2+} . Similar trends were also noted with ion-exchange out of the zeolite, with Ag^+ being held most strongly by the zeolite, e.g. 0.35 mmol/l of Ag^+ was released from the ternary sample, compared to a maximum of 96.2 mmol/l that could be released. MIC of single, binary and ternary ion-exchanged zeolite A towards *S. aureus* (MRSA, ATCC 43300) and *Candida tropicalis* (ATCC 90874) and *P. aeruginosa* (ATCC 27853) were determined. The concentration of zeolite was varied from 2 to 1024 ppm with 5×10^5 CFU/ml of bacteria. Ag^+ containing samples exhibited the highest activity e.g. with Ag^+ -A, MIC of 2, 512 and 128 ppm ($\mu\text{g/g}$) towards *C. tropicalis*, MRSA and *P. aeruginosa* was observed. Co-exchange with Zn^{2+} and Cu^{2+} decreased the amount of Ag^+ , and in some cases increased MIC.

Zhou et al. studied the antimicrobial property of Ag^+ -ion exchanged zeolite A (36.6 wt% Ag) towards *E. coli* (ATCC 8739) and *S. aureus* (ATCC 6538) [115]. MIC of 1 $\mu\text{g/ml}$ and 3.5 $\mu\text{g/ml}$ towards *E. coli* and *S. aureus* was found. These are some of the lowest numbers for MIC that are reported, but since the description of the biological experiments were poorly presented (lack of CFU, times of exposure), it is difficult to compare this study with others.

Jiaroj et al. compared the antimicrobial properties of Ag^+ -ion exchanged zeolite A and AgNP-zeolite A (prepared by NaBH_4 reduction, $\sim 1 \mu\text{m}$ zeolite particle, weight loadings of Ag not reported) [116]. There was surface roughening of the zeolite upon Ag^+ incorporation. From the electron microscopy data, the size of the AgNP appears $< 10 \text{ nm}$ (present in both the ion-exchanged and metallic samples). Gram-negative *E. coli* (ATCC 25922) and Gram-positive *S. aureus* (ATCC 6538) at $\sim 10^7$ CFU/ml was used to examine the antibacterial activity towards the zeolite (25–200 $\mu\text{g/ml}$) for exposures of 0–3 h. General observations were that higher concentrations and longer exposure times to silver zeolite were more effective at killing cells. Killing of *S. aureus* took higher concentrations and longer times than *E. coli*. Towards *E. coli*, the AgNP-zeolite was less effective than Ag^+ -zeolite, though this effect disappeared with longer incubation times. Thus, at 3 h, $\geq 50 \mu\text{g}$ zeolite/ml caused $\sim 100\%$ *E. coli* mortality at 3 h for both Ag^+ and AgNP zeolite.

Demirci et al. studied Ag^+ , Zn^{2+} and Cu^{2+} -exchanged zeolite A and X and their antimicrobial activity towards bacteria (*S. aureus*, *E. coli*, *P. aeruginosa*, *B. cereus*, 10^7 CFU/ml), yeast (*C. albicans*, *C. glabrata* 10^5 CFU/ml) and fungi (*A. Niger*, *P. vinaceum* 10^3 spore/ml) [117]. Incubation times were 24 h, 48 h and 72 h for bacteria, yeast and fungi, respectively. The best antibacterial results were obtained with Ag^+ -exchanged samples. For a phase-pure Ag^+ -X

(Ag-z2 from the paper), the MIC value for *P. aeruginosa* was 32 $\mu\text{g/ml}$, whereas for the other 3 bacteria, MIC was 64 $\mu\text{g/ml}$. With the optimum Ag^+ -A sample (Ag-z3) the MIC towards *B. cereus* was 16 $\mu\text{g/ml}$, whereas for the other three bacteria, MIC was 32 $\mu\text{g/ml}$. This sample (Ag-z3) also exhibited the highest rate of release of Ag^+ into the media (39–70 ppm Ag^+ over 0.5–24 h with 2.048 mg zeolite/ml). For the Cu^{2+} and Zn^{2+} exchanged zeolites, the MIC value for the bacteria ranged from 256 to 2048 $\mu\text{g/ml}$. Towards the yeast and fungi, MIC for the Ag^+ -zeolites varied from 128–1024 $\mu\text{g/ml}$.

Summary of this section is:

- Closer contact of silver zeolite with microorganism promotes antibacterial activity.
- Bacteria with thicker walls required more silver zeolites.
- Silver zeolites exhibit antimicrobial activity under anaerobic conditions, but at a considerable lower rate.
- For multiply ion-exchanged silver zeolite (e.g. with Zn^{2+} and Cu^{2+}), the presence of a co-cation influences the ion-exchange kinetics of the Ag^+ release.

4.2.1.2. Faujasitic zeolites. Zeolites X and Y are representative of faujasitic zeolites, and their structure is shown in Fig. 3. Zeolite X and Y have the same framework, and are only distinguished by their Si/Al ratios, with zeolite X being defined as Si/Al < 1.5 and zeolite Y with Si/Al > 1.5 .

Kwayke-Awuah et al. examined the antimicrobial activity of Ag^+ -zeolite X (2–9 μm zeolite, 5.8 wt% Ag) towards *E. coli* (K12 W-T), *P. aeruginosa* (NCIMB 8295) and *S. aureus* (NCIMB6571) [118]. With all three bacteria ($\sim 5 \times 10^5$ CFU/ml), exposure to zeolite loadings of 150–1000 $\mu\text{g/ml}$ led to complete cell death after 2 h. With 150 $\mu\text{g/ml}$ zeolite, no viable cells were detected in *E. coli* after 45 min and the same observation was made with *S. aureus* and *P. aeruginosa* after 60 min of exposure. The amount of Ag^+ released from the zeolite was higher in presence of microorganisms than in broth alone, suggesting uptake of Ag^+ by the bacteria. Ag^+ concentrations were < 10 ppm for 45 min exposure, indicating that the majority of Ag^+ ($\sim 97\%$) is retained in the zeolite. Antimicrobial activity with the same sample was repeatable (experiments done 3 times), since most of the Ag^+ is retained in the zeolite.

Inoue et al. proposed that light irradiation was responsible for creating bactericidal active oxygen species (superoxide) responsible for killing *E. coli* (NIH CJ2), since the Ag^+ -zeolite Y did not exhibit antibacterial activity in the dark [119]. A control sample of Na^+ -zeolite Y under light irradiation did not show activity. It is unclear how the intrazeolitic superoxide is formed and transported out of the zeolite within 5 min to kill $\sim 10^6$ bacteria.

Shameli et al. studied AgNP (2–3 nm) on micron-sized zeolite Y crystals prepared by reduction of Ag^+ -Y with NaBH_4 [120]. Antibacterial activity towards *E. coli* (ATCC 25922), *Shigella dysenteriae* (ATCC 9753), (both Gram-negative), and *S. aureus* (ATCC 25923), *S. aureus* (MRSA, ATCC 700689) (both Gram-positive) was examined by the disk diffusion method. All AgNP-Y exhibited antimicrobial activity; zeolites with smaller AgNP particles exhibiting higher activity.

Ferreira et al. studied Ag^+ -ion exchanged zeolite X (9.8 wt% Ag) and Ag^+ -ion exchanged zeolite Y (9.7 wt% Ag), both containing micron sized zeolite particles [121]. The MIC values for the bacteria (*E. coli*, *B. subtilis*) were 300 $\mu\text{g/ml}$ for AgX and 200 $\mu\text{g/ml}$ for AgY (24 h exposure) and for the yeast *S. cerevisiae* and *C. albicans*, MIC were 1000 $\mu\text{g/ml}$ for both Ag^+ zeolite X and Y (42 h exposure). The lower MIC value for the bacteria in the case of AgY as compared to AgX was explained as arising from the metallic Ag (presence concluded by Auger spectroscopy) in AgX. Fig. 9 compares the antimicrobial efficiency between the two zeolites towards *E. coli* as a function of zeolite content. With the yeast samples, the more

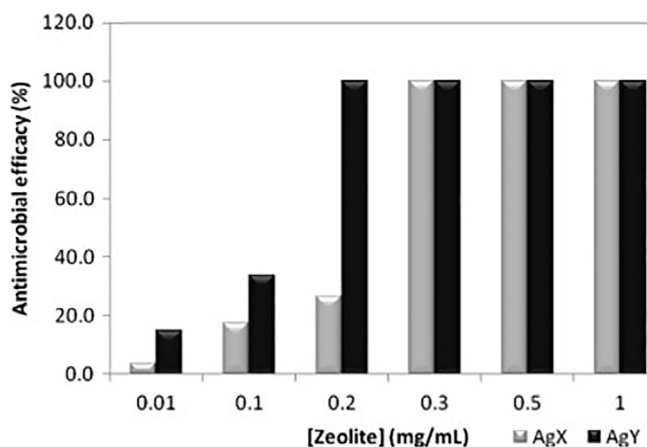


Fig. 9. Antimicrobial efficacy (%) of Ag^+ -exchanged zeolite X and Y against the Gram-negative bacteria *E. coli* (adapted from Ref. [121]).

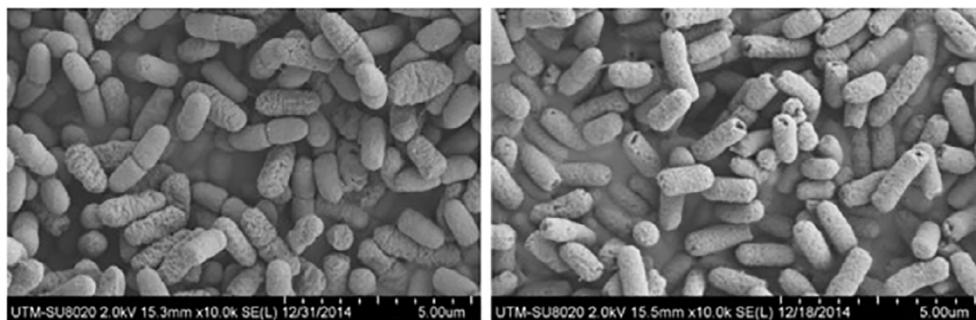


Fig. 10. Morphology of *E. coli* before (left) and after (right) the treatment with Ag^+ -Y, holes are evident in the bacteria ($\times 10\text{ k}$ magnification, adapted from Ref. [126]).

complex cell structure of the yeast necessitated the need for higher levels of Ag^+ zeolite to inhibit growth.

The effect of Ag^+ -exchanged zeolite X on antibiotic activity of rifampicin, nalidixic acid, benzylpenicillin and chloramphenicol towards *E. coli* (NIHJ JC2) (10^6 CFU/ml) was reported by Inoue et al. [122]. The exposure times were kept to 3 min, since at these short times, it was reasoned that the Ag^+ -zeolite would have no effect. Only in the case of rifampicin, Ag-Y had a synergistic effect. It was proposed that that effect of the silver zeolite arose from its ability to create reactive oxygen species.

Ferreira et al. examined bimetallic samples of zeolite Y, containing two of three ions Ag^+ , Cu^{2+} and Zn^{2+} (six samples starting with the monometallic form) for antimicrobial activity towards *E. coli* (CECT 423) (24 h exposure) [123]. Towards *E. coli*, the ZnAg-Y (Zn^{2+} exchanged first followed by Ag^+) was the most active, with a MIC of 500 $\mu\text{g/ml}$, while AgZnY had a MIC of 1000 $\mu\text{g/ml}$. Bimetallic samples were more active than Ag-Y or Zn-Y (both with MIC > 2000 $\mu\text{g/ml}$). The loading of Ag and Zn in AgZnY and ZnAgY were 1.04 wt% (Ag), 4.61 wt%(Zn) and 3.31 wt% (Zn), 1.85 wt% (Ag), respectively. The ion-exchange out of the zeolite is dependent in which order the metallic ion was introduced. For the yeast sample, the best results were also obtained with AgZn-Y and ZnAg-Y, both exhibiting MIC values of 2000 $\mu\text{g/ml}$, expectedly higher for the more complex eukaryotic yeast cell.

Singh et al. noted that sputtered Ag metal on zeolite crystals can react with H_2O_2 producing O_2 that results in movement of these crystals within a fluid medium [124]. These Ag metal-zeolites can be ion-exchanged with Ag^+ and was found to exhibit antibacterial properties towards *E. coli*. The self propelled motion promoting enhanced contact with the bacteria was of interest in this study.

Ferreira et al. continued their studies with the bimetallic ZnAgY, and tested for activity against *E. coli* (CECT423), *B. subtilis* (4886), yeast *C. albicans* (JGC 3456T) and *S. cerevisiae* (BY 4741) [125]. Samples with different Ag loadings were examined. The optimal sample ZnAgY had 3.03 wt% Zn and 6.04 wt% Ag and exhibited MIC of 100, 100, 300, 300 $\mu\text{g/ml}$ towards *E. coli*, *B. subtilis*, *C. albicans* and *S. cerevisiae*, respectively. For AgY with 9.70 wt% Ag loading, comparable MIC values were higher, 200 $\mu\text{g/ml}$ for bacteria and 1000 $\mu\text{g/ml}$ for yeast, indicating enhancement of activity with both ions present. The Zn^{2+} and Ag^+ distribution in the zeolite was non-uniform, with Ag^+ proposed to be in the supercage sites. A synergistic effect of Ag^+ and Zn^{2+} was clearly present. The zeolite/antimicrobial assays were reproducible even after two years of zeolite sample storage.

Hanim et al. carried out surface derivatization of Ag^+ -zeolite Y with 3-aminopropyltriethoxysilane [126]. The surface derivatization leads to $-\text{NH}_2$ groups, which get protonated in the media, leading to positively charged zeolite particles (confirmed by zeta potential measurements). Several concentrations of AgNO_3 were chosen for ion-exchange, and the extent of surface functionalization was also altered. Surface derivatization tended to improve the MIC compared to the underivatized sample e.g. with *E. coli* (ATCC 11229). MIC of 100 and 50 $\mu\text{g/ml}$ was noted for underivatized and derivatized sample, respectively. Enhanced interaction of positively charged zeolite particles with negatively charged bacteria was proposed to explain the improved MIC for functionalized samples. Higher loadings of Ag^+ did not improve MIC significantly, and zeolite structural changes were noted at high loadings of Ag^+ . Similar observations were made with *S. aureus* (ATCC 6538). Fig. 10

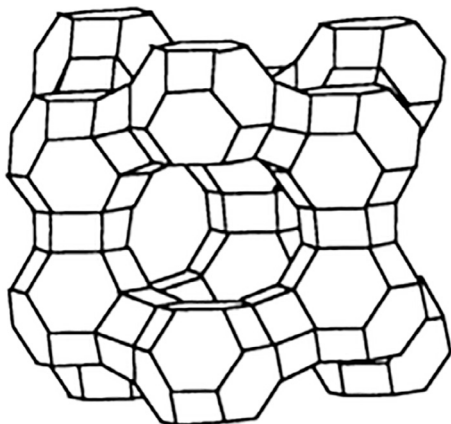


Fig. 11. The structure of EMT.

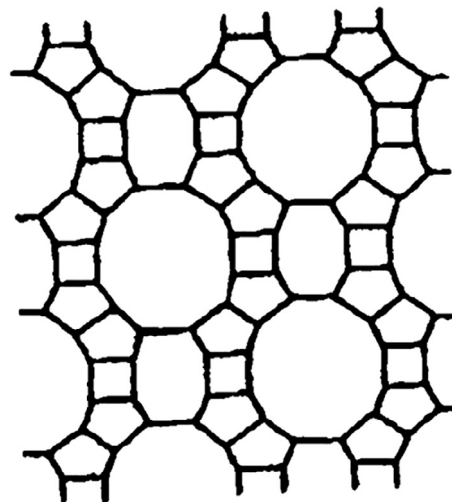


Fig. 12. The structure of mordenite.

shows electron micrographs of zeolite-exposed *E. coli* with holes in the bacterial cell surface. With *S. aureus*, the morphology was unchanged, indicating difference in the killing mechanism between these two bacteria.

Chen et al. compared the MIC and MBC for Ag⁺-exchanged zeolite X of varying morphology [127]. Submicron aggregates of 100–700 nm containing ~24 nm primary particles was compared with ~2 μm particles. The nanostructured zeolite had a hierarchical structure with both micro- and mesopores. The amount of Ag⁺ loading in both morphologies was comparable, about 20–22 wt%. However, the Ag⁺ release characteristics in a flow-through cell (with Na⁺ eluent) indicated faster and higher amount release of Ag⁺ from the nanozeolite. The micron and nano zeolites exhibited MIC and MBC values towards *S. aureus* (MRSA) of 16 and 32 μg/ml, respectively (24 h test). The faster Ag⁺ release from the nanozeolite was evident in short-term experiments (10 min), where 400 μg/ml of the zeolite killed MRSA (10⁸ CFU/ml) in 3 min versus 7 min for comparable levels of the micron zeolite. The Ag⁺ nanozeolite was ineffective at inhibiting MRSA biofilm, rather appeared to promote film formation. The cytotoxicity against human skin epithelial cells (WM-115) required >128 μg/ml of Ag⁺-hierarchical zeolite, whereas for human skin fibroblasts (Detroit 551) and monocytes (U-937) concentrations of 64 μg/ml was required for significant reduction in viability. These cytotoxic concentrations are significantly higher than the MIC/MBC concentrations.

Youseff et al. also compared zeolites analcime, faujasite and zeolite A in both micron and nanosizes (~200 nm) [128]. Upon Ag⁺ exchange, the nanozeolites were degraded, but the micron sized zeolites were stable. Very high levels of Ag⁺ were found in faujasite (48 wt%) and analcime (50 wt%) for the micron sized zeolites, with zeolite A containing 24.6 wt%. The agar plate diffusion method showed antimicrobial activity in the following order analcime > faujasite > zeolite A towards *S. aureus*, *P. aeruginosa*, *C. albicans* and *A. niger*. No difference in antimicrobial activity was noted between the micron and nano-sized zeolites.

Summary of observations of faujasitic zeolites are

- Smaller zeolite crystal exhibit faster Ag⁺ release.
- Nanosized zeolite crystals may be damaged with high Ag⁺ loadings.
- Ion-exchange of Ag⁺ from a bimetallic Ag⁺, Zn²⁺ zeolite depends on which of the two ions is introduced first into the zeolite.
- Presence of microorganism alters available Ag⁺ in broth media.
- As in case of clinoptilolite, high Ag⁺ loadings can lead to Ag⁰ formation and slow the antimicrobial activity.
- Smaller the size of AgNP on the zeolite, higher the activity.
- Yeast requires more silver zeolite than bacteria for cell death.
- Surface modification of the silver zeolite to generate a positive charge improves antimicrobial activity.
- Gram positive and Gram negative bacteria exhibit different morphological changes upon treatment with silver zeolites.
- Silver zeolites exhibit activity even after two years of storage.

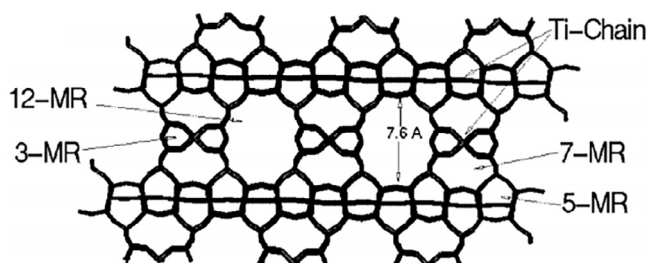


Fig. 13. The structure of ETS-10.

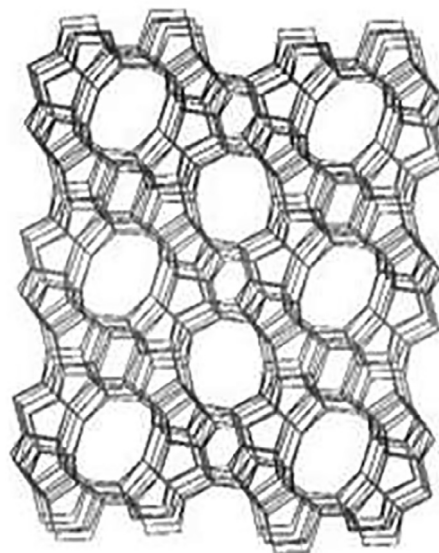


Fig. 14. The structure of ZSM-5.

4.2.1.3. EMT. The structure of EMT is shown in Fig. 11.

Dong et al. ion-exchanged nanosized (10–20 nm) crystals of EMT with Ag⁺ (2–6 h) to form Ag⁺-EMT [129]. The Ag content increased to 14 wt% with 6 h of ion-exchange. These samples were subjected to microwave radiation in the presence of trimethylamine to form AgNP-EMT. The size of the AgNP varied from 0.6 nm to 2–5 nm, the latter with the high-loading Ag⁺. The NP were on the surface of the zeolite. Spot inoculation of *E. coli* (ATCC 8739, 10⁸ CFU/ml) onto thioglycollate agar plates in the presence of Ag⁺-EMT and Ag-EMT showed that the cells were instantly killed. MIC values were not reported, since the goal was to qualitatively compare the killing efficiency of Ag⁺ and AgNP EMT samples. The NP tended to perform better than the ion-exchange samples, and was attributed to the presence of the NP in a mesoporous zeolite environment, thereby promoting Ag mobility.

In summary.

- Direct composition of the antimicrobial activity of AgNP and Ag⁺-zeolite with comparable silver loadings show that the AgNP-zeolite performed better.

4.2.2. High Si/Al zeolites

4.2.2.1. Mordenite. The structure of mordenite is shown in Fig. 12.

Jaime-Acuna et al. synthesized mordenite with entrapped AgNP in a one-pot experiment using silica, alumina sources and AgNO₃ [130]. The mordenite crystal size was 40 μm length with 70 nm needle shaped crystals, and AgNP of average size of 5–6 nm resident on the surface of the zeolite. The Ag loading was found to be 1.5 at.%. With 10⁴ CFU/ml *E. coli* (MC4100), MIC and MBC of the AgNP-mordenite was 2 and 3 μg/ml, respectively (overnight incubation). Silver release from the zeolite was ~15 ppm. Exposure to the solution alone was slower in killing cells, as compared to direct contact with the zeolite.

4.2.2.2. ETS. ETS-10, unlike the aluminosilicate zeolites discussed in this paper is a titanosilicate, and its structure is shown in Fig. 13.

Lv et al. examined the antimicrobial activity of Ag⁺-exchanged ETS-10 and AgNP ETS-10 (reduction by NaBH₄) towards *E. coli* [131]. The Ag⁺ loading varied from 6.4 to 17.8 wt% for Ag⁺-ETS-10 and the AgNP loading in AgNP ETS-10 was 5.3–16.2 wt% of Ag. The size of the AgNP was in the range of 0–5 nm. With Ag⁺-ETS-10 (0.5 mg/ml), the viable cell number decreased by a factor of

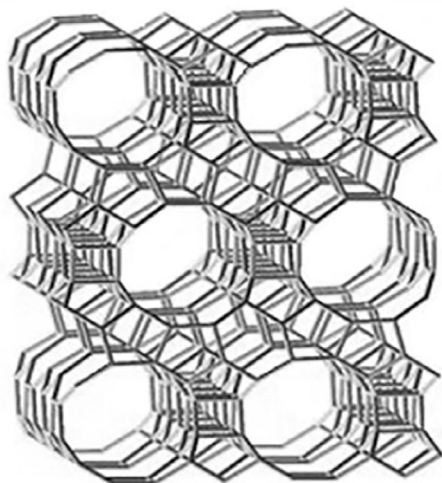


Fig. 15. The structure of zeolite beta.

100 within 1 h (starting with 10^7 CFU/ml). The activity was enhanced with AgNP-ETS-10, with $3.5 \log_{10}$ decrease within an hour. This study also noted that both the rate of Ag^+ release and the amount of Ag^+ released are different for the ion-exchanged and NP samples. Over ~ 40 min, Ag^+ -ETS released 125 ppb Ag^+ , whereas AgNP-ETS (of similar Ag loading, 16.2 wt%) released 35 ppb Ag^+ . However, in that time period, cell amount decreased by a factor of ~ 100 for Ag^+ -ETS-10, whereas exposure to AgNP-ETS-10 decreased cell count by a factor of ~ 1000 . This is contrary to what might be expected, if Ag^+ is solely causing cell death, and suggests that physical contact of AgNP ETS-10 with the bacteria may be playing a role. Even though the aggregate Ag^+ release may be lower with AgNP-ETS-10, the local concentration of Ag^+ around the bacteria upon AgNP dissolution may be higher.

In another study, Guerra et al. prepared AgNP (2–20 nm) on TS-1 by H_2 reduction at 500°C [132]. These particles were effective in reducing *E. coli* and *Salmonella typhi* colonies (100 CFU/ml of *E. coli* reduced to 0 in few minutes, whereas *S. typhi* showed a decrease over 60 min, but not completely eliminated).

4.2.2.3. ZSM-5. With siliceous zeolites, the ion-exchange capacity is lower, and thus amount of silver that can be incorporated by ion-exchange is lower. The structure of ZSM-5 is shown in Fig. 14.

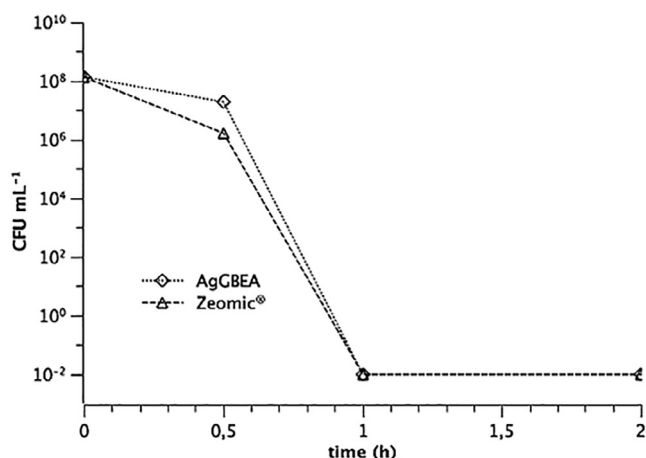


Fig. 16. Activity of Ag^+ -BEA (synthesized without structure directing agent) and Zeomic[®] over a two-hour time period (adapted from Ref. [137]).

Lauleza et al. ion-exchanged Ag^+ into H^+ -ZSM-5 (Si/Al = 15, particle size of zeolite 1–2 μm) using a 1 wt% AgNO_3 solution [133]. The low Al content of the zeolite resulted in a low Ag^+ loading of ~ 0.2 wt%. These Ag^+ -ZSM-5 samples showed a $4 \log_{10}$ unit decrease in 24 h for *S. aureus* strain 9213 (10^9 CFU/ml). Within the first 4–6 h of exposure, 25,000 ppm Ag^+ was released to the culture medium from 300 mg/ml of zeolite with 0.23 wt% Ag. At longer times (24 h), though more Ag^+ is released, the biofilm formed (observed by SEM) around the zeolite hindered the migration of Ag^+ , diminishing antimicrobial activity.

In another study, Lalueza et al. loaded peracetic acid (PAA, 8–9 wt%) into Ag^+ -ZSM5 and AgNP-ZSM-5 (prepared by NaBH_4 reduction, Ag loading 0.2 wt%) and their antibacterial activity towards *S. aureus* (9213, 10^9 CFU/ml) was examined [134]. The combination of peracetic acid, itself a strong disinfectant with Ag exhibited stronger bactericidal ($9 \log_{10}$ decrease) effect than the acid ($2 \log_{10}$ decrease) or Ag-zeolite ($6 \log_{10}$ decrease) (using 30 mg/ml of zeolite). It was proposed that the presence of PAA disrupted the biofilm, allowing for Ag^+ activity. The AgNP-ZSM5 did not exhibit any activity, but with PAA exhibited a $7 \log_{10}$ reduction. In the case of AgNP-ZSM5, PAA was proposed to enhance the dissolution of NP.

Yee et al. reduced Ag^+ -ZSM-5 (1–5 μm zeolite, Ag content 0.8–10 wt%) with citrate to produce AgNP (~ 1.48 nm), visible by TEM both outside and inside the zeolite [135]. The adherent bacterial biomass (using *H. pacifica*, a common marine fouling organism) was reduced by 81% with the 10 wt% Ag^+ sample (compared to zeolite alone). The biofilm inhibition was correlated with the Ag loading of the zeolite. The Ag zeolite also inhibited the growth of other marine microalgae *D. tertiolecta* and *Isochrysis* sp. The amount of silver in the zeolite was very high considering that ZSM-5 is a siliceous zeolite.

Sanchez et al. ion-exchanged Ag^+ into high Si/Al ZSM-5, and examined their antimicrobial activity towards *E. coli* and *P. aeruginosa* and antifungal activity towards *C. albicans* [136]. Both inhibition halo test and bacterial growth curves showed that the silver-ZSM-5 exhibited antibacterial and antifungal activity. Growth curves for the bacteria exhibited a 50% decrease in growth as measured by decrease in the optical density (400 min). The antifungal property was not as pronounced, with a decrease of 15% in growth after 400 min.

4.2.2.4. Zeolite beta. The structure of zeolite beta is shown in Fig. 15.

Saint-Cricq et al. examined three zeolites, beta (3D pore structure), MTW (1D pores) and zeolite A (3D pores, commercial Zeomic) [137]. For zeolite beta and MTW, zeolite samples were prepared with and without structure-directing agent (SDA). Ag^+ was incorporated by ion-exchange. The samples with the structure-directing agent needed to be calcined and incorporated lower levels of Ag^+ upon ion-exchange. There were several unexpected observations. First, the MTW prepared with structure-directing agent (0.5 wt% Ag) exhibited no antibacterial activity, whereas MTW prepared without structure-directing agent (1.3 wt% Ag) completely killed all bacteria (10^8 CFU/ml) within 8 h (2 mg/ml of zeolite used). Zeolite beta prepared with structure directing agent (0.5 wt% Ag) killed all bacteria within 8 h, whereas zeolite beta without the structure directing agent (0.7 wt% Ag) was far more active, with complete bacterial death for 10^8 CFU/ml within one hour. Zeomic with 2 wt% Ag also killed all bacteria (10^8 CFU/ml) within an hour. Fig. 16 compares the antimicrobial activity of beta with Zeomic. The poor antibacterial activity of MTW was explained due to the presence of extraframework Al blocking the one-dimensional pore, and stopping the release of Ag^+ . This hypothesis was not verified by Ag^+ release into the media. However, it was shown that Zeomic releases Ag^+ faster than zeolite

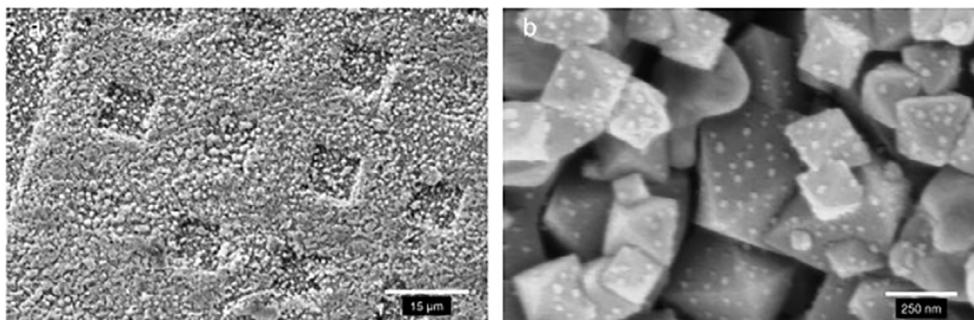


Fig. 17. SEM micrographs of (a) the zeolite film after growth of silver particles and (b) a magnified image of the surface, showing the AgNP (adapted from Ref. [139]).

beta, and was considered the reason for the enhanced activity of Zeomic at the 30 min mark (Fig. 16). What is puzzling is the significant difference between the two forms of zeolites beta with comparable silver loadings (0.5 and 0.7 wt%). The comparison of the release of Ag^+ from the two samples would have been instructive. One possibility could be differences in particle size of the zeolite prepared by the two methods, which can alter the cell-zeolite interaction. The morphological data was not provided. The nonlinearity of activity over time for Zeomic and beta (also observed previously with Zeomic) could be due to the kinetics of ion-exchange.

Tosheva et al. examined both small (18–200 nm) and large (1.2–2.2 μm) crystals of zeolite X, as well as zeolite beta, small (200–300 nm) and large (400–500 nm) [138]. The Ag^+ loading by ion-exchange in zeolite X was ~10.7 wt%, and in beta ~2.3 wt%. The larger crystals tended to release more Ag^+ into solution e.g. at 50 μg/ml zeolite X, 0.02 and 0.11 ppm Ag were found after a 7 min exposure for small and large crystals, respectively. Zeolite beta at 0.05 mg/ml released 1.10 ppm (small) and 2.52 ppm (large) Ag^+ within 7 min. Antimicrobial tests were carried out with *E. coli* (ATCC 8734) and a yeast *C. albicans* (NCYC 1363). With a sample of 500 μg/ml, small zeolite X showed complete killing (with 5×10^5 CFU/ml) within 5 min, whereas for the larger crystals it took 3 min. With comparable amounts of zeolite beta, the trends were similar, but complete killing took place in a minute. This study also looked at cytotoxicity towards peripheral blood mononuclear cells. Apoptosis measured with flow cytometry, indicated that silver zeolites with a dosage of 50 μg/ml or below did not cause toxicity.

For high Si/Al zeolites, the following observations can be made.

- Direct contact of microorganism with silver zeolite promotes killing efficiency as compared to the broth in which the zeolite is suspended.
- AgNP-zeolite released Ag^+ slower than Ag^+ of comparable Ag loading, but the AgNP-zeolite was more active.
- Highly siliceous zeolites store lower amounts of silver.
- Formation of biofilm around the zeolite can decrease antimicrobial activity due to decreased release of silver.
- Antibacterial activity of silver exceeds antifungal activity.
- For the same framework, use of a structure-directing agent (SDA) in the synthesis step and its subsequent removal decreases the antimicrobial activity, as compared to the zeolite that was synthesized without the SDA (comparable Ag^+ content).
- More Ag^+ is released from larger crystals (minutes time frame) as compared to smaller zeolite crystals with comparable Ag^+ content.
- Siliceous zeolites released Ag^+ faster than more aluminous zeolites.

4.2.3. Zeolite membranes

Zeolite membranes are an effective support for separations and purification, and two studies have been reported on AgNP generated on zeolite membranes.

Sabbani et al. generated Ag-NP (~50 nm) on patterned zeolite Y membranes (micron size features formed by soft lithography) and antibacterial activity towards XL-1 blue *E. coli* was studied [139]. Within 120 min, all bacteria (5×10^4 CFU/ml) were killed upon exposure to the AgNP-zeolite membrane. The rationale for creating the patterned zeolite structure was to increase the contact points with the bacteria, as is evident from Fig. 17, a micrograph of the patterned zeolite.

Nagy et al. investigated the antibacterial activity of AgNP embedded within a zeolite membrane towards XL-1 blue *E. coli* and *S. aureus* (MRSA) [10]. Bacterial growth was completely inhibited over a 3 h incubation period for *E. coli* (10^6 CFU/ml). The supernatant from the membrane in broth also exhibited comparable activity, indicating that Ag^+ release from the AgNP is responsible for the antibacterial activity. Concentrations of ~20 ppm Ag^+ were noted in the broth after 48 h. The AgNP-zeolite membrane was bacteriostatic towards *S. aureus*. This study also showed upregulation of several antioxidant genes as well as genes coding for metal transport, metal reduction and ATPase pumps upon exposure of *E. coli* to AgNP-membrane. The antibacterial mechanism of AgNP was related to minimization of antioxidant capacity.

Summarizing, we note that

- Ag-exchanged self-standing zeolite membranes on supports are effective antimicrobials.
- Ag^+ released from zeolite membranes showed upregulation of several antioxidant genes.

5. Zeolite-silver supported on matrices and their antimicrobial activity

5.1. Zeolite/polymer composites

Incorporation of silver zeolites into polymers is an active area of research, motivated by numerous possible applications, considering the ubiquity of polymers.

5.1.1. Synthetic polymers

5.1.1.1. Polyvinylidene fluoride. Inoue et al. investigated antibacterial activity towards *E. coli* (NIHJCC2) of silver ion exchanged zeolite X incorporated into polyvinylidene fluoride (PVDF) films [140]. There was no activity in N_2 -saturated media, while under aerobic conditions, bacterial count of 10^7 CFU/ml was reduced to ~1 CFU/ml within 5 min. The Ag^+ released from the zeolite/PVDF composites was $<10^{-7}$ M, and was not considered relevant for antimicrobial activity. Bactericidal activity was proposed to be arising from

superoxide, hydrogen peroxide, hydroxyl radicals and singlet oxygen based on results with various ROS scavengers. The exact mechanism by which Ag^+ -zeolite X is activating the dissolved oxygen to form the ROS was not discussed.

Shi et al. examined the antimicrobial effectiveness of a dual layer hollow fiber PVDF ultrafiltration membranes containing Ag^+ -zeolite Y or AgNP-zeolite Y (6.4 wt% silver) in salt water [141]. The silver zeolites were incorporated in the outer part of the hollow fiber in a dry-jet wet-spinning process. Silver ion release from the AgNP membrane was slower than with the Ag^+ membrane, upon exposure to PBS buffer or salt water. In deionized water, the Ag^+ release from the AgNP-membrane was higher than the Ag^+ -membrane. The antibacterial activity of the AgNP-membrane, as measured by killing of *E. coli* was longer term as compared to the Ag^+ -membrane. These silver-loaded PVDF zeolite membranes were resistant to bacterial adhesion.

5.1.1.2. Polyterephthalate. Abo El Ola et al. studied fiber filaments prepared by mixing Ag^+ exchanged zeolite X (1–4 μm) with hydrophobic poly(trimethylene terephthalate) chips (0.5 wt% zeolite) (75,500 g/mol MW) and then sent through a screw extruder (256 °C, 4000 m/min) [142]. The tensile strength and T_g were slightly altered from the native filament. There was a color change during the processing, possibly due to formation of metallic silver. With Ag content of 516 ppm in the polymer, 91% reduction of *E. coli* (10^5 CFU/ml) was noted with 200 mg/ml of fiber in phosphate buffer. No zones of inhibition were noted with the agar assay, indicating lack of release of Ag^+ from the fiber into the agar medium.

5.1.1.3. Polyurethane. Kamisoglu et al. incorporated Ag^+ -exchanged zeolite beta (Si/Al \sim 9.4, 5.53 wt% Ag) and zeolite A (Si/Al \sim 1.2, 10.6 wt% Ag) into a polyurethane polymer [143]. The mechanical properties of the polymer improved upon zeolite incorporation. Both zeolite/polymer samples exhibited antimicrobial effect towards *E. coli* as measured by the disc diffusion method. Qualitatively, the zone of inhibition around Ag^+ zeolite A/polymer pellet was greater.

Kaali et al. incorporated Ag^+ -zeolite A (Zeomic) into polyurethane via injection molding and into silicone rubber (prior to cross linking) [144,145]. The antimicrobial properties of polymer test pieces towards *S. aureus* (MRSA) (ATCC 43300), *P. aeruginosa* (ATCC 27853) and several fungi strains were investigated. In general, increase in the Ag^+ -zeolite content (1–5 wt%) resulted in improved antimicrobial effect. Decrease by a factor of \sim 8 was noted for MRSA (8×10^6 CFU/ml) over a 24 h period for the polyurethane and factor of two for silicone with 5 wt% zeolite. Fungal growth on the polymer specimens also decreased with zeolite

content. Incorporation of the zeolite enhanced the degradation of the polyurethane and silicone towards artificial body fluids.

In another study, Kaali et al. incorporated Ag^+ , Zn^{2+} and Cu^{2+} -exchanged zeolite (single, binary and ternary ions) (Zeomic) into thermoplastic polyether type polyurethanes [145]. The antimicrobial activity towards *S. aureus* (MRSA), *P. aeruginosa* and *C. tropicalis* was tested. Ag^+ containing samples exhibited the strongest inhibition effect, e.g. 10^7 CFU/ml to $<10^5$ CFU/ml for MRSA in 24 h, and Cu^{2+} -zeolite decreased the number of *C. tropicalis*. Combination of ions increased the inhibition effect. Incorporation of zeolite altered the water uptake of the polyurethane due to the hydrophilic nature of the zeolite and zeolite migration to the surface of the polymer was noted. The contact angle of the polymer decreased as a function of time upon exposure to artificial body fluids (24 weeks), possibly due to water adsorption by the zeolite. Increased degradation of the polyurethane was noted by infrared spectroscopy, especially with samples that contained >3 wt% zeolite.

5.1.1.4. Polyamide. Lind et al. incorporated Ag^+ -zeolite A into polyamide film by introducing zeolite nanocrystals (140 nm) during the interfacial polymerization step [146]. The Ag^+ -zeolite powder exhibited significant antimicrobial activity towards *Pseudomonas putida* (10^6 – 10^7 cells/ml) based on a qualitative assessment of fluorescence from live and dead cells. However, upon incorporation of the Ag^+ -zeolite in the polymer, the bactericidal activity disappeared. The interfacial polymerization reaction resulted in darkening of the film due to formation of insoluble silver species. Silver precipitation within the polymer and inability to escape from the polymer was held responsible for the lack of bactericidal activity.

5.1.1.5. Polyethylene. Xu et al. surface modified (chemistry not specified) Ag^+ , Zn^{2+} -zeolite (not specified) followed by incorporation into polyethylene by melt extrusion [147]. Mechanical properties of the polyethylene worsened with increasing zeolite, but <6 wt% zeolite provided acceptable polymer samples. The 6 wt% zeolite/polymer showed a reduction of 99.99% growth of *S. aureus*, *Colibacillus* (starting with 2×10^5 CFU/ml).

Boschetto et al. studied low density polyethylene films containing 1–10 wt% of Ag^+ -zeolite Y (5 wt% Ag) prepared by hot casting and wet casting methods [148]. The melting and crystallization temperature of the polymer was unaltered upon zeolite incorporation. The zeolite powder exhibited a MIC of 0.5 mg zeolite/ml (24 h test) with *E. coli* ATCC 25922. The antimicrobial property of the polymer film prepared by the wet casting method was superior, though based on the inhibition halos, these films were in general, poor antimicrobial materials, possibly due to inability of the Ag^+ from the polymer encapsulated zeolite to be released into the medium.

Cushen et al. incorporated commercially available Ag^+ -zeolites (Aglon) into polyethylene via a screw extruder extrusion process (0.5–2 wt% loading of zeolite) [149]. Migration of Ag^+ from these composites into water and a 3% acetic acid was examined for a period of 10 days at 40 °C. For a 2 wt% zeolite loading, 6.07×10^{-3} and 3.32×10^{-2} mg/l of Ag^+ was found in water and acetic acid, respectively. It was concluded that <0.5 wt% of zeolite needs to be used in contact with non-acidic foods to meet the regulatory level of 0.001 mg/kg of dissolved silver.

5.1.1.6. Polysulfone. Hoek et al. incorporated Ag^+ -exchanged zeolite A (250 nm) and Ag^+ , Cu^{2+} micron sized zeolite A (1.8–6.5 μm , Aglon) into polysulfone ultrafiltration membrane [150]. The zeolite incorporated membranes were more wettable, but with lower mechanical strength as compared to polysulfone membranes. The larger zeolite particles had poor binding with the polymer. Membranes with the Ag^+ -nanozeolite A had lower bacterial adhesion,

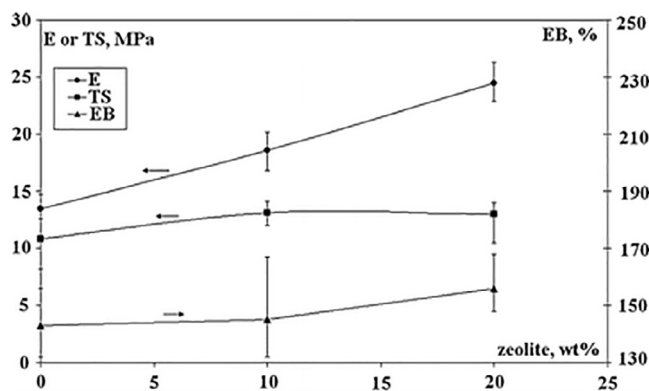


Fig. 18. Mechanical properties of PVC/zeolite composites as a function of silver zeolite content: EB elongation at break, TS tensile stress and E elastic modulus (adapted from Ref. [151]).

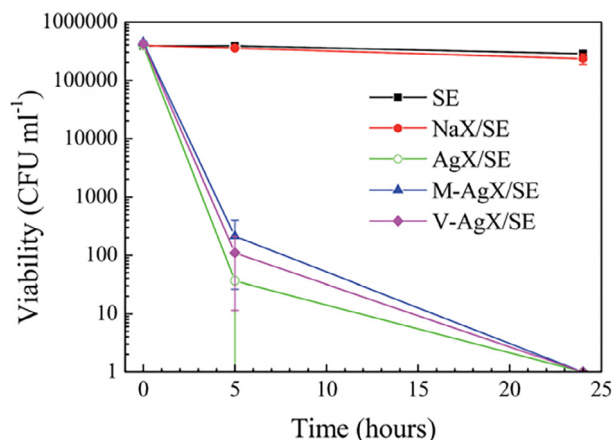


Fig. 19. Viability of *E. coli* in the presence of silicone elastomers (SE) and SE containing zeolites. M-AgX/SE and V-AgX/SE were surface modified zeolite Ag⁺-X with 3(trimethoxysilyl) propylmethacrylate and triethoxy vinylsilane, respectively (adapted from Ref. [154]).

possibly due to lower contact angles and better bactericidal properties as compared to the membrane with metallic NP.

5.1.1.7. Polyvinylchloride. Zampino et al. incorporated commercial sample of Ag⁺-zeolite (Aglon) into PVC by melt mixing [151]. With 2–20 wt% zeolite incorporation, the elongation at break (EB), and tensile strength (TS) of PVC were mostly unchanged, whereas the elastic modulus increased as shown in Fig. 18. Stiffening of the composite with increasing zeolite was noted, though processing ability was unchanged. The Ag⁺-zeolite/PVC (20 wt% Ag) inhibited growth of *E. coli* (5×10^3 CFU/ml) up to 7 days, whereas it was lower for *S. epidermis* (no growth for 24 h). A 7 log₁₀ reduction was noted in sterile urine for *E. coli* (10^8 CFU/ml) within 24 h and activity was maintained for 20 days. With *S. epidermis*, activity was maintained for 5 days, consistent with the thicker cell wall of the Gram-positive bacteria. The amount of silver released into urine varied with time with 0.365 ppm in the first 24 h (38% of total amount eventually released), and decreased to 0.07 ppm for days 2–5 and 0.02 ppm from days 6–20.

5.1.1.8. Polyvinylalcohol. Kim et al. incorporated zeolite nanoparticles (50 ± 10 nm) with 5–10 nm Ag particles (commercial sample from Miji Tech Co, Korea) into polyvinylalcohol (PVA) hydrogels [152]. The polymerization reaction was initiated with UV radiation. The hydrogel hardness decreased with increasing amounts of Ag-zeolite, and had the consistency of a soft elastomer at 5 wt% zeolite. Reduction of *S. aureus* and *Klebsiella pneumonia* by 99.9% within 18 h was noted with the PVA-zeolite composite with a zeolite loading of 3 wt%.

Wu et al. modified the surface of Ag⁺-zeolite X (150 nm) with 3-aminopropylmethyl diethoxysilane and coated the modified zeolites on nanofiltration membrane using either polyvinylalcohol (PVA) or polydopamine (PDA) [153]. The membranes were reduced with NaBH₄ to generate AgNP. Zeolites were clearly observable by SEM on the membrane surfaces. Two PVA coatings with 22 and 13 wt% zeolite coatings, which corresponds to 37.5 and 18.6 mg/m² of silver loading, respectively were prepared. The coatings with the zeolite led to significant decreases in water permeability through the membrane, being more significant with PVA. Also, two PDA coatings with 20.5 and 9.6 mg/m² of silver and zeolite surface coverage of 15% were prepared. All samples showed significant antimicrobial activity towards *P. aeruginosa* (ATCC 700829), with higher loading Ag samples showing more activity e.g. the higher loading PVA sample completely inactivated the bacteria in

the culture suspension for 5 days (starting concentration 1×10^8 CFU/ml) with repeated 24 h exposures. Cell attachment to the membrane surface was also reduced with the zeolite-coated samples, even after 9 days of repeated incubation, well after the inhibitory influence in the suspension (5 days). The Ag⁺ release into NaCl solution from the AgNP sample was lower than the Ag⁺ exchanged sample (e.g. with the high loaded PVA, 45.71% versus 32.2% after 7 days for Ag⁺ and AgNP, respectively). All samples reached steady state of Ag⁺ release within 4–5 days, with 31–54% of Ag still retained in the membrane. Though the higher loading Ag samples exhibited better antimicrobial activity, the activity did not correlate with the cumulative release of Ag, indicating that measured bulk concentration may be lower than at the membrane surface.

5.1.1.9. Silicone elastomers. Belkhair et al. incorporated organosilane surface-derivatized Ag⁺-exchanged zeolite X (Ag 8.8–14.1 wt %) into silicone elastomers [154]. The zeolite surface functionalization led to uniform dispersion and good mechanical properties of the polymer. The antimicrobial properties of these polymers were tested with *E. coli* (ATCC 8739) (4×10^6 CFU/ml) and *Staphylococcus epidermis* (NTCC 11046) (2×10^5 CFU/ml), and yeast *C. albicans* (NCYC 1363) (2×10^4 CFU/ml). With 24 h exposure, *E. coli* decreased by 5 log₁₀ and *S. epidermis* by 4 log₁₀ counts. *C. albicans* was not influenced by the AgX-polymer. Silver dissolution from the polymer was of the order of 0.005 ppm, and no trend was observed between dissolved Ag and antimicrobial activity. With *E. coli*, the surface modified and unmodified Ag-X exhibited similar activity after 5 h incubation, as shown in Fig. 19. For *S. epidermis*, the derivatized sample was not as effective (cell counts was higher by two orders of magnitude). It is possible that surface derivatization slowed the ion-exchange process. This study also used a neutralizing agent (thiosulfate + thioglycollate) to stop further activity of Ag⁺ prior to bacterial counts.

5.1.1.10. Polyetherketone. Hamciuc et al. silylated zeolite L (~200 nm) with 3-aminopropyl(diethoxy)methylsilane, ion exchanged the zeolite with Ag⁺, and incorporated into aromatic poly(etheretherketone) (PEEK), at zeolite loading of 2, 7 and 12 wt % [155]. The antimicrobial activity towards *S. aureus* (25923), *S. aureus* MRSA (TCC43300) and *E. coli* (ATCC 25922) was noted by the agar diffusion method, and best antimicrobial results were obtained with the 12 wt% Ag-zeolite sample (24 h). Cell viability with rabbit fibroblasts, as measured by the MTT assay was 82.3% of control zeolite for the 12 wt% Ag-zeolite sample (24 h exposure).

5.1.2. Biopolymers

5.1.2.1. Polylactic acid. Films of polylactic acid and with commercial (Zeomic) Ag⁺-zeolite A were prepared by solution casting and melt method with a zeolite loading of 5 wt% by Fernandez et al. [156]. These films are mimics for food packaging, and the release of Ag⁺ in simulated food solvents was examined. After 24 h contact, 0.043 ppm Ag⁺ in distilled water, 0.35 ppm in TSB broth, 0.029 ppm in 95% ethanol, and 0.71 ppm in acetic acid was released from the solution casted polymers. In water, about 1 log₁₀ unit decrease (10^6 CFU/ml) was noted for both *E. coli* (CECT 515) and *S. aureus* (CECT 86) for the solution cast films, whereas the melt films did not exhibit any activity. The amount of Ag⁺ released in water is small since ion-exchange is minimal. The study concludes that food matrices require higher amounts of Ag⁺ (~5 ppm Ag⁺) for activity due to chelating agents and salts that can precipitate the Ag⁺. Regulations, however, limit exposure of foods to 0.05 ppm Ag⁺.

Prapruddivongs et al. prepared polylactic acid (PLA) and wood flour/PLA composites with Ag⁺-zeolite A (Zeomic, 0.5–10.5 wt%) using a twin screw extruder [157]. The tensile strength decreased

with addition of zeolite e.g. with 1.5 wt% zeolite, from 49.48, 48.16, 41.77 MPa to 48.61, 43.8 and 11.01 MPa for PLA, 5% wood/PLA and 10% wood/PLA, respectively. The zeolitic water was proposed to promote PLA hydrolysis. None of the PLA samples with zeolite retarded *S. aureus* growth. Biodegradation was also enhanced in the presence of zeolite, possibly related to the hydrolysis.

5.1.2.2. Natural rubber. Ag⁺-exchanged zeolite (structure not specified) were incorporated into natural rubber (1–5 wt% zeolite) by Jai-eau et al. and vulcanized by 3 different methods [158]. The presence of zeolite did not influence the vulcanization reaction. With 5 wt% zeolite in the rubber, 3 log₁₀ reduction was noted with *E. coli* (ATCC 25922) and 2 log₁₀ reduction with *S. aureus* (ATCC 25923) for a contact time of 240 min.

5.1.2.3. Alginate (polysaccharide). Ag⁺-zeolite (micron size, structure not specified) was incorporated into alginate (polysaccharide extracted from seaweed) films by Shankar et al. [159]. The transparency was reduced by a factor of 4, and the thermal strength decreased by 40%, and the water permeability was unchanged. These films exhibited potent antibacterial activity against *E. coli* and *L. monocytogenes*, with MIC/MBC of 3.125/12.5 µg/ml and 6.25/12.5 µg/ml, respectively. The Ag concentration in the films that exhibited the antimicrobial effect was 7.5 µg/ml, considerably lower than the levels required for toxicity against C2C12 cells at >40 µg/ml, against BRL 3A rat liver cells >24 µg/ml and human fibroblast (IMR-90) and glioblastoma cells (U251) at >25 µg/ml.

Much work has been done on silver zeolite incorporation in polymers, and can be summarized as

- Processing of zeolite into polymers can be carried out at high temperature (256 °C).
- Processing has included screw extrusion, melt mixing, melt extrusion, injection molding, interfacial polymerization, photochemical polymerization.
- Mechanical properties of polymers can improve or degrade depending on the polymer and the processing conditions.
- Incorporation of zeolite into the polymer can enhance water uptake and permeability and also promote degradation.
- Polymer can entrap the silver zeolite, or precipitate the silver stopping release of Ag⁺ and diminishing antimicrobial activity.
- Transparency of the polymer can be reduced by silver zeolite incorporation.
- AgNP-zeolite loaded membranes exhibited longer term antimicrobial effects in high ionic strength solutions as compared to Ag⁺-zeolite loaded membranes.
- Silver zeolite in polymers exhibited cytotoxicity towards eukaryotic cells at concentrations higher than that required for antimicrobial activity.

5.2. Zeolite/textile composites

5.2.1. Cellulose

Lim et al. deposited Ag⁺-zeolite Y dispersions mixed with binders on cellulose fibers [160]. The fibers with the smaller Ag⁺ zeolite particles (~300 nm) exhibited better deodorant properties towards NH₃ than micron-sized particles, though both exhibited comparable antimicrobial activity towards *Staphylococcus* ATCC 6538.

Cellulose mats were generated by an electrospinning process by Rieger et al., and zeolites were introduced in the mats [161]. Three samples were investigated, zeolite A (~6 µm) was grown on top of the cellulose, nanocrystals (~150 nm) and mesoporous zeolite A was incorporated inside the cellulose by electrostatic attraction. Electron micrograph of mesoporous zeolite particles attached to the fiber are shown in Fig. 20. These samples were ion-

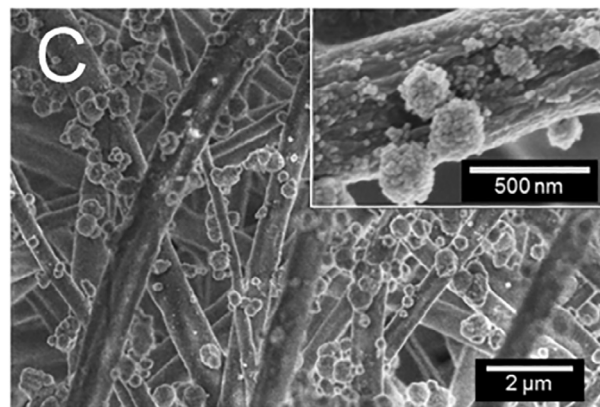


Fig. 20. Micrographs of the mesostructured zeolite A attached to the surface of cellulose nanofiber mats postsynthesis (adapted from Ref. [161]).

exchanged with Ag⁺ and examined for their antimicrobial activity towards *E. coli* (K12 MG1655, 10⁷ cells/ml). Maximum exchange of Ag⁺ was 60–67% of theoretical ion-exchange capacity of zeolite. Viability loss of the bacteria was determined by a fluorescence assay. The 30 min incubation time provided the most instructive results. Ag⁺-zeolite A grown on cellulose killed 70%, nano Ag⁺-zeolite A killed 90% and Ag⁺ mesoporous zeolite A killed 85% of cells. The amount of silver released was 0.3150, 0.0275, 0.007 and 0.007 mg for the zeolite A in suspension (4 mg of zeolite), zeolite A/cellulose (0.3488 mg of zeolite), nanozeolite/cellulose (0.697 mg of zeolite) and mesoporous zeolite/cellulose (0.0687 mg of zeolite), respectively. Clearly, use of the cellulose enhances the biocidal activity, though releasing less Ag⁺ into solution. It was proposed that the microstructure of the cellulose promoted bacteria transport, providing more intimate contact with Ag⁺.

5.2.2. Cotton

Scaccheti examined cotton fabrics with chitosan, Ag⁺ zeolite A (3–5 µm zeolite, Ag-0.3 wt%) and composite of chitosan/Ag-A. A pad-dry-cure process was used for incorporation of zeolite into cellulose [162]. The fabric with chitosan/silver zeolite was effective (100% reduction in 20 h, 10⁴–10⁶ CFU/ml) towards *E. coli*, *S. aureus*, *C. albicans* and *T. rubrum*. A synergistic effect was noted with chitosan/zeolite as compared to fabric with chitosan or zeolite. The amount of Ag⁺ released from the fabrics was of the order of ~70 ppb.

Release of Ag from textiles during washing has been noted, though no such studies exist with silver zeolites embedded in textiles [18,163,164].

The observations on silver zeolite textiles can be summarized as

- Zeolites can be incorporated into cellulose by binders and electrospinning and pad-dry process for cotton.
- Silver with smaller zeolite crystals are more effective antimicrobial agents.
- Chitosan and Ag⁺ combination in cotton had synergistic antimicrobial effect.
- Microstructure of cellulose enhanced bacterial transport, thereby promoting interaction with entrapped zeolites.

5.3. Zeolite/metal coatings

5.3.1. Stainless steel

Galeano et al. coated stainless steel coupons with Ag⁺ (2.5 wt%), Zn²⁺ (14 wt%) exchanged zeolite A (commercial sample Aglon) and

exposed them to vegetative cells of the three *Bacillus* spores, *B. anthracis* Sterne, *B. cereus* strain T and *B. subtilis* strain 168 (10^6 – 10^7 CFU/ml) [165]. There was a 3 \log_{10} inhibition of the vegetative cells (2–24 h) but no effect on the viability of the spores (24–48 h). Autoclaving decreased efficiency of the coated steel.

Cowan et al. coated zeolite (commercial sample AgIon) containing 14% Zn^{2+} and 2.5% Ag^+ on stainless steel with the help of epoxy by a wet and dry (electrical) method and heat treated the sample to form a continuous film [166]. It was proposed that the Zn^{2+} provides a slower release of Ag^+ , though the media/conditions in which these experiments were carried out was not specified. The antimicrobial activity towards *E. coli* ATCC 25922, *P. aeruginosa* 27853 and *S. aureus* ATCC 25923 was investigated. With the zeolite powder alone, the MBC was 3.13 mg/ml (78 μ g Ag/ml , grown in LB) for *E. coli* and 1.56 mg/ml (39 μ g Ag/ml) for *S. aureus* and *P. aeruginosa* (grown in TSB). The ionic strength of the two media is different and so the ion-exchange dynamics of Zn^{2+}/Ag^+ from the zeolite are different. With the zeolite-coated stainless steel, *S. aureus* ($>1 \times 10^6$ CFU) was reduced by 3.6 \log_{10} , and 5 \log_{10} reduction for *E. coli*, both with a 6 h exposure. Both bacteria exhibited >99.9% reduction in 24 h. Repeated tests and washing exhibited decreased efficacy, especially at the 4 h mark, but the 24 h efficacy was still >90% over 11 trials. *P. aeruginosa* exhibited similar sensitivity to the other two bacterial species.

Zeolite A was grown on stainless steel coupons, and ion-exchanged with 0.01 M Ag^+ solution by McDonnell et al. [167]. These coupons were exposed to *E. coli* (JM 109, 1×10^6 cells/ml), and immediately upon contact, the average count decreased by five orders of magnitude, whereas stainless steel and zeolite coated stainless steel had no bactericidal activity. Within 24 h, there were no surviving cells on the Ag^+ -zeolite coupons.

Bedi et al. ion-exchanged Ag^+ into zeolite A-coated stainless steel with 38–40 wt% Ag loading [168]. These materials were very effective in killing bacteria, *E. coli*, *Listeria innocua*, *S. epidermis*, fungus *Aureobasidium pullulans* and marine yeast *Rhodotorula mucilaginosa*. *E. coli* (10^6 – 10^7 CFU/ml) was completely killed upon contact, even after 24 repeats of the test. The Ag^+ was not released from the zeolite upon storage in water, and lost $\sim 0.4\%$ upon each bacterial challenge (buffer used in the bacterial tests contained K^+ , which replaces the Ag^+ in the zeolite), as shown in Fig. 21. For all four bacterial samples, similar bactericidal effect was observed.

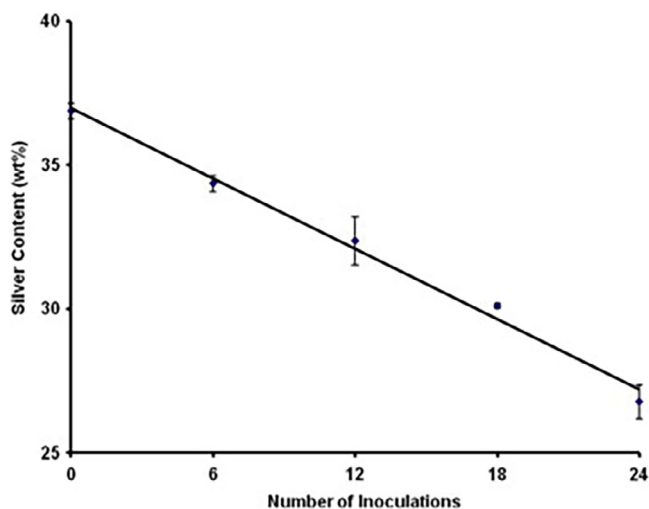


Fig. 21. Percentage Ag (g/g) within the Ag^+ -zeolite A coating on stainless steel after up to 24 repeated *E. coli* challenges (24 h incubation) (adapted from Ref. [168]).

5.3.2. Titanium alloys

Using a hydrothermal method, zeolite A coatings was grown on titanium alloys by Wang et al. [169]. The sample was ion exchanged with Ag^+ , and antibacterial activity towards *S. aureus* (MRSA) evaluated. Ag^+ release into simulated body fluid occurred rapidly within the first 24 h (70% of Ag from 2.3 wt% silver in zeolite) and then slowed down. The Ag^+ -A/alloy completely stopped the growth of *S. aureus* ($\sim 10^6$ cells/ml), and exhibited no cytotoxicity towards L-929 fibroblasts by MTT assay.

Silver zeolite coatings on metals can be summarized as

- Zeolites grown hydrothermally on stainless steel can ion-exchange with Ag^+ to generate an antimicrobial surface.
- Zeolite coatings on steel can be made with epoxy.
- Autoclaving the zeolite-coated stainless steel can decrease activity.
- Repeated tests with silver zeolite on stainless steel maintained antimicrobial activity.

5.4. Dental materials

Padachey et al. incorporated commercial Zeomic (zeolite A) into a glass ionomer cement (0.2 wt% zeolite) to be used as a root canal sealer [170]. This *in vitro* study showed that the inclusion of the zeolite did not alter or inhibit the growth of *Enterococcus faecalis* with the zeolite-based root canal sealer. The zeolite-glass composite in a direct contact test is known to suppress the adherence of *E. faecalis*.

Abe et al. incorporated Ag^+ -zeolite A (Zeomic) into polymethylmethacrylate as a model for tissue conditioner for dental use [171]. Antimicrobial activity in human saliva towards *S. aureus*, MRSA, *C. albicans* was noted but not towards *P. aeruginosa*, possibly because it produced a biofilm on the tissue conditioner.

Dentures made from acrylic resins tend to attract bacteria and can cause infections. Biofilm formation has also been noted on these polymer surfaces. Infections by *C. albicans* yeast is common and causes candidiasis. Casemri et al. incorporated 2.5 wt% Ag^+ -zeolite (commercial Irgaguard B5000) into acrylic resins prepared by microwave and heat polymerization and found antimicrobial activity against *C. albicans* and *S. mutans*, as measured by the agar diffusion method [172]. Both the flexural strength and impact strength of the resin decreased upon incorporation of 2.5–5.0 wt % zeolite.

Odabus et al. added Ag^+ -exchanged zeolite A (0.2–2 wt%) to the dental cement material, mineral trioxide aggregate and antimicrobial activity towards several microorganisms was tested by the agar diffusion method [173]. Presence of the silver zeolite inhibited growth of *E. faecalis*, *S. aureus*, *Prevotella intermedia*, *Actinomyces israelii*, *Porphyromonas gingivalis*, *C. albicans* but had no effect on *P. intermedia* and *A. israelii*. About 0.86 ppm of Ag^+ was released into water in 24 h from the 2 wt% silver zeolite-cement sample. The material properties of the cement in the presence of zeolite was not evaluated.

Soft liners are used by denture wearers and used during other dental procedures as a tissue conditioner. Over time, these liners can be host to bacteria and fungi. To minimize the colonization, Saravan et al. investigated the use of silver zeolite (details not specified) introduced into acrylic soft liners [174]. The viscoelastic properties of the acrylic was not compromised as compared to control sample. The growth of *C. albicans* and a bacteria (not specified) was decreased by 65% for a patient over a period of 28 days.

The effectiveness of Ag^+ -zeolite (structure not specified) as a root canal irrigant was investigated by Ghivari et al. against biofilms made from *C. albicans*, *E. faecalis* and *S. aureus* [175]. Exposures for 1 min showed that the zeolite was not as effective as NaOCl, chlorhexidine and octenidine.

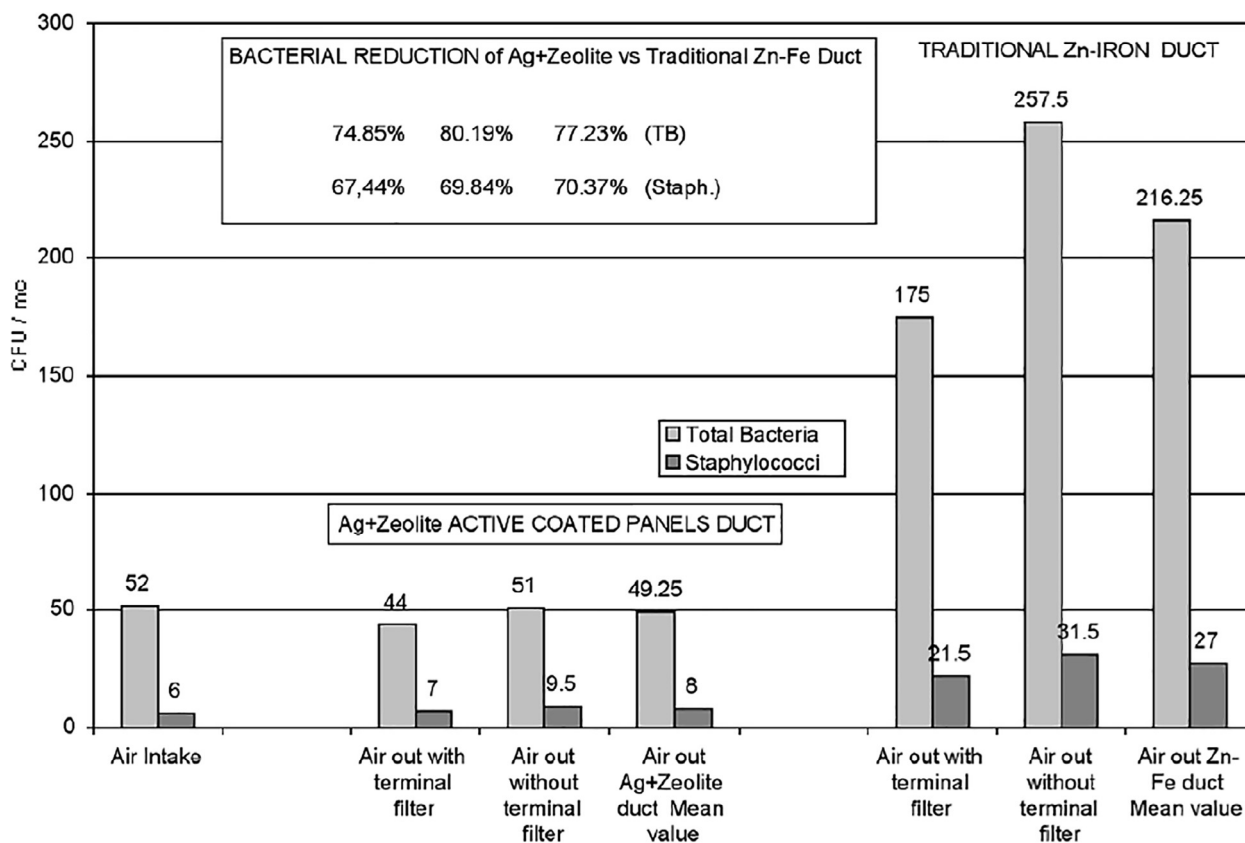


Fig. 22. Total Bacterial Count (cfu/mc) in the air at outlet ducts with Ag⁺-zeolite A coated and uncoated ducts (adapted from Ref. [177]).

The summary of dental materials is

- Zeolites can be incorporated into glass-based cements and polymers for dental applications.
- Acrylic resin strength decreased with zeolite incorporation, whereas viscoelastic properties were not compromised.

5.5. Environmental/consumer materials

5.5.1. Odor prevention

The effectiveness of a Ag-zeolite powder spray (Zeomic dispersed into oil and propellant) towards skin-resident odor causing bacteria was studied by Nakane et al. [176]. The bacterial strains *Micrococcus luteus* (JCM 1464), *Brevibacterium epidermis* (JCM 2593), *Corynebacterium amycolatum* (JCM 7447) and *S. epidermis* (IFO3762) were isolated from human skin. The MIC of Ag-zeolite against these bacteria were 5–50 μg/cm² (starting CFU of 5 × 10⁵/cm² of skin contact area). Powder sprays with >5 wt% zeolite exhibited 3–4 log₁₀ reduction of bacteria in a 6 h period. Clinical studies with human volunteers showed that 10 wt% powder sprays applied to the axilla was an effective antimicrobial. Human patch tests and a 4-week safety test of the powder zeolite spray showed no adverse events.

5.5.2. Ventilation/air conditioning

Rizzetto et al. reported that ventilation and air conditioning system ducts (traditional galvanized iron lined with polyurethane tiles) when coated with Ag⁺-zeolite (commercial Aglon) reduced the bacterial load of the emerging air by 75–80% as compared to the air from a traditional galvanized air duct [177]. Fig. 22 shows the bacterial reduction with the zeolite-coated duct as compared to a traditional zinc-iron duct.

Ag⁺-zeolite was incorporated into aluminum cladding panels and HVAC duct panels (procedure of incorporation or types of zeolite not specified) by Tinteri et al. [178]. The laminates were 80–120 μm thick, and exhibited antibacterial property towards *Legionella pneumophila* (ATCC 33152), *S. aureus* (ATCC 6538), *P. aeruginosa* (ATCC 15422), *E. coli* (ATCC 8739), *C. albicans* (ATCC 10231) and *A. niger* (ATCC 6275), with 5–7 log₁₀ unit decrease in CFU/ml over a 24 h period. Samples of polyurethane covered by silver zeolite aluminum panels placed in a hospital environment exhibited antimicrobial activity after 2½–3 years. In such HVAC applications, only bacteria on the panels can be killed, if the right moisture conditions and ion-exchanging ions are available.

5.5.3. Metal door handles

Potter et al. reported on a study of door handles. 60–70 μm thick coatings containing 2–5 μm silver zeolite particles were applied on door handles in a university campus [179]. Over a 3-year period, the door handles were sampled weekly for bacteria. A statistically significant difference of bacterial populations between the control and silver-coated door handles was observed. However, there were instances when the silver zeolite-coated door handles had higher bacterial count, or the differences with the control handles was minimal. Several reasons were proposed for these observations, including silver zeolite being effective only on a subset of bacteria and insufficient release of silver. It is possible that the silver zeolite crystals embedded deep within the coatings are also not being effective.

5.5.4. Cement/concrete

Haile et al. noted that impregnation of Ag⁺-commercial zeolite (Aglon, with co-cations of Cu²⁺ or Zn²⁺) on the surface of mortar specimens reduced bacterial-induction corrosion, as measured by

leaching of Ca^{2+} and Si^{4+} from the cement [180]. Activity of *thiobacilli* species, responsible for corrosion is reduced in the presence of Ag^+ -zeolite, as noted by the drop in pH.

In another study, Haile et al. measured bacterial induced corrosion of zeolite coated (commercial Aglon) concrete against *Acidithiobacillus thiooxidans* by measuring biomass dry cell weight, sulfate generation and oxygen uptake [181]. Zeolite bonding to the concrete was done with epoxy. Use of the zeolite (5 wt% Ag) reduced planktonic and *A. thiooxidans* biofilm formation.

5.5.5. Paper

FDA has approved the use of micron-sized zeolites at ≤ 5 wt% in food contact surfaces. Lee et al. impregnated commercial Aglon (2.5 wt% zeolite A) on tissue papers and tested for their ability to prevent bacterial growth of *P. putida* [182]. With 4% silver zeolite paper, there were fewer bacterial colonies as compared to controls. Storage of beef, pork and turkey for 3 days on the zeolite paper led to 1.2, 0.9 and 1.0 \log_{10} reduction in *P. putida* growth at 10 °C. At 4 °C, the silver zeolite did not have any effect. It appears that silver zeolites are more effective in broth as compared to real foods, since ion-exchange is facilitated.

Jederzejczyk et al. incorporated Ag^+ -exchanged zeolite Y into paper prepared by pulling vacuum on a mixture of the wet pulp and zeolite, followed by drying of the sheets [183]. The zeolite content in the paper was 44 wt%. Antibacterial activity towards *Serratia marcescens*, *E. coli*, *B. subtilis*, and lower activity towards *B. megaterium* was noted using the LuciPac Pen test (measures the relative content of ATP and AMP). The Ag^+ -zeolite containing paper exhibited higher antimicrobial activity than a paper with AgNP. Several fungi samples were also investigated, and except for *M. alpine*, decreased growth was noted for *Chaetomium globosum*, *Cladosporium cladosporioides* and *A. niger*. The paper also discusses using Na_2EDTA to remove surface bound Ag^+ from the zeolite.

5.5.6. Food-related

Mortero et al. noted that three commercially available cutting boards containing silver zeolites and nanosilver exhibited antimicrobial activity towards *S. aureus* only under humid conditions (35–93% relative humidity) [184]. In the presence of growth medium, no antibacterial activity of the boards were observed. This study concluded that under practical food preparation conditions, the cutting boards were not effective antimicrobial agents.

Griffith et al. grew zeolite films on stainless steel (the XRD of the deposit on the steel was not analyzed, so it is unclear if zeolite growth did occur, though SEM and AFM show a coating) [185]. Upon Ag^+ exchange, the stainless steel coupons inhibited bacterial growth on the surface (*L. innocua*, *E. coli*). This study proposed that zeolite coated stainless steel can be used in food processing.

Ag^+ -zeolite (micron size structure not specified) was incorporated into low density polyethylene (LDPE), fabricated into active layers of multilayer films (LDPE – polyamide-active LDPE) via a blown film extraction process by Soysal et al. [186]. These films were used to store chicken for 0–6 days. The meat was analyzed for total coliform, aerobic mesophilic bacterial, molds and yeasts. Along with silver zeolite, polymer films were also made with chitosan, nisin, potassium sorbate. All films had a protective effect. The performance of the films for total coliform and bacteria was in the order chitosan > nisin > Ag-zeolite > sorbate, and for mold and yeast reduction chitosan > sorbate > nisin > Ag-zeolite (5 °C for 6 days). Fig. 23 shows the data with the aerobic mesophilic bacteria (APC).

Summary for consumer applications of silver zeolites is

- Zeolites can be incorporated into a powder spray.
- Human patch tests of the powder spray showed no adverse events over a 4-week test.

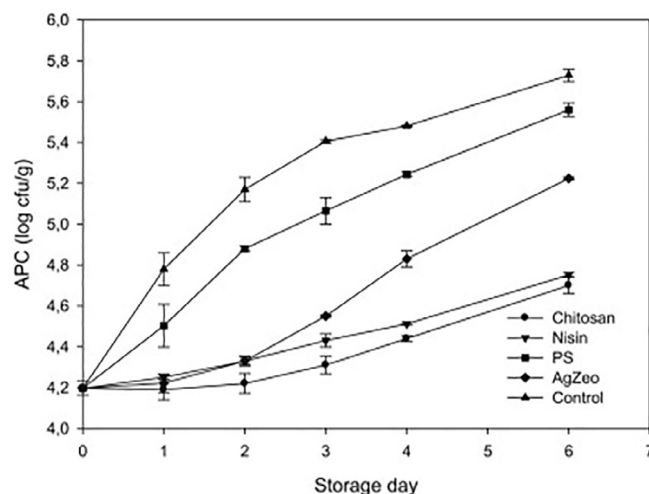


Fig. 23. Effects of antimicrobial packages on aerobic mesophilic bacteria (log cfu/g) of chicken drumsticks stored at 5 °C for 6 days (adapted from Ref. [186]).

- Silver zeolites incorporated into HVAC duct panels exhibited antimicrobial activity over 3 years.
- Bacterial corrosion of concrete is reduced by incorporation of silver zeolites.
- Zeolites can be incorporated into paper by wet pulp method.
- Humid conditions are necessary for zeolite-incorporated cutting boards to exhibit antimicrobial activity.

6. Environmental, toxicity and regulatory issues

It is fair to say that almost all of the regulatory issues are being driven by the increased use of silver colloids. Silver zeolites are not yet treated as a separate entity. It is expected that regulations of silver zeolite will be driven by decisions made with silver colloids. Also, most environmental and toxicity studies focus on silver colloids, and only a few studies exist with silver zeolites. Since it is apparent that silver colloids will drive the regulations on silver zeolites, this section is focused primarily on silver colloids. Even though our discussion on silver colloids is brief, since there are many recent reviews covering this area, we do discuss all the papers dealing with *in vitro* studies of silver zeolites with eukaryotic cells.

6.1. Environmental concerns with silver colloids

There is concern that since the amount of nanosilver is increasing, this will result in release of the silver into the environment [187–189]. Estimates of 4 tons per year 2005 increasing to 563 tons per year of silver nanoparticles in 2008 is reported [7]. The data confirming these estimates are not available. Another model in 2009 suggests that amount of silver is 0.5–2 ng/L in water, and 32–111 ng/L in outflow of sludge (low to high values 15–85%), and that these numbers will increase [190]. There is concern that silver present in mud and sewage can spread to agricultural fields. Silver used in building materials, such as paints can be released into the soil [191]. Silver in soil can be absorbed by plants, and appear in foods consumed by humans and animals [192].

Another environmental concern is the possibility of development of antimicrobial resistance towards silver [193]. Jelenko et al. noted as early as 1969 that *E. coli* isolated from prolonged (47 days) silver-nitrate-treated-burn was silver-resistant [194]. A silver-resistant *salmonella typhimurium* strain was isolated from silver nitrate treated burn in the 1970s [195]. There are reports of a *Bacillus sp.* bacterial to nanosilver [196]. In 2015, a *E. coli* strain

tolerant to nanosilver upon prolonged exposure was reported [197]. Thus, vigilance is required for monitoring for resistance development as more widespread use of nanosilver becomes prevalent.

6.2. Silver zeolite interactions with eukaryotic cells

As far as *in vitro* eukaryotic cell culture studies, there are numerous papers using AgNP or Ag⁺, and has been recently catalogued [21]. Since our focus is on silver zeolites, we refer the reader to the review and references, therein. Cells studies included alveolar epithelial cells, astrocytes, embryonic testicular carcinoma cells, embryonal stem cells, epithelial HeLa cells, fibroblasts, hepatocellular carcinoma cells, gill cells, lung cells, macrophages, mesenchymal stem cells, adrenal medulla cells, ovary cells, prosteoblasts, and T cells. It can be generally stated that for cytotoxic effect, concentration of 1–10 µg/ml for Ag⁺ and 10–100 µg/ml for AgNP is required.

Several studies of cytotoxicity with zeolites (without silver) with a wide variety of cell lines are reported. The most critical observation is that cytotoxicity is dependent on dosage. With silicalite, high dosages in excess of 0.5 mg/ml exhibited toxicity for 30 and 150 nm particles [198,199]. With nanosized zeolite L, ZSM-5, and zeolite A, necrosis was noted with HeLa cells at dosages exceeding 50 µg/ml. Presence of aluminum in the framework was considered relevant for cytotoxicity [200]. Zeolites used in hemostatic dressings were nontoxic at concentrations below 100 µg/ml [201]. In another study with 25–100 nm zeolite Y and A, no toxicity was noted up to doses of 500 µg/ml, and the zeolite particles were less toxic than amorphous silica [202]. Silicalite was found to cause reactive oxygen species generation and DNA fragmentation at 100 µg/ml, though no effect on cellular proliferative capacity was noted [203]. With nanosized EMT and zeolite L, no cytotoxicity towards HeLa cells was noted at concentrations of 400 µg/ml. Disc-shaped zeolite L was internalized by HeLa cells, and exhibited cytotoxicity at concentrations >100 µg/ml, with positively charged particles exhibiting higher toxicity [204,205]. PEG-modified zeolite A had a cytotoxic effect only at dosages of 50 µg/ml after 72 h treatment, with longer chain PEG having a more protective effect [206]. Zeolites are considered Generally Regarded As Safe (GRAS) materials for use in cosmetics [207].

The number of studies with eukaryotic cells and silver zeolites is much smaller and the focus of this section. The cytotoxicity against human skin epithelial cells (WM-115) required >128 µg/ml of Ag⁺-hierarchical zeolite, and for human skin fibroblasts (Detroit 551) and monocytes (U-937) concentrations of 64 µg/ml was required for reduction in viability. These cytotoxic concentrations were significantly higher than the MIC/MBC concentrations [127]. With peripheral blood mononuclear cells, silver zeolites with a dosage of 50 µg/ml or below did not cause toxicity [138]. Cell viability with rabbit fibroblasts, as measured by the MTT assay was 82.3% of control (24 h exposure) [155]. The silver concentration for the antimicrobial effect was 7.5 µg/ml, considerably lower than the levels required for toxicity against C2C12 cells at >40 µg/ml, against BRL 3A rat liver cells >24 µg/ml and human fibroblast (IMR-90) and glioblastoma cells (U251) at >25 µg/ml [159]. The Ag⁺-A/alloy exhibited no cytotoxicity towards L-929 fibroblasts by MTT assay [169].

The potential cytotoxicity of Ag⁺-EMT and AgNP-EMT nanosized zeolites on human glioblastoma, human embryonic kidney cells as well as astrocytes from cerebral cortices of neonatal mice and cultures from mouse embryos were studied [208]. The dosages were 50, 100 and 400 µg/ml of zeolite for periods of 24 and 45 h. Cell viability was measured WST-1 assay, (similar to MTT assay). With the glioblastoma and kidney cells, 50 µg/ml of Ag⁺ EMT killed all the cells, (24 h), whereas with 400 µg/ml of AgNP EMT, a loss of

73.5 ± 20.51% was noted after 24 h relative to control. The kidney cells were more resistant to Ag⁺-EMT (83.64 ± 2.31% decrease relative to central at 50 µg/ml dosage for 24 h). With AgNP EMT at 400 µg/ml, after 24 h, a loss of 62.3 ± 17.96% in cell viability compared to control was noted. For neurons, both Ag⁺ EMT and AgNP EMT exhibited similar toxicity with no viable cells after 24 h at 50 µg/ml. AgNP EMT was more toxic to astrocytes as compared to Ag⁺EMT for comparable dosages (with 50 µg/ml, loss in cell viability of 34.37 ± 23.90% and 97.95 ± 3.31% for Ag⁺ EMT and AgNP EMT, respectively). *E. coli* growth even at 50 µg/ml of Ag⁺EMT was completely stopped, whereas with AgNP EMT, it required 400 µg/ml to stop all growth.

These studies with eukaryotic cells show that by proper control of the type and amount of silver zeolite, it is possible to exhibit antibacterial effect with minimal effect on eukaryotic cell viability.

6.3. Animal studies with silver colloids

There are studies on the adverse effect of silver nanoparticles on daphnia (planktonic crustaceans), Eurasian perch and zebrafish embryos [209–211].

The effect of silver nanoparticles on mice, rats, chickens and rabbits are reported.

Exposure of mice to silver nanoparticles (5 ± 2 nm) by inhalation caused pulmonary inflammation (inhalation doses of AgNP were 3–3 mg m⁻³, 4 h d⁻¹ for 10 days) [212]. Silver nanoparticles (18 nm) were found mainly in lungs and liver of rats, but no evidence of genotoxicity was noted [213]. Other studies with 18 nm silver particles in rats noted reduced lung volume, increased alveolar inflammation and silver accumulation in the bodies of rats [214,215]. Inhalation of AgNP by rats for 28-days did not cause health effects, though 90-day study showed accumulation in the lungs and liver. High doses of AgNP were required to cause any toxic response [216]. Inhalation of ~35 nm silver nanoparticles by rats did not cause any significant changes in the respiratory and circulatory systems, though accumulation of particles in the body was noted [217]. At high concentration, 100–1000 mg/kg AgNP, neurotoxicity was noted in mouse brain [218]. Damage was noted with doses above 300 mg of particles assessed over a period of 28 days [219]. Neurotoxicity and immunotoxicity was noted in mice that inhaled AgNP with dosage of 1.91 × 10⁷ particles/cm³ for 6 h d⁻¹ and 5 d week⁻¹ [220].

Penetration and inflammatory properties of AgNP on porcine skin indicated that the toxic response were arising from the contaminants in the AgNP suspensions [221].

Broiler chickens fed a diet of ~18 nm silver particles (4 ppm) resulted in accumulation of particles in hepatocytes. With increased concentration (12 ppm) of particles, growth of fibrous tissue and necrosis of hepatocytes was noted [222].

With rabbits, 10 and 20 nm silver particles led to skin edema and erythema. Death of liver cells, spleen hyperaemia and cerebral edema was also noted. Nanoparticles were found to cause more adverse effects than large particles [223].

Animal studies have also shown positive effects of silver [12]. With laboratory mice, nanosilver particles effectively controlled platelet clumping and prevented platelet adhesion [224]. Liver damage of mice induced by CCl₄ was cured with AgNP [225]. Silver not only kills pathogens in wounds, but also stimulates tissue and bone regrowth. AgNP is proposed to play a role in decreasing inflammation in chronic inflections and wounds [226]. A mouse model of allergic airway disease noted that AgNP attenuated antigen-induced airway inflammation and hyper-responsiveness [227].

There are a few studies with humans. Decades ago, Rendin et al. noted that colloidal silver oxide given via oral ingestion to 88 peptic ulcer patients for a period of 9 days healed 87 patients [228]. More recently, Munger et al. carried out a 14-day human oral

Table 1
Chronological summary of literature (since 2000).

Reference	Zeolite used	Microorganism used	Conditions	Comments
Kawahara 2000 [110]	Ag ⁺ zeolite A (Zeomic), 2.5 wt% Ag	<i>P. gingivalis</i> , <i>P. intermedia</i> , <i>A. actinomycetemcomitans</i> , <i>S. mutans</i> (other dental bacteria also studied)	1 × 10 ⁷ cells/ml 24–72 h incubation	<ul style="list-style-type: none"> – 14 different bacterial strains (oral) were studied under anaerobic conditions – MIC of Ag⁺-A varied from 256 to 2048 μg/ml – Gram-negative species more susceptible – 75% of Ag⁺ was released into the broth within 30 min and unaltered at longer times
Padachey 2000 [170]	Zeomic (0.2 wt%) – glass composite	<i>E. faecalis</i>	10 ⁶ –10 ⁷ CFU/ml	<ul style="list-style-type: none"> – Zeolite-glass root canal sealer did not stop bacteria ingress
Inoue 2002 [140]	Ag ⁺ zeolite X in polyvinylidene fluoride films PVF	<i>E. coli</i>	10 ⁷ CFU/ml 0.1 g PVF	<ul style="list-style-type: none"> – No activity in N₂ saturated media – Over 5 min, complete cell death – OH radical, H₂O₂, O₂ relevant to bactericidal activity – Ag⁺ <10⁻⁷ M – ROS proposed as antibacterial species
Cowan 2003 [166]	Zn ²⁺ /Ag ⁺ zeolite on stainless steel via epoxy binding	<i>E. coli</i> , <i>S. aureus</i> , <i>P. aeruginosa</i>	>1 × 10 ⁶ CFU/ml	<ul style="list-style-type: none"> – MBC to <i>E. coli</i> 3.13 mg/ml (78 μg Ag/ml), 1.56 mg/ml (39 μg/ml) to <i>S. aureus</i> – Zeolite on stainless steel exhibited >99.9% efficacy in 24 h – Antimicrobial efficacy maintained over repeated washing steps
Galeano 2003 [165]	Stainless steel coated with commercial Agion zeolite A	Vegetative cells and spores of <i>B. anthracis</i> Sterne, <i>B. cereus</i> , <i>B. subtilis</i> 168	10 ⁶ –10 ⁷ CEU/ml	<ul style="list-style-type: none"> – coating produced 3 log₁₀ decrease of vegetative cells – no effect on spores
Matsumura 2003 [111]	Ag ⁺ zeolite A (Zeomic), 2.5 wt% Ag	<i>E. coli</i>	2 × 10 ⁷ CFU/ml zeolite (concentration units inconsistent)	<ul style="list-style-type: none"> – Aerobic conditions promoted antimicrobial activity – Close proximity of bacteria and zeolite necessary for activity
Abe 2004 [171]	Zeomic in PMMA as a tissue conditioner for dental use	<i>S. aureus</i> , MRSA, <i>P. aeruginosa</i> , <i>C. albicans</i>	10 ⁶ –10 ⁷ CFU	<ul style="list-style-type: none"> – Antibacterial activity towards <i>P. aeruginosa</i> not observed – Other microorganisms activated noted – <i>P. aeruginosa</i> formed biofilm
Abo El Ola 2004 [142]	Ag ⁺ -zeolite X in poly(trimethylene terephthalate films) 0.5 wt% zeolite 1–4 μm	<i>E. coli</i>	10 ⁵ CFU/ml Agar method	<ul style="list-style-type: none"> – Zeolite incorporation during spinning at 256 °C – Ag⁺ reduction to Ag⁰ during processing – Antimicrobial activity in buffer
Top 2004 [106]	Ag ⁺ -clinoptilolite (natural zeolite)	<i>P. aeruginosa</i> , <i>E. coli</i>	Agar disk diffusion method	<ul style="list-style-type: none"> – Ag⁺ exhibits selectivity over Na⁺ for ion-exchange into clinoptilolite – Ag⁺-zeolite more antibacterial than Zn²⁺ or Cu²⁺-zeolite
McDonnell 2005 [167]	Ag ⁺ zeolite A grown on stainless steel	<i>E. coli</i>	>1 × 10 ⁶ CFU/stainless steel	<ul style="list-style-type: none"> – Zeolite coatings had excellent adhesion to stainless steel – Bactericidal action immediately upon contact with Ag⁺-zeolite/stainless steel coupon (5.5 log₁₀ decrease) – No surviving colonies after 24 h
Lim 2006 [160]	Ag ⁺ -Y zeolite on cellulose fibers	<i>Staphylococcus</i> ATCC 6538	Deodorization towards NH ₃	<ul style="list-style-type: none"> – Smaller zeolite particles had better deodorization properties
Nakane 2006 [176]	Zeomic dispersed in oil and propellant as an odor spray	Several bacterial strains isolated from skin	10 ⁵ –10 ⁶ CFU/ml 0–40 wt% zeolite	<ul style="list-style-type: none"> – MIC of spray 5–50 μg/cm² – Human patch test show no adverse effect
Kwyake-Awuah 2007 [118]	Ag ⁺ -zeolite X, 5.8 wt% Ag, 2–9 μm zeolite	<i>E. coli</i> , <i>P. aeruginosa</i> , <i>S. aureus</i>	5 × 10 ⁵ CFU/ml	<ul style="list-style-type: none"> – 150 μg/ml of Ag⁺-X killed all <i>E. coli</i> within 45 min and <i>S. aureus</i> and <i>P. aeruginosa</i> within 60 min – Dissolved Ag⁺ <10 ppm (45 min, 97% retained in zeolite) – Same sample repeatable activity (measured 3 times)
Kamisoglu 2008 [143]	Ag ⁺ -zeolite beta (Si/Al = 9.4, 5.53 wt% Ag), Ag ⁺ -zeolite A (Si/Al = 1.2, 10.6 wt% Ag) incorporated into polyurethane	<i>E. coli</i>	Disc diffusion method	<ul style="list-style-type: none"> – Both samples exhibited antibacterial activity – Mechanical properties improved with zeolite incorporation
Inoue 2008 [119]	Ag ⁺ -faujasite	<i>E. coli</i>	10 ⁷ CFU/ml	<ul style="list-style-type: none"> – Light irradiation in the presence of Ag⁺-zeolite exhibit 6 log₁₀ decrease in 5 min
Casemiro 2008 [172]	Commercial Ag ⁺ -zeolite in acrylic resin for dentures (2.5–5 wt% zeolite)	<i>C. albicans</i> , <i>S. mutans</i>	Agar diffusion method	<ul style="list-style-type: none"> – Antimicrobial activity increased with zeolite loading – Flexural and impact strength decreased with zeolite incorporation
Haile 2008 [180]	Agion with Cu ²⁺ , Zn ²⁺ on mortar specimens	<i>A. thiooxidans</i>	Ca ²⁺ , Si ⁴⁺ leaching pH monitoring	<ul style="list-style-type: none"> – Cumulative leaching of Ca²⁺, Si⁴⁺ reduced in zeolite coated concrete (28 days) – pH profile indicated antimicrobial activity
Rizzetto 2008 [177]	Commercial Agion coated on HVAC ducts	<i>S. aureus</i> , <i>L. pneumophila</i> , <i>P. aeruginosa</i> , <i>C. albicans</i> , <i>A. niger</i> , <i>E. coli</i>	5 month study Bacterial count in air	<ul style="list-style-type: none"> – 75% reduction in bacterial/mold load with Ag-duct

(continued on next page)

Table 1 (continued)

Reference	Zeolite used	Microorganism used	Conditions	Comments
Zhang 2009 [112]	Ag ⁺ -zeolite A prepared by ion-exchange with microwave	<i>E. coli</i> , <i>B. subtilis</i> , <i>S. aureus</i>	10 ⁶ cells/ml	– MIC of microwave Ag ⁺ -A was 50 µg/ml for all three bacteria as compared to 100 µg/ml for conventional ion-exchange
Lind 2009 [146]	Ag ⁺ -nanozeolite A (140 nm) incorporated in polyamide film	<i>P. putida</i>	10 ⁶ –10 ⁷ cells/ml	– Ag ⁺ -zeolite powders exhibited activity (measured by fluorescence) – Ag ⁺ -zeolite/polymer showed no bactericidal activity, due to silver species precipitation during polymerization
Lv 2009 [131]	Ag ⁺ ETS-10 (6.4–17.8 wt%) AgNP ETS-10 (5.3–16.2 wt%) (NaBH ₄ reducing agent)	<i>E. coli</i>	10 ⁷ CFU/ml 500 µg zeolite/ml	– AgNP ETS-10 higher bactericidal activity over Ag ⁺ ETS-10 – Ag ⁺ release higher with Ag ⁺ ETS-10 over AgNP-10 (1 h) – Decrease of 4 log ₁₀ units with AgNP ETS-10 (1 h) – Decrease of 2 log ₁₀ units with Ag ⁺ ETS-10 (1 h)
Haile 2010 [181]	Agion bound to concrete by epoxy	<i>A. thoxidans</i>	Biomass weight Biological SO ₄ ²⁻ production Ca ²⁺ , Si ⁴⁺ leaching	– Zeolite coating improves bacterial induced corrosion – Zeolite inhibitory to biofilm formation – Leaching reduced with zeolite coating
Sabbani 2010 [139]	AgNP-lithographically patterned zeolite Y membrane (N ₂ H ₄ reducing agent)	<i>E. coli</i>	5 × 10 ⁴ CFU/ml	Within 120 min, all cells killed upon exposure to Ag ⁺ -Y membrane
Fernandez 2010 [156]	Ag ⁺ -zeolite A incorporated in polylactic acid	<i>E. coli</i> , <i>S. aureus</i>	10 ⁶ CFU/ml	– 1 log ₁₀ decrease in distilled water – Ag ⁺ release in distilled water ~0.043 ppm
Kaali 2010 [144]	Zeomic in polyurethane and silicon rubber (1–5 wt% zeolite)	MRSA, <i>P. aeruginosa</i> , Several fungi	8 × 10 ⁶ CFU/ml	– Ag ⁺ -zeolite in both polymers exhibited strong antibacterial and antifungal effect
Xu 2010 [147]	Ag ⁺ , Zn ²⁺ zeolite in polyethylene via melt extrusion	<i>S. aureus</i> , <i>Colibacillus</i>	2 × 10 ⁵ CFU/ml	– 6 wt% zeolite/polymer exhibited 99.99% reduction of both microorganisms
Hoek 2011 [150]	Ag ⁺ -zeolite in polysulfone ultrafiltration membranes (250 nm, 1.8–6.5 µm zeolites)	<i>P. putida</i>		– Ag ⁺ nanozeolite/polysulfone membrane exhibited low bacterial adhesion and good protein fouling – Micron zeolite/polymer had poor particle-polymer binding
Kaali 2011 [145]	Zeomic (Ag ⁺ , Zn ²⁺ , Cu ²⁺) in polyurethane	MRSA, <i>P. aeruginosa</i> , <i>C. tropicalis</i>	10 ⁷ CFU/ml 24 h	– Ag ⁺ -zeolite most antimicrobial – degradation of polyurethane in artificial body fluid
Lalueza 2011 [133]	Ag ⁺ ZSM-5 (0.16–0.23 wt% Ag)	<i>S. aureus</i>	– 10 ⁹ CFU/ml, 30 mg/ml (0.23 wt% zeolite)	– 4 log ₁₀ unit decrease after 24 h – 4 h Ag ⁺ release (25,000 ppm) correlates with higher bacterial death – 24 h-bacterial film formation and entrapment of Ag ⁺ – No correlation between Ag ⁺ release and bacterial activity at long times
Lee 2011 [182]	Agion in tissue paper	<i>P. putida</i> on raw beef, pork, turkey	Bacterial growth inhibition 10 ³ CFU/ml	– Lower visible signs of colonies on 4% Ag-zeolite paper – Paper reduced spoilage bacteria on raw meals
Nagy 2011 [10]	AgNP-zeolite Y membrane	<i>E. coli</i> <i>S. aureus</i> (MRSA)	10 ⁶ CFU/ml	– Ag ⁺ released from the membrane was considered the active species – <i>E. coli</i> decreased by 6 log ₁₀ in 180 min – AgNP-zeolite membrane bacteriostatic towards <i>S. aureus</i> – Gene expression studies suggest exhaustion of antioxidant capacity of bacteria with Ag ⁺
Odabas 2011 [173]	Ag ⁺ -zeolite A (0.2–2 wt%) in mineral trioxide aggregate, a dental cement.	<i>S. Aureus</i> , <i>E. faecalis</i> , <i>E. coli</i> , <i>P. aeruginosa</i> , <i>C. albicans</i> , <i>P. gingivalis</i> , <i>A. israeli</i> , <i>P. intermedia</i>	Agar Diffusion method	– No antimicrobial activity towards <i>P. intermedia</i> <i>A. israeli</i> – Activity towards other listed microorganisms – 0.86 ppm of Ag ⁺ released into H ₂ O from 2 wt% sample (24 h)
Wang 2011 [169]	Ag ⁺ -zeolite A on titanium alloys 2.3 wt% Ag	<i>S. aureus</i> (MRSA)	10 ⁶ cells/ml	– Ag ⁺ -A/alloy stopped growth of <i>S. aureus</i> – Ag ⁺ release reached 20% of total in 1 day – Ag ⁺ -A/alloy exhibited no cytotoxicity towards fibroblasts
Shameli 2011 [120]	AgNP/zeolite Y (AgNP 2–3 nm) (NaBH ₄ reductant)	<i>E. coli</i> , <i>S. dysenteriae</i> , <i>S. aureus</i> , <i>S. aureus</i> (MRSA)	Disc diffusion method	– All AgNP-Y exhibited antimicrobial activity towards all 4 bacteria
Zampino 2011 [151]	2–3 µm AgION commercial Ag ⁺ -zeolite (Ag –10.4 wt%) incorporated into PVC by melt mixing (2–20 wt% zeolite)	<i>E. coli</i> , <i>S. epidermis</i>	10 ⁶ –10 ⁸ CFU/ml	– 20 wt% Ag ⁺ zeolite in PVC 4–6 log ₁₀ decrease in 24 h – <i>E. coli</i> growth inhibited for 20 days – <i>S. epidermis</i> inhibited for 5 days

Table 1 (continued)

Reference	Zeolite used	Microorganism used	Conditions	Comments
Saint-Cricq 2012 [137]	Ag ⁺ Zeomic (commercial) Ag ⁺ -Beta Ag ⁺ -MTW	<i>E. coli</i>	10 ⁸ CFU/ml 2 mg zeolite/ml	<ul style="list-style-type: none"> - Ag⁺ release primarily occurs in the first 24 h (for 20 wt% zeolite in PVC, 0.365 ppm in 24 h, 0.07 ppm over 2–5 days, 0.2 ppm over 6–20 days) - Zeolite A, beta significantly more active than MTW - Preparation of the same framework (Beta) with and without structure directing agent (SDA) has profound differences in activity - 8 log₁₀ decrease for Zeomic and beta (w/o SDA) in 1 h
Bedi 2012 [168]	Ag ⁺ -zeolite A/stainless steel (38–40% Ag)	<i>E. coli</i> , <i>L. innocua</i> , <i>S. epidermidis</i> , <i>P. putida</i> , <i>A. pullulans</i> , <i>R. mucilaginosa</i>	10 ⁶ –10 ⁷ CFU/ml	<ul style="list-style-type: none"> - Cells killed on contact - Ag⁺ released only in presence of buffer (0.4 wt% Ag release over 24 h) - 24 repeated exposures towards <i>E. coli</i> exhibited activity
Boschetto 2012 [148]	Ag ⁺ -zeolite Y in polyethylene (1–10 wt% zeolite, 5 wt% Ag)	<i>E. coli</i>	Optical density Agar diffusion	<ul style="list-style-type: none"> - 5% Ag zeolite MIC 0.5 Mg/ml - Film thermal properties unchanged with zeolite incorporation - Antimicrobial activity of Ag⁺-zeolite/polymer poor
Laluzea 2012 [134]	Peracetic acid (PAA) (8–9%) in Ag ⁺	<i>S. aureus</i> 9213	10 ⁹ CFU/ml, 30 mg zeolite/ml	<ul style="list-style-type: none"> - PAA-ZSM5 2 log₁₀ reduction in 24 h - Ag⁺-ZSM5 6 log₁₀ reduction (24 h) - AgNP-ZSM5 no activity - PAA-AgNP ZSM5 7 log₁₀ reduction (24 h) - PAA-Ag⁺-ZSM5 9 log₁₀ reduction (24 h) - PAA proposed to disrupt biofilm
Krishnani 2012 [113]	Ag ⁺ -zeolite A (2–3 μm, 39.4 wt% Ag)	<i>E. coli</i> , <i>V. harveyi</i> , <i>V. cholera</i> , <i>V. parahaemolyticus</i>	10 ⁹ CFU/ml, 5–60 μg/ml of zeolite	<ul style="list-style-type: none"> - MIC for <i>E. coli</i>, <i>V. harveyi</i>, <i>V. cholerae</i> and <i>V. parahaemolyticus</i> were 40, 40, 50 and 60 μg/ml respectively (48 h duration) - NH₃ had a synergistic effect with Ag⁺-zeolite
Ferreira 2016 [125]	Ag ⁺ -zeolite X (0.5–3.3 μm) Ag ⁺ -zeolite Y (0.5–1.1 μm) (9.8 wt% Ag)	Bacteria: <i>E. coli</i> , <i>B. subtilis</i> Yeast: <i>S. cerevisiae</i> , <i>C. Albicans</i>	10 μg–1000 μg/ml zeolite	<ul style="list-style-type: none"> - MIC for <i>E. coli</i>, <i>B. subtilis</i> AgX 300 μg/ml; AgY 200 μg/ml - MIC for <i>S. Cerevisiae</i> and <i>C. albicans</i> 1000 μg/ml for both AgX and AgY
Guerra 2012 [108]	AgNP-clinoptilolite Ag NP 0.9–7.4 nm, Ag 4 wt%	<i>E. coli</i> , <i>Salmonella typhi</i>	150 CFU/ml	<ul style="list-style-type: none"> - 1.7 mg/ml of AgNP-zeolite killed all <i>E. coli</i> (1 h) - 6.7 μg/ml of AgNP-zeolite killed all <i>S. typhi</i> (1 h)
Inoue 2012 [122]	Ag ⁺ -zeolite Y	<i>E. coli</i>	10 ⁶ –10 ⁷ CFU/ml	<ul style="list-style-type: none"> - Ag⁺-Y enhanced the effect of antibiotic rifampicin towards <i>E. coli</i>
Flores-Lopez 2012 [109]	AgNP-chabazite (natural) Thermal annealing in air to generate NP (Ag 18.57 wt%) (NP size 2–20 nm)	<i>S. epidermis</i> , <i>S. aureus</i> , <i>Salmonella</i> , <i>Typhimurium</i> , <i>E. coli</i> , <i>Shigella flexneri</i> , <i>P. aeruginosa</i>	10 ⁵ CFU/ml 1, 0.1, 0.001 and 0.00001 wt% zeolite 1–48 h	<ul style="list-style-type: none"> - At 0.001 wt% AgNP-chabazite (10 μg/ml) only <i>S. aureus</i> not completely killed (48 h duration)
Moretro 2012 [184]	Cutting boards contain 9 ng Ag-zeolite	<i>S. aureus</i>	>10 ³ CFU/ml	<ul style="list-style-type: none"> - Antibacterial effect in high humidity (>70%) - Antibacterial effect of cutting board reduced in broth
Tinteri 2012 [178]	Ag zeolite on HVAC duct panels	<i>L. pneumophila</i> , <i>S. aureus</i> , <i>P. aeruginosa</i> , <i>E. coli</i> , <i>C. albicans</i> , <i>A. niger</i>	Analyzing microbial activity of panel 2 year test 10 ⁷ –10 ⁹ CFU/ml	<ul style="list-style-type: none"> - NaCl necessary with AgNP in cutting board - ~5–8 log₁₀ decreases in bacteria (24 h) in broth - Even after 2 years 99.999978% reduction in <i>P. aeruginosa</i>
Kaali 2013 [114]	Single, binary and ternary mixtures of Ag ⁺ , Cu ²⁺ , Zn ²⁺ -exchanged zeolite A	<i>S. aureus</i> (MRSA) <i>P. aeruginosa</i> , <i>C. tropicalis</i>	– 5 × 10 ⁵ CFU/ml – 2–1024 μg/g zeolite	<ul style="list-style-type: none"> - MIC of Ag⁺-A towards MRSA, <i>C. tropicalis</i>, <i>P. aeruginosa</i> of 512, 2 and 128 μg/g, respectively - Ag⁺-A exhibits highest activity - Co-exchange with Zn²⁺/Cu²⁺ increased MIC
Jai-eau 2013 [158]	Ag ⁺ -exchanged zeolite in vulcanized rubber	<i>E. coli</i> , <i>S. aureus</i>	1–5 wt% zeolite in rubber	<ul style="list-style-type: none"> - 5 wt% zeolite shows 3 log₁₀ reduction of <i>E. coli</i> and 2 log₁₀ reduction of <i>S. aureus</i> over 240 min
Jiraroj 2014 [116]	Ag ⁺ -zeolite A AgNP-zeolite A (NaBH ₄ reduction), Ag NP <10 nm	<i>E. coli</i> , <i>S. aureus</i>	10 ⁷ CFU/ml 25–200 μg/ml zeolite, duration 0–3 h	<ul style="list-style-type: none"> - 200 μg/ml of Ag⁺-A caused >95% and 84% reduction in <i>E. coli</i> and <i>S. aureus</i> in 3 h, respectively - AgNP less effective than Ag⁺-A, except at longer times
Cushen 2014 [149]	Commercial Agion (0.5–2 wt% zeolite) in polyethylene 3 μm zeolite		Studied the release of Ag ⁺ in fluids	0.5 wt% of zeolite had Ag ⁺ release of 3.4 × 10 ⁻⁴ mg/kg, <0.001 mg/kg regulatory limit

(continued on next page)

Table 1 (continued)

Reference	Zeolite used	Microorganism used	Conditions	Comments
Kim 2014 [152]	5–10 nm AgNP on 50 nm zeolite in polyvinylalcohol hydrogels (1, 3, 5 wt% zeolite)	<i>S. aureus</i> , <i>K. pneumoniae</i>		<ul style="list-style-type: none"> – Zeolite incorporation/polymer by UV radiation – 99.9% reduction in <i>S. aureus</i> with 3 wt% zeolite/polymer sample
Zhou 2014 [115]	Ag ⁺ -zeolite A (36 wt% Ag)	<i>E. coli</i> <i>S. aureus</i>	Not provided	<ul style="list-style-type: none"> – MIC of 1 µg/ml Ag⁺-A towards <i>E. coli</i> and 3.5 µg/ml towards <i>S. aureus</i> (poor data presentation makes it difficult to compare with other studies)
Demirci 2014 [117]	Ag ⁺ -zeolite A and X Also studied zeolite with Cu ²⁺ and Zn ²⁺	<i>E. coli</i> , <i>P. aeruginosa</i> , <i>B. cereus</i> , <i>S. aureus</i>	<ul style="list-style-type: none"> – 10⁷ CFU/ml – 24 h exposure 	<ul style="list-style-type: none"> – MIC of 32–64 µg/ml towards <i>E. coli</i>, <i>S. aureus</i> – Activity correlates with rate of ion release
Potter, 2014 [179]	Aglon coated on door handles	<i>Staphylococcus</i>	Samples recovered from door handles with cotton swab	– Bacterial counts lower on silver zeolite coated door handles most of the time (there were exceptions)
Dong 2014 [129]	Ag ⁺ -EMT AgNP-EMT (microwave/trimethylamine) zeolite size 10–20 nm Ag size 0.6–5 nm	<i>E. coli</i> (ATCC 8739)	Qualitative assessment	– AgNP EMT performed better than Ag ⁺ EMT
Akhigbe 2014 [107]	Ag ⁺ -exchanged natural clinoptilolite Ag 4.34 wt% loading	<i>E. coli</i>	10 ⁸ CFU/ml	<ul style="list-style-type: none"> – 2 mg/ml Ag⁺-zeolite 10 log₁₀ reduction in 30 min – Presence of Pb²⁺, Cd²⁺, Zn²⁺ in solution enhanced activity
Ferriera 2015 [123]	Bimetallic zeolite Y (combination of Ag ⁺ , Zn ²⁺ , Cu ²⁺ (metal loading 1.02 to 4.33 wt%))	<i>E. coli</i> , Yeast: <i>Saccharomyces cerevisiae</i>	CFU not specified 24 h exposure to <i>E. coli</i> . 42 h to yeast	<ul style="list-style-type: none"> – ZnAg-Y (Zn²⁺ exchanged first) most active towards bacteria, better than AgZnY – MIC for ZnAg-Y towards <i>E. coli</i> 500 µg/ml – MIC for ZnAg-Y towards yeast 2000 µg/ml
Belkhair 2015 [154]	AgX surface functionalized and dispersed in silicone polymer (Ag-8.8–14.1%)	<i>E. coli</i> , <i>S. epidermis</i> , <i>C. albicans</i>	<ul style="list-style-type: none"> 4 × 10⁶ <i>E. coli</i> 2 × 10⁵ <i>S. epidermis</i> 2 × 10⁴ <i>C. albicans</i> 	<ul style="list-style-type: none"> – 3 log₁₀ reduction (5 h), 5 log₁₀ reduction for <i>E. coli</i> (24 h) – 1 log₁₀ reduction (5 h), 4 log₁₀ reduction for <i>S. epidermis</i> (24 h) – No effect on <i>C. albicans</i> – Organosilane modified zeolite dispersed well in silicone polymer
Griffith 2015 [185]	Ag ⁺ zeolite on stainless steel (0.5–1.0 wt% zeolites (400–1000 nm thick coating))	<i>L. innovia</i> , <i>E. coli</i>	<ul style="list-style-type: none"> – 10⁶–10⁸ CFU/ml – Cresyl violet quantification of bacteria on stainless steel 	– Ag ⁺ -zeolite inhibited bacterial growth on surface
Praprudivongs 2015 [157]	Commercial zeomic in polylactic acid and wood flour/polylactide acid composites (1.5 wt% zeolite)	<i>S. aureus</i>	10 ⁷ –10 ⁸ CFU/ml	– Zeolite/polymer had minimal antibacterial effect
Saravanan 2015 [174]	Silver zeolite (not specified) into acrylic soft liners for denture wearers	<i>C. albicans</i>	In vivo study	<ul style="list-style-type: none"> – 65% decrease in <i>C. albicans</i> growth in 24 h – Visoelectric properties of acrylic not altered by zeolite
Soysal, 2015 [186]	Ag ⁺ zeolite-X in polyvinylidene polyamide films to	– Total aerobic mesophilic bacteria, coliforms molds, yeasts	– Agar (potato Dextrose, plato count, Violet Red Bile	– Ag zeolite not as effective as chitosan, nisin (5 °C for 6 days)
Yee 2015 [135]	AgNP-ZSM-5 (1–5 µm zeolite 0.8–10 wt%, Ag) AgNP ~1.5 µm reduction with citrate	<i>H. pacifica</i> , <i>Microalgae</i> , <i>D. tertiolecto</i> , <i>Isochrysis</i> sp.	Adherent Biomass	<ul style="list-style-type: none"> – 10 wt% Ag loaded sample reduced biofilm attachment by 81% – Growth of microalgae inhibited
Hanim 2016 [126]	Amine-functionalized zeolite Y	<i>E. coli</i> , <i>S. aureus</i>	<ul style="list-style-type: none"> 1.5 × 10⁸ CFU/ml 25 µg–10 mg/ml zeolite 24 h incubation 	<ul style="list-style-type: none"> – Optimum MIC value for <i>E. coli</i> and <i>S. aureus</i> was 50 µg/ml – positively charged zeolite surface improved activity
Rieger 2016 [161]	Zeolite A grown on cellulose Nano and meso zeolite A incorporated in cellulose	<i>E. coli</i>	<ul style="list-style-type: none"> 10⁷ cells/ml 4 mg Ag⁺ zeolite A suspension, 0.07–0.35 mg Ag⁺-zeolite A/cellulose mat 	<ul style="list-style-type: none"> – Ag⁺-A in suspension killed 53% of bacteria (30 min) – Ag⁺ zeolite incorporated in cellulose more active (70–90% kill in 30 min) – Ag⁺ zeolite in cellulose releases lower levels of Ag⁺, as compared to crystals – Cellulose porous matrix provides better contact with bacteria
Rieger 2016 [161]	Zeolite A grown on cellulose mat, nanocrystals and mesoporous zeolite A inside cellulose fibers	<i>E. coli</i> K12	<ul style="list-style-type: none"> 10⁷ CFU/ml 60–67% Ag⁺ exchange in zeolite Viability by fluorescence 	<ul style="list-style-type: none"> – 70–90% cells killed within 90 min with Ag⁺-zeolite/cellulose samples – Microstructure of cellulose promotes contact with bacteria

Table 1 (continued)

Reference	Zeolite used	Microorganism used	Conditions	Comments
Shankar 2016 [159]	Ag ⁺ -zeolite in alginate films	<i>E. coli</i> , <i>L. monocytogenes</i>	10 ⁶ –10 ⁷ UFU/ml	– MIC/MBC of Ag ⁺ -zeolite alginate film 3.125/12.5 µg/ml for <i>E. coli</i> and 6.25/12.5 µg/ml for <i>L. monocytogenes</i>
Jaime-Acuna 2016 [130]	AgNP-mordenite synthesized in a one-pot process. Zeolite 40 µm AgNP 5–6 nm	<i>E. coli</i>	MIC/MBC determined with 10 ⁵ CFU/ml	– AgNP mordenite exhibited a MIC and MBC of 2 and 3 µg/ml, respectively – Direct contact of zeolite and bacteria promoted activity
Ferreira 2016 [125]	Zn ²⁺ + Ag ⁺ exchanged zeolite Y	<i>E. coli</i> , <i>B. subtilis</i> , <i>C. albicans</i> , <i>S. cerevisiae</i>	CFU for MIC not specified	– For the optimal ZnAgY, MIC values for bacteria were 100 µg/ml, and 300 µg/ml for the yeast – Bimetallic samples are more active than singly ion-exchanged zeolite
Chen 2017 [127]	Ag ⁺ -zeolite X of varying morphology (100–700 nm, 2 µm) 20–22 wt% Ag	MRSA, human epithelial cells, skin fibroblasts, monocytes	10 ⁷ –10 ⁸ CFU/ml MRSA USA 300 biofilms	– MRSA killed with dosages of (MIC) 4–8 µg/ml in 24 h – Nanozeolite release Ag ⁺ faster than micron zeolite – Cytotoxicity to human cells require >128 µg/ml of nano-zeolite
Ghivari 2017 [175]	Silver zeolite (not specified) applied to biofilms (root canal irrigant)	Biofilm of <i>C. albicans</i> , <i>S. aureus</i> , <i>C. albicans</i>	Biofilm on nitrocellulose membrane	– Zeolite not as effective as NaOCl, chlorhexidine octenidine
Jedrzejczyk 2017 [183]	Ag zeolite Y incorporated in paper	<i>E. coli</i> , <i>A. niger</i> , <i>S. Marcescens</i> , <i>B. subtilis</i> , <i>B. megaterium</i> , <i>M. alpine</i> , <i>T. viride</i> , <i>C. globosum</i> , <i>C. cladosporioides</i>	Lucipac Pentest (measures ATP)	– AgNP and Ag ⁺ -zeolite Y in paper show similar antimicrobial and antifungal activity
Sanchez 2017 [136]	Ag ⁺ -ZSM-5	<i>E. coli</i> , <i>P. aeruginosa</i> , <i>C. albicans</i>	Agar diffusion method, bacterial growth curves	– Antibacterial and antifungal effect noted – Growth of bacteria retarded by 50% in 3 h
Scacchetti 2017 [162]	Ag ⁺ -zeolite A, Ag ⁺ -zeolite A/chitosan in cotton fabric	<i>E. coli</i> , <i>S. aureus</i> , <i>S. Albicans</i> , <i>T. rubrum</i>	10 ⁴ –10 ⁶ CFU/ml	– Ag ⁺ -zeolite/chitosan exhibited antimicrobial activity towards all 4 species. – Chitosan/zeolite combination better activity than chitosan, zeolite alone
Tosheva 2017 [138]	Small (180–230 nm) and large (1.2–2.2 µm) zeolite X Ag ~10.7 wt% Small (200–300 nm) and large (400–500 nm) zeolite Beta Ag ~2.3 wt%	<i>E. coli</i> , <i>C. albicans</i>	10 ⁵ CFU/ml 7 min assay (500 µg/ml)	– Large crystals were more effective than smaller crystals (e.g. small zeolite X decreases 5 log 10 in 5 min, large zeolite X 5 log 10 reduction in 3 min – Zeolite beta more effective than zeolite X (though with significantly lower Ag content)
Wu 2017 [153]	Surface modified nanozeolite Y (150 nm) incorporated into polyvinyl alcohol and polydopamine	<i>P. aeruginosa</i>	10 ⁸ CFU/ml	– AgNP – PVA and PBA coating showed significant antimicrobial activity e.g. bacterial growth inhibited for 9 days on membrane surface
Youssef 2017 [128]	Ag – analcime, faujasite, zeolite A 200 nm and micron zeolite 50 wt% Ag	<i>S. aureus</i> , <i>P. aeruginosa</i> , <i>C. albicans</i> , <i>A. niger</i>	Agar diffusion method	– Antimicrobial activity analcime > faujasite > zeolite A – No major difference between nano and micron size in activity
Hamiciuc 2018 [155]	Silylated zeolite L (200 nm) in polyether-ether-ketone (2, 7, 12 wt % zeolite)	<i>S. aureus</i> , MRSA, <i>E. coli</i>	Agar diffusion	– 12 wt% sample showed activity towards all 3 bacteria – Upon 24 exposure fibroblast viability decreased to 82% of control

exposure to a commercial colloidal silver product and no significant changes were noted in pulmonary ROS or pro-inflammatory cytokine generation [229]. No morphological changes were noted in the lungs, heart or abdominal organs. Baral et al. noted that colloidal silver alleviated the inflammatory symptoms in cystic fibrosis [230].

Human patch tests and a 4-week safety test of the powder zeolite spray showed no adverse events [176].

6.4. Regulatory issues

Many of the world's regulatory agencies have put a limit on the exposure to silver [7,231]. World Health Organization (WHO) in 2004 proposed a No observable Adverse Effect Level (NOAEL) for humans of 0.39 mg/person/day (corresponds to 6.5 µg/kgbw/day, assuming an adult weighs 60 kgbw). These values led WHO to conclude that silver levels of 0.1 mg/l is tolerable in drinking water. EFSA (European Food Safety Agency) recommends 0.05 mg/l in water and 0.05 mg/kg in food. US EPA recommends 0.1 mg/l

(100 ppb) in drinking water [232]. The basis for these recommendation is that LOAEL (Lowest Observable Adverse Effect Level) silver causes argyria in humans following intravenous application. Considering oral absorption of 4%, body weight of 70 kg and lifetime of 70 years, US EPA has come up with a dose of 5 µg/kgbw for chronic exposure to silver.

A tolerable daily intake (TDI) of 2.5 µg/kgbw/day is proposed for all for oral exposure to ~22 nm silver nanoparticles based on elevation of TNF-α in serum of mice exposed to these particles [233].

For silver zinc zeolites, the acceptable daily intake (ADI) of 0.3 µg/kgbw/day has been proposed, based on a 2 year study in rats focused on liver toxicity, organ pigmentation and endometrial polyps [231].

The regulations relating to silver in contact with food materials varies widely between different countries [234]. In 2014, USEPA warned a company to stop selling a silver-containing food container since the claim that the container keeps food fresh was not approved by the EPA. In 2013, the Brazilian authorities rejected a bill that proposed labeling products that use nanotechnology.

7. Assessment of the literature

It is difficult to compare the antimicrobial performance of the silver zeolites from different authors, even for the same zeolite. The broth media, number of viable cells and amounts of zeolite and the silver content used very widely. Thus, it is not surprising that MIC values as reported in Table 1 vary significantly. However, comparisons can be drawn from a single study or if experimental conditions are well defined.

Conclusions related to the structure of zeolites that can be made are

- Different zeolite frameworks exhibit different activity, even for comparable silver loading. This could arise from differences in the Ag^+ release characteristics due to the varying framework – Ag^+ electrostatic interactions.
- For the same framework, higher Ag^+ loading leads to increased antimicrobial activity, unless at higher loading metallic Ag is formed.
- Surface charge modification of the zeolite particle to a positive charge improves antimicrobial effect. The possible explanation is that the positively charged zeolite is attracted to the negatively charged bacterial surface. However, the charge that the particle acquires in the broth is dependent on adsorption of salts/proteins (protein corona) and can be different from the magnitude and sign of the charge on the as-synthesized particle.
- Co-cations such as Zn^{2+} and Cu^{2+} increases antimicrobial activity, though the exact synergy is difficult to evaluate because introducing a second cation alters the amount and release characteristics of the Ag^+ . The order in which the ions are exchanged also becomes relevant because different sites have different energetics which influences the release of the ions.
- For the same framework, AgNP supported zeolite exhibits higher activity than Ag^+ /Zeolite, though there are inconsistencies in the literature of this issue.
- AgNP supported on nanozeolite had a slightly higher activity.
- In a direct comparison, high Si/Al ratio zeolite beta was comparable in performance to zeolite A, though the latter had five times the amount of silver.
- Large zeolite particles were more active than smaller ones for the same framework, though results on this point are inconsistent.
- More siliceous zeolites tend to be more potent, if silver levels are comparable to more aluminous zeolites.

From a practical point of view, the following conclusion can be drawn

- Common methods of polymer fabrication can incorporate silver zeolites.
- Silver zeolites can be applied as coatings on metal, textiles and polymers.
- Zeolite membranes containing silver can be synthesized on polymers, metals.
- Zeolites in some cases can compromise the mechanical properties of polymers.
- Manufacturing processes that incorporate silver zeolites need to be optimized so that the zeolites are accessible to the external environment.
- Long term use of silver zeolites on variety of matrices is possible because of the storage of large amounts of silver with slow release.
- Humid conditions are required for antimicrobial activity.
- Uniform of distribution of silver zeolites in matrices depends on formulation methodology, and needs to be optimized.

8. Future trends

The numerous studies discussed above clearly demonstrates that silver zeolite function as antimicrobial agents, as well as show potent activity against fungi, yeasts and viruses. Thus, silver zeolites are an alternative to silver salts and silver colloids. Silver zeolites are capable of storage and release of Ag^+ and AgNP. There are growing concerns about the use of silver colloids, because of their eventual release into the environment, soils and possibly even into drinking water and foods for living species. Regulations are being proposed for controlling the release and amounts of silver. Silver zeolites will possibly be subject to similar regulations as silver colloids. Other concern is that microbes may develop resistance to silver. Paracelsus the founder of toxicology stated that “dosage makes a material a poison or a remedy (*dosis sola facit venenum*)” applies to silver-based compounds [12]. So, the ideal goal should be to use the least amount of silver, while exploiting its antimicrobial properties. Do silver zeolites offer any advantages over silver salts and silver colloids? The answer to this question is application specific. Future trends on the use of silver zeolites will depend on a better understanding of its mechanism of action and the advantages that the zeolite host provides in enhancing the antimicrobial properties of the guest silver species.

From a basic research viewpoint, the dynamics of release of Ag^+ from Ag^+ -zeolite as well as AgNP- zeolite needs to be better understood as a function of

- Zeolite framework
- Zeolite Si/Al ratio
- Silver loading
- Presence of co-cations

These experiments should be done in a solution of fixed ion strength (e.g. 0.1 M NaNO_3).

Another area of research is the zeolite-cell interaction. The parameters here are

- Gram positive and negative bacteria.
- Zeolite morphology, spheres, cubes and needles.
- Zeolite size, nano versus micron.

Of interest are if nanosized zeolites can be engulfed by the bacteria. Microscopy, both optical and electron can help in evaluating the zeolite-bacteria interaction.

In a practical sense, it is possible that silver zeolites can be more effective than silver salts or silver colloids for the following reasons. Control of Ag^+ release from silver zeolites is different from silver salts since it is controlled by the ion-exchange process. In the case of silver colloids, there are ligands on the surface, whereas AgNP on zeolite requires no ligand, thus altering Ag^+ release. Zeolite cages and cavities can also store species, such as Zn^{2+} that can enhance the antimicrobial activity of silver. Zeolite surfaces contain –OH groups that can be modified to alter surface charge, and promote electrostatic interactions with the bacteria, thereby increasing potency. Nanozeolites can act as a Trojan horse delivering their content within the bacteria. Numerous possibilities exist for formulation of the optimized silver zeolite into products, including high temperature and harsh environment processing.

These features suggest that the zeolite as a support is unique and can increase the potency of the guest silver species, thereby requiring less silver, alleviating the environment concerns. The fate of silver zeolites in the environment will depend on the conditions. Zeolites are stable at pH's between 3 and 12, and under these conditions, the silver will be retained on the zeolite and release by ion-exchange mechanisms and AgNP dissolution.

Silver-zeolite antimicrobials, optimized by size, surface charge, co-species can be an alternative to silver salts and silver colloids with higher potency and lower environmental footprint.

References

- J.W. Alexander, History of the medical use of silver, *Surg. Infect.* 10 (2009) 289–292, <https://doi.org/10.1089/sur.2008.9941>.
- H.J. Klaseen, Historical review of the use of silver in the treatment of burns. I. Early uses, *Burns* 26 (2000) 117–130, [https://doi.org/10.1016/S0305-4179\(99\)00108-4](https://doi.org/10.1016/S0305-4179(99)00108-4).
- G. Zhao, S.E. Stevens, Multiple parameters for the comprehensive evaluation of the susceptibility of *Escherichia coli* to the silver ion, *Biometals* 11 (1998) 27–32, <https://doi.org/10.1023/A:10092532230055>.
- Q.L. Feng, J. Wu, G.Q. Chen, F.Z. Cui, T.N. Kim, J.O. Kim, A mechanistic study of the antibacterial effect of silver ions on *Escherichia coli* and *Staphylococcus aureus*, *J. Biomed. Mater. Res.* 52 (2000) 662–668, [https://doi.org/10.1002/1097-4636\(20001215\)52:4<662::AID-JBM10>3.0.CO;2-3](https://doi.org/10.1002/1097-4636(20001215)52:4<662::AID-JBM10>3.0.CO;2-3).
- J. Pulit-Prociak, M. Banach, Silver nanoparticles – a material of the future...?, *Open Chem* 14 (2016), <https://doi.org/10.1515/chem-2016-0005>.
- FDA, code of federal regulations (21 CFR parts 174–186), (n.d.), <https://www.ecfr.gov/cgi-bin/text-idx?SID=6ba0a6620c258cee683e814692be783d&mc=true&node=pt21.3.174&rgn=div5> (accessed June 18, 2018).
- P. Hartemann, P. Hoet, A. Proykova, T. Fernandes, A. Bann, W. De Jong, J. Filser, A. Hensten, C. Kneuer, J.-Y. Maillard, H. Norppa, M. Scheringer, S. Wijnhoven, Nanosilver: safety, health and environmental effects and role in antimicrobial resistance, *Mater. Today* 18 (2015) 122–123, <https://doi.org/10.1016/j.matod.2015.02.014>.
- S.M. Auerbach, K.A. Carrado, P.K. Dutta, *Handbook of Zeolite Science and Technology*, CRC Press, 2003.
- D.W. Breck, *Zeolite Molecular Sieves: Structure, Chemistry, and Use*, Wiley, 1973.
- A. Nagy, A. Harrison, S. Sabhani, J. Robert, S. Munson, P.K. Dutta, W.J. Waldman, Silver nanoparticles embedded in zeolite membranes: release of silver ions and mechanism of antibacterial action, *Int. J. Nanomed.* 6 (2011) 1833–1852, <https://doi.org/10.2147/IJN.S24019>.
- M. Severance, P.K. Dutta, Evolution of silver nanoparticles within an aqueous dispersion of nanosized zeolite Y: mechanism and Applications, *J. Phys. Chem. C* 118 (2014) 28580–28591, <https://doi.org/10.1021/jp5074957>.
- K. Naik, M. Kowshik, The silver lining: towards the responsible and limited usage of silver, *J. Appl. Microbiol.* 123 (2017) 1068–1087, <https://doi.org/10.1111/jam.13525>.
- J.A. Lemire, J.J. Harrison, R.J. Turner, Antimicrobial activity of metals: mechanisms, molecular targets and applications, *Nat. Rev. Microbiol.* 11 (2013) 371–384, <https://doi.org/10.1038/nrmicro3028>.
- K. Zheng, M.I. Setyawati, D.T. Leong, J. Xie, Antimicrobial silver nanomaterials, *Coord. Chem. Rev.* 357 (2018) 1–17, <https://doi.org/10.1016/j.ccr.2017.11.019>.
- B. Khalandi, N. Asadi, M. Milani, S. Davaran, A.J.N. Abadi, E. Abasi, A. Akbarzadeh, A review on potential role of silver nanoparticles and possible mechanisms of their actions on bacteria, *Drug Res.* 11 (2017) 70–76, <https://doi.org/10.1055/s-0042-113383>.
- N. Durán, M. Durán, M.B. de Jesus, A.B. Seabra, W.J. Fávaro, G. Nakazato, Silver nanoparticles: a new view on mechanistic aspects on antimicrobial activity, *Nanomed. Nanotechnol. Biol. Med.* 12 (2016) 789–799, <https://doi.org/10.1016/j.nano.2015.11.016>.
- M. Konop, T. Damps, A. Misicka, L. Rudnicka, Certain aspects of silver and silver nanoparticles in wound care: a minireview, *J. Nanomater.* 2016 (2016) 7614753, <https://doi.org/10.1155/2016/7614753>.
- B. Simončič, D. Klemenčič, Preparation and performance of silver as an antimicrobial agent for textiles: a review, *Text. Res. J.* 86 (2016) 210–223, <https://doi.org/10.1177/0040517515586157>.
- H.J. Park, H.M. Lim, Antimicrobial properties of Ag-exchanged natural and synthetic zeolites: a short review, *Curr. Green Chem.* 2 (2015) 354–361.
- B. Le Ouay, F. Stellacci, Antibacterial activity of silver nanoparticles: a surface science insight, *Nano Today* 10 (2015) 339–354, <https://doi.org/10.1016/j.nantod.2015.04.002>.
- S. Chernousova, M. Epple, Silver as antibacterial agent: ion, nanoparticle, and metal, *Angew. Chem. Int. Ed.* 52 (2013) 1636–1653, <https://doi.org/10.1002/anie.201205923>.
- K. Mijnenonckx, N. Leys, J. Mahillon, S. Silver, R.V. Houdt, Antimicrobial silver: uses, toxicity and potential for resistance, *BioMetals* 26 (2013) 609–621, <https://doi.org/10.1007/s10534-013-9645-z>.
- D.R. Monteiro, L.F. Gorup, A.S. Takamiya, A.C. Ruvollo-Filho, E.R. de Camargo, D.B. Barbosa, The growing importance of materials that prevent microbial adhesion: antimicrobial effect of medical devices containing silver, *Int. J. Antimicrob. Agents* 34 (2009) 103–110, <https://doi.org/10.1016/j.ijantimicag.2009.01.017>.
- C. Marambio-Jones, E.M.V. Hoek, A review of the antibacterial effects of silver nanomaterials and potential implications for human health and the environment, *J. Nanoparticle Res.* 12 (2010) 1531–1551, <https://doi.org/10.1007/s11051-010-9900-y>.
- S.Y. Liao, D.C. Read, W.J. Pugh, J.R. Furr, A.D. Russell, Interaction of silver nitrate with readily identifiable groups: relationship to the antibacterial action of silver ions, *Lett. Appl. Microbiol.* 25 (2003) 279–283, <https://doi.org/10.1046/j.1472-765X.1997.00219.x>.
- W. Ghandour, J.A. Hubbard, J. Deistung, M.N. Hughes, R.K. Poole, The uptake of silver ions by *Escherichia coli* K12: toxic effects and interaction with copper ions, *Appl. Microbiol. Biotechnol.* 28 (1988) 559–565, <https://doi.org/10.1007/BF00250412>.
- W.J. Schreurs, H. Rosenberg, Effect of silver ions on transport and retention of phosphate by *Escherichia coli*, *J. Bacteriol.* 152 (1982) 7–13.
- P. Dibrov, J. Dzioba, K.K. Gosink, C.C. Häse, Chemiosmotic mechanism of antimicrobial activity of Ag⁺ in *Vibrio cholerae*, *Antimicrob. Agents Chemother.* 46 (2002) 2668–2670, <https://doi.org/10.1128/AAC.46.8.2668-2670.2002>.
- K.B. Holt, A.J. Bard, Interaction of silver(I) ions with the respiratory chain of *Escherichia coli*: an electrochemical and scanning electrochemical microscopy study of the antimicrobial mechanism of micromolar Ag⁺, *Biochemistry (Mosc.)* 44 (2005) 13214–13223, <https://doi.org/10.1021/bi0508542>.
- C.-N. Lok, C.-M. Ho, R. Chen, Q.-Y. He, W.-Y. Yu, H. Sun, P.K.-H. Tam, J.-F. Chiu, C.-M. Che, Proteomic analysis of the mode of antibacterial action of silver nanoparticles, *J. Proteome Res.* 5 (2006) 916–924, <https://doi.org/10.1021/pr0504079>.
- A.L. Semejckina, V.P. Skulachev, Submicromolar Ag⁺ increases passive Na⁺ permeability and inhibits the respiration-supported formation of Na⁺ gradient in *Bacillus* FTU vesicles, *FEBS Lett.* 269 (1990) 69–72, [https://doi.org/10.1016/0014-5793\(90\)81120-D](https://doi.org/10.1016/0014-5793(90)81120-D).
- E.M. Luther, Y. Koehler, J. Diendorf, M. Epple, R. Dringen, Accumulation of silver nanoparticles by cultured primary brain astrocytes, *Nanotechnology* 22 (2011), <https://doi.org/10.1088/0957-4484/22/37/375101>.
- R. Foldbjerg, D.A. Dang, H. Autrup, Cytotoxicity and genotoxicity of silver nanoparticles in the human lung cancer cell line, A549, *Arch. Toxicol.* 85 (2011) 743–750, <https://doi.org/10.1007/s00204-010-0545-5>.
- W.K. Jung, H.C. Koo, K.W. Kim, S. Shin, S.H. Kim, Y.H. Park, Antibacterial activity and mechanism of action of the silver ion in *Staphylococcus aureus* and *Escherichia coli*, *Appl. Environ. Microbiol.* 74 (2008) 2171–2178, <https://doi.org/10.1128/AEM.02001-07>.
- R. Kaegi, A. Voegelin, B. Sinnet, S. Zuleeg, H. Hagendorfer, M. Burkhardt, H. Siegrist, Behavior of metallic silver nanoparticles in a pilot wastewater treatment plant, *Environ. Sci. Technol.* 45 (2011) 3902–3908, <https://doi.org/10.1021/es1041892>.
- G.A. Martínez-Castañón, N. Niño-Martínez, J.P. Loyola-Rodríguez, N. Patiño-Marín, J.R. Martínez-Mendoza, F. Ruiz, Synthesis of silver particles with different sizes and morphologies, *Mater. Lett.* 63 (2009) 1266–1268, <https://doi.org/10.1016/j.matlet.2009.02.061>.
- A. Panáček, L. Kvítek, R. Prucek, M. Kolář, R. Večeřová, N. Pizúrová, V.K. Sharma, T. Nevěčná, R. Zbořil, Silver colloid nanoparticles: synthesis, characterization, and their antibacterial activity, *J. Phys. Chem. B* 110 (2006) 16248–16253, <https://doi.org/10.1021/jp0638226>.
- Z.S. Pillai, P.V. Kamat, What factors control the size and shape of silver nanoparticles in the citrate ion reduction method?, *J. Phys. Chem. B* 108 (2004) 945–951, <https://doi.org/10.1021/jp037018r>.
- S. Sharma, M. Thakur, M.K. Deb, Synthesis of silver nanoparticles using N 1, N 2-diphenylbenzamide by microwave irradiation method, *J. Exp. Nanosci.* 2 (2007) 251–256, <https://doi.org/10.1080/17458080701753744>.
- V.K. Sharma, R.A. Yngard, Y. Lin, Silver nanoparticles: green synthesis and their antimicrobial activities, *Adv. Colloid Interface Sci.* 145 (2009) 83–96, <https://doi.org/10.1016/j.cis.2008.09.002>.
- A. Varki, R. Cummings, J. Esko, H. Freeze, G. Hart, J. Marth, *Saccharide Structure and Nomenclature*, Cold Spring Harbor Laboratory Press, 1999, <https://www.ncbi.nlm.nih.gov/books/NBK20732/> (accessed June 18, 2018).
- S.K. Batabyal, C. Basu, A.R. Das, G.S. Sanyal, Green chemical synthesis of silver nanowires and microfibers using starch, *J. Biobased Mater. Bioenergy.* 1 (2007) 143–147, <https://doi.org/10.1166/jbmb.2007.016>.
- H. Huang, X. Yang, Synthesis of polysaccharide-stabilized gold and silver nanoparticles: a green method, *Carbohydr. Res.* 339 (2004) 2627–2631, <https://doi.org/10.1016/j.carres.2004.08.005>.
- D. Manno, E. Filippo, M. Di Giulio, A. Serra, Synthesis and characterization of starch-stabilized Ag nanostructures for sensors applications, *J. Non-Cryst. Solids.* 354 (2008) 5515–5520, <https://doi.org/10.1016/j.jnoncrysol.2008.04.059>.
- M. Singh, I. Sinha, R.K. Mandal, Role of pH in the green synthesis of silver nanoparticles, *Mater. Lett.* 63 (2009) 425–427, <https://doi.org/10.1016/j.matlet.2008.10.067>.
- E.A. Venediktov, V.A. Padokhin, Synthesis of silver nanoclusters in starch aqueous solutions, *Russ. J. Appl. Chem.* 81 (2008) 2040–2042, <https://doi.org/10.1134/S1070427208110323>.
- S. Li, Y. Shen, A. Xie, X. Yu, L. Qiu, L. Zhang, Q. Zhang, Green synthesis of silver nanoparticles using *Capsicum annuum* L. extract, *Green Chem.* 9 (2007) 852–858, <https://doi.org/10.1039/B615357G>.
- R. Sanghi, P. Verma, Biomimetic synthesis and characterisation of protein capped silver nanoparticles, *Bioresour. Technol.* 100 (2009) 501–504, <https://doi.org/10.1016/j.biortech.2008.05.048>.
- D.M. Eby, N.M. Schaeublin, K.E. Farrington, S.M. Hussain, G.R. Johnson, Lysozyme catalyzes the formation of antimicrobial silver nanoparticles, *ACS Nano.* 3 (2009) 984–994, <https://doi.org/10.1021/nn900079e>.
- J. Kasthuri, S. Veerapandian, N. Rajendiran, Biological synthesis of silver and gold nanoparticles using apii as reducing agent, *Colloids Surf. B*

- Biointerfaces 68 (2009) 55–60, <https://doi.org/10.1016/j.colsurfb.2008.09.021>.
- [51] S.S. Shankar, A. Ahmad, M. Sastry, Geranium leaf assisted biosynthesis of silver nanoparticles, *Biotechnol. Prog.* 19 (2003) 1627–1631, <https://doi.org/10.1021/bp034070w>.
- [52] J.Y. Song, B.S. Kim, Rapid biological synthesis of silver nanoparticles using plant leaf extracts, *Bioprocess Biosyst. Eng.* 32 (2009) 79, <https://doi.org/10.1007/s00449-008-0224-6>.
- [53] A. Ahmad, P. Mukherjee, S. Senapati, D. Mandal, M.I. Khan, R. Kumar, M. Sastry, Extracellular biosynthesis of silver nanoparticles using the fungus *Fusarium oxysporum*, *Colloids Surf. B Biointerfaces* 28 (2003) 313–318, [https://doi.org/10.1016/S0927-7765\(02\)00174-1](https://doi.org/10.1016/S0927-7765(02)00174-1).
- [54] K. Kalishwaralal, V. Deepak, S. Ramkumarandian, H. Nellaiah, G. Sangiliyadi, Extracellular biosynthesis of silver nanoparticles by the culture supernatant of *Bacillus licheniformis*, *Mater. Lett.* 62 (2008) 4411–4413, <https://doi.org/10.1016/j.matlet.2008.06.051>.
- [55] N. Mokhtari, S. Daneshpajouh, S. Seyedbagheri, R. Atashdehghan, K. Abdi, S. Sarkar, S. Minaian, H.R. Shahverdi, A.R. Shahverdi, Biological synthesis of very small silver nanoparticles by culture supernatant of *Klebsiella pneumoniae*: the effects of visible-light irradiation and the liquid mixing process, *Mater. Res. Bull.* 44 (2009) 1415–1421, <https://doi.org/10.1016/j.materresbull.2008.11.021>.
- [56] P. Mukherjee, A. Ahmad, D. Mandal, S. Senapati, S.R. Sainkar, M.I. Khan, R. Parishcha, P.V. Ajaykumar, M. Alam, R. Kumar, M. Sastry, Fungus-mediated synthesis of silver nanoparticles and their immobilization in the mycelial matrix: a novel biological approach to nanoparticle synthesis, *Nano Lett.* 1 (2001) 515–519, <https://doi.org/10.1021/nl0155274>.
- [57] S. Senapati, D. Mandal, A. Ahmad, Fungus mediated synthesis of silver nanoparticles: a novel biological approach, *Indian J. Phys.* 78 (2004) 101–105.
- [58] S. Sharma, M. Thakur, M.K. Deb, Preparation of silver nanoparticles by microwave irradiation, *Curr. Nanosci.* 4 (2008) 138–140.
- [59] N. Vigneshwaran, N.M. Ashtaputre, P.V. Varadarajan, R.P. Nachane, K.M. Paralikar, R.H. Balasubramanya, Biological synthesis of silver nanoparticles using the fungus *Aspergillus flavus*, *Mater. Lett.* 61 (2007) 1413–1418, <https://doi.org/10.1016/j.matlet.2006.07.042>.
- [60] Y. Li, Y.N. Kim, E.J. Lee, W.P. Cai, S.O. Cho, Synthesis of silver nanoparticles by electron irradiation of silver acetate, *Nucl. Instrum. Methods Phys. Res. Sect. B Beam Interact. Mater. At.* 251 (2006) 425–428, <https://doi.org/10.1016/j.nimb.2006.06.019>.
- [61] J.P. Abid, A.W. Wark, P.F. Brevet, H.H. Girault, Preparation of silver nanoparticles in solution from a silver salt by laser irradiation, *Chem. Commun.* (2002) 792–793, <https://doi.org/10.1039/B200272H>.
- [62] H. Jia, W. Xu, J. An, D. Li, B. Zhao, A simple method to synthesize triangular silver nanoparticles by light irradiation, *Spectrochim. Acta. A. Mol. Biomol. Spectrosc.* 64 (2006) 956–960, <https://doi.org/10.1016/j.saa.2005.09.004>.
- [63] D. Long, G. Wu, S. Chen, Preparation of oligochitosan stabilized silver nanoparticles by gamma irradiation, *Radiat. Phys. Chem.* 76 (2007) 1126–1131, <https://doi.org/10.1016/j.radphyschem.2006.11.001>.
- [64] S.K. Mahapatra, K.A. Bogle, S.D. Dhole, V.N. Bhoraskar, Synthesis of gold and silver nanoparticles by electron irradiation at 5–15 keV energy, *Nanotechnology* 18 (2007), <https://doi.org/10.1088/0957-4484/18/13/135602>.
- [65] N. Yanagihara, Y. Tanaka, H. Okamoto, Formation of silver nanoparticles in Poly(methyl methacrylate) by UV irradiation, *Chem. Lett.* 30 (2001) 796–797, <https://doi.org/10.1246/cl.2001.796>.
- [66] H. Yin, T. Yamamoto, Y. Wada, S. Yanagida, Large-scale and size-controlled synthesis of silver nanoparticles under microwave irradiation, *Mater. Chem. Phys.* 83 (2004) 66–70, <https://doi.org/10.1016/j.matchemphys.2003.09.006>.
- [67] H. Zeng, C. Zhao, J. Qiu, Y. Yang, G. Chen, Preparation and optical properties of silver nanoparticles induced by a femtosecond laser irradiation, *J. Cryst. Growth.* 300 (2007) 519–522, <https://doi.org/10.1016/j.jcrysgro.2006.11.308>.
- [68] S. Stoeva, K.J. Klabunde, C.M. Sorensen, I. Dragieva, Gram-scale synthesis of monodisperse gold colloids by the solvated metal atom dispersion method and digestive ripening and their organization into two- and three-dimensional structures, *J. Am. Chem. Soc.* 124 (2002) 2305–2311, <https://doi.org/10.1021/ja012076g>.
- [69] A.B. Smetana, K.J. Klabunde, G.R. Marchin, C.M. Sorensen, Biocidal activity of nanocrystalline silver powders and particles, *Langmuir* 24 (2008) 7457–7464, <https://doi.org/10.1021/la800091y>.
- [70] S.S. Djokić, R.E. Burrell, Behavior of silver in physiological solutions, *J. Electrochem. Soc.* 145 (1998) 1426–1430, <https://doi.org/10.1149/1.1838499>.
- [71] C.-M. Ho, C.-K. Wong, S.K.-W. Yau, C.-N. Lok, C.-M. Che, Oxidative dissolution of silver nanoparticles by dioxigen: a kinetic and mechanistic study, *Chem. Asian J.* 6 (2011) 2506–2511, <https://doi.org/10.1002/asia.201100034>.
- [72] C.-N. Lok, C.-M. Ho, R. Chen, Q.-Y. He, W.-Y. Yu, H. Sun, P.K.-H. Tam, J.-F. Chiu, C.-M. Che, Silver nanoparticles: partial oxidation and antibacterial activities, *JBC J. Biol. Inorg. Chem.* 12 (2007) 527–534, <https://doi.org/10.1007/s00775-007-0208-z>.
- [73] S. Kittler, C. Greulich, J. Diendorf, M. Köller, M. Epple, Toxicity of silver nanoparticles increases during storage because of slow dissolution under release of silver ions, *Chem. Mater.* 22 (2010) 4548–4554, <https://doi.org/10.1021/cm100023p>.
- [74] Z. Xiu, Q. Zhang, H.L. Puppala, V.L. Colvin, P.J.J. Alvarez, Negligible particle-specific antibacterial activity of silver nanoparticles, *Nano Lett.* 12 (2012) 4271–4275, <https://doi.org/10.1021/nl301934w>.
- [75] C. Levard, B.C. Reinsch, F.M. Michel, C. Oumahi, G.V. Lowry, G.E. Brown, Sulfidation processes of PVP-coated silver nanoparticles in aqueous solution: impact on dissolution rate, *Environ. Sci. Technol.* 45 (2011) 5260–5266, <https://doi.org/10.1021/es2007758>.
- [76] X. Li, J.J. Lenhart, Aggregation and dissolution of silver nanoparticles in natural surface water, *Environ. Sci. Technol.* 46 (2012) 5378–5386, <https://doi.org/10.1021/es204531y>.
- [77] M. Baalousha, Y. Nur, I. Römer, M. Tejamaya, J.R. Lead, Effect of monovalent and divalent cations, anions and fulvic acid on aggregation of citrate-coated silver nanoparticles, *Sci. Total Environ.* 454–455 (2013) 119–131, <https://doi.org/10.1016/j.scitotenv.2013.02.093>.
- [78] K.A. Huynh, K.L. Chen, Aggregation kinetics of citrate and polyvinylpyrrolidone coated silver nanoparticles in monovalent and divalent electrolyte solutions, *Environ. Sci. Technol.* 45 (2011) 5564–5571, <https://doi.org/10.1021/es200157h>.
- [79] J. Dobias, R. Bernier-Latmani, Silver release from silver nanoparticles in natural waters, *Environ. Sci. Technol.* 47 (2013) 4140–4146, <https://doi.org/10.1021/es304023p>.
- [80] A. Henglein, Colloidal silver nanoparticles: photochemical preparation and interaction with O₂, CCl₄, and some metal ions, *Chem. Mater.* 10 (1998) 444–450, <https://doi.org/10.1021/cm970613j>.
- [81] O. Choi, T.E. Cleveenger, B. Deng, R.Y. Surampalli, L. Ross, Z. Hu, Role of sulfide and ligand strength in controlling nanosilver toxicity, *Water Res.* 43 (2009) 1879–1886, <https://doi.org/10.1016/j.watres.2009.01.029>.
- [82] B.C. Reinsch, C. Levard, Z. Li, R. Ma, A. Wise, K.B. Gregory, G.E. Brown, G.V. Lowry, Sulfidation of silver nanoparticles decreases *Escherichia coli* growth inhibition, *Environ. Sci. Technol.* 46 (2012) 6992–7000, <https://doi.org/10.1021/es203732x>.
- [83] C. Levard, E.M. Hotze, B.P. Colman, A.L. Dale, L. Truong, X.Y. Yang, A.J. Bone, G. E. Brown, R.L. Tanguay, R.T. Di Giulio, E.S. Bernhardt, J.N. Meyer, M.R. Wiesner, G.V. Lowry, Sulfidation of silver nanoparticles: natural antidiote to their toxicity, *Environ. Sci. Technol.* 47 (2013) 13440–13448, <https://doi.org/10.1021/es403527n>.
- [84] J. Liu, D.A. Sonshine, S. Shervani, R.H. Hurt, Controlled release of biologically active silver from nanosilver surfaces, *ACS Nano.* 4 (2010) 6903–6913, <https://doi.org/10.1021/nn102272n>.
- [85] W. Zhang, Y. Yao, N. Sullivan, Y. Chen, Modeling the primary size effects of citrate-coated silver nanoparticles on their ion release kinetics, *Environ. Sci. Technol.* 45 (2011) 4422–4428, <https://doi.org/10.1021/es104205a>.
- [86] E. Bae, H.-J. Park, J. Lee, Y. Kim, J. Yoon, K. Park, K. Choi, J. Yi, Bacterial cytotoxicity of the silver nanoparticle related to physicochemical metrics and agglomeration properties, *Environ. Toxicol. Chem.* 29 (2010) 2154–2160, <https://doi.org/10.1002/etc.278>.
- [87] S. Pal, Y.K. Tak, J.M. Song, Does the antibacterial activity of silver nanoparticles depend on the shape of the nanoparticle? A study of the Gram-negative bacterium *Escherichia coli*, *Appl. Environ. Microbiol.* 73 (2007) 1712–1720, <https://doi.org/10.1128/AEM.02218-06>.
- [88] B. Sadeghi, F.S. Garmaroudi, M. Hashemi, H.R. Nezhad, A. Nasrollahi, S. Ardalan, Comparison of the anti-bacterial activity on the nanosilver shapes: nanoparticles, nanorods and nanoplates, *Adv. Powder Technol.* 23 (2012) 22–26, <https://doi.org/10.1016/j.apt.2010.11.011>.
- [89] J.R. Morones, J.L. Elechiguerra, A. Camacho, K. Holt, J.B. Kouri, J.T. Ramírez, M.J. Yacaman, The bactericidal effect of silver nanoparticles, *Nanotechnology* 16 (2005) 2346–2353, <https://doi.org/10.1088/0957-4484/16/10/059>.
- [90] J. Schnadt, J. Knudsen, X.L. Hu, A. Michaelides, R.T. Vang, K. Reuter, Z. Li, E. Lægsgaard, M. Scheffler, F. Besenbacher, Experimental and theoretical study of oxygen adsorption structures on Ag(111), *Phys. Rev. B* 80 (2009), <https://doi.org/10.1103/PhysRevB.80.075424>.
- [91] I. Sondi, B. Salopek-Sondi, Silver, nanoparticles as antimicrobial agent: a case study on *E. coli* as a model for Gram-negative bacteria, *J. Colloid Interface Sci.* 275 (2004) 177–182, <https://doi.org/10.1016/j.jcis.2004.02.012>.
- [92] E.-J. Park, J. Yi, Y. Kim, K. Choi, K. Park, Silver nanoparticles induce cytotoxicity by a Trojan-horse type mechanism, *Toxicol. In Vitro.* 24 (2010) 872–878, <https://doi.org/10.1016/j.tiv.2009.12.001>.
- [93] N. Lewinski, V. Colvin, R. Drezek, Cytotoxicity of nanoparticles, *Small Weinheim. Bergstr. Ger.* 4 (2008) 26–49, <https://doi.org/10.1002/smll.200700595>.
- [94] M. Banerjee, S. Mallick, A. Paul, A. Chattopadhyay, S.S. Ghosh, Heightened reactive oxygen species generation in the antimicrobial activity of a three component iodinated chitosan-silver nanoparticle composite, *Langmuir* 26 (2010) 5901–5908, <https://doi.org/10.1021/la9038528>.
- [95] A.M. El Badawy, R.G. Silva, B. Morris, K.G. Scheckel, M.T. Suidan, T.M. Tolaymat, Surface charge-dependent toxicity of silver nanoparticles, *Environ. Sci. Technol.* 45 (2011) 283–287, <https://doi.org/10.1021/es1034188>.
- [96] D. Walczyk, F.B. Bombelli, M.P. Monopoli, I. Lynch, K.A. Dawson, What the cell “sees” in bionanoscience, *J. Am. Chem. Soc.* 132 (2010) 5761–5768, <https://doi.org/10.1021/ja910675v>.
- [97] T.-O. Peulen, K.J. Wilkinson, Diffusion of nanoparticles in a biofilm, *Environ. Sci. Technol.* 45 (2011) 3367–3373, <https://doi.org/10.1021/es103450g>.
- [98] M. Golmohamadi, R.J. Clark, J.G.C. Veinot, K.J. Wilkinson, The role of charge on the diffusion of solutes and nanoparticles (silicon nanocrystals, nTiO₂, nAu) in a biofilm, *Environ. Chem.* 10 (2013) 34–41, <https://doi.org/10.1071/EN12106>.
- [99] O. Choi, C.-P. Yu, G. Esteban Fernández, Z. Hu, Interactions of nanosilver with *Escherichia coli* cells in planktonic and biofilm cultures, *Water Res.* 44 (2010) 6095–6103, <https://doi.org/10.1016/j.watres.2010.06.069>.

- [100] C. Baerlocher, D.H. Olson, W.M. Meier, *Atlas of zeolite framework types (formerly: atlas of zeolite structure types)*, Elsevier, 2001.
- [101] C. Colella, Ion exchange equilibria in zeolite minerals, *Miner. Deposita* 31 (1996) 554–562, <https://doi.org/10.1007/BF00196136>.
- [102] H.S. Sherry, The ion-exchange properties of zeolites. I. Univalent ion exchange in synthetic faujasite, *J. Phys. Chem.* 70 (1966) 1158–1168, <https://doi.org/10.1021/j100876a031>.
- [103] B. Wang, Y. Li, C. Shao, M. Cui, P.K. Dutta, Rapid and high yield synthesis method of colloidal nano faujasite, *Microporous Mesoporous Mater.* 230 (2016) 89–99, <https://doi.org/10.1016/j.micromeso.2016.05.001>.
- [104] S.H. Lee, Y. Kim, K. Seff, Weak Ag⁺–Ag⁺ bonding in zeolite X. Crystal structures of Ag₉₂Si₁₀₀Al₉₂O₃₈₄ hydrated and fully dehydrated in flowing oxygen, *Microporous Mesoporous Mater.* 41 (2000) 49–59, [https://doi.org/10.1016/S1387-1811\(00\)00270-5](https://doi.org/10.1016/S1387-1811(00)00270-5).
- [105] Y.M. Lee, S.J. Choi, Y. Kim, K. Seff, Crystal structure of an ethylene sorption complex of fully vacuum-dehydrated fully Ag⁺-exchanged zeolite X (FAU). Silver atoms have reduced ethylene to give CH₂²⁻ carbanions at framework oxide vacancies, *J. Phys. Chem. B* 109 (2005) 20137–20144, <https://doi.org/10.1021/jp058185p>.
- [106] A. Top, S. Ülkü, Silver, zinc, and copper exchange in a Na-clinoptilolite and resulting effect on antibacterial activity, *Appl. Clay Sci.* 27 (2004) 13–19, <https://doi.org/10.1016/j.clay.2003.12.002>.
- [107] L. Akhigbe, S. Ouki, D. Saroj, X.M. Lim, Silver-modified clinoptilolite for the removal of *Escherichia coli* and heavy metals from aqueous solutions, *Environ. Sci. Pollut. Res.* 21 (2014) 10940–10948, <https://doi.org/10.1007/s11356-014-2888-6>.
- [108] R. Guerra, E. Lima, M. Viniegra, A. Guzmán, V. Lara, Growth of *Escherichia coli* and *Salmonella typhi* inhibited by fractal silver nanoparticles supported on zeolites, *Microporous Mesoporous Mater.* 147 (2012) 267–273, <https://doi.org/10.1016/j.micromeso.2011.06.031>.
- [109] N.S. Flores-López, J. Castro-Rosas, R. Ramírez-Bon, A. Mendoza-Córdova, E. Larios-Rodríguez, M. Flores-Acosta, Synthesis and properties of crystalline silver nanoparticles supported in natural zeolite chabazite, *J. Mol. Struct.* 1028 (2012) 110–115, <https://doi.org/10.1016/j.molstruc.2012.05.080>.
- [110] K. Kawahara, K. Tsuruda, M. Morishita, M. Uchida, Antibacterial effect of silver-zeolite on oral bacteria under anaerobic conditions, *Dent. Mater.* 16 (2000) 452–455, [https://doi.org/10.1016/S0109-5641\(00\)00050-6](https://doi.org/10.1016/S0109-5641(00)00050-6).
- [111] Y. Matsumura, K. Yoshikata, S. Kunisaki, T. Tsuchido, Mode of bactericidal action of silver zeolite and its comparison with that of silver nitrate, *Appl. Environ. Microbiol.* 69 (2003) 4278–4281, <https://doi.org/10.1128/AEM.69.7.4278-4281.2003>.
- [112] Y. Zhang, S. Zhong, M. Zhang, Y. Lin, Antibacterial activity of silver-loaded zeolite A prepared by a fast microwave-loading method, *J. Mater. Sci.* 44 (2009) 457–462, <https://doi.org/10.1007/s10853-008-3129-5>.
- [113] K.K. Krishnani, Y. Zhang, L. Xiong, Y. Yan, R. Boopathy, A. Mulchandani, Bactericidal and ammonia removal activity of silver ion-exchanged zeolite, *Bioresour. Technol.* 117 (2012) 86–91, <https://doi.org/10.1016/j.biortech.2012.04.044>.
- [114] P. Kaali, G. Czél, Single, binary and ternary ion exchanged zeolite as an effective bioactive filler for biomedical polymer composites, *Mater. Sci. Forum* 729 (2013) 234–239, <https://doi.org/10.4028/www.scientific.net/MSF.729.234>.
- [115] Y. Zhou, Y. Deng, P. He, F. Dong, Y. Xia, Y. He, Antibacterial zeolite with a high silver-loading content and excellent antibacterial performance, *RSC Adv.* 4 (2014) 5283–5288, <https://doi.org/10.1039/C3RA44750B>.
- [116] D. Jiraroj, S. Tungasmita, D.N. Tungasmita, Silver ions and silver nanoparticles in zeolite A composites for antibacterial activity, *Powder Technol.* 264 (2014) 418–422, <https://doi.org/10.1016/j.powtec.2014.05.049>.
- [117] S. Demirci, Z. Ustaoglu, G.A. Yilmazer, F. Sahin, N. Baç, Antimicrobial properties of zeolite-X and zeolite-A ion-exchanged with silver, copper, and zinc against a broad range of microorganisms, *Appl. Biochem. Biotechnol.* 172 (2014) 1652–1662, <https://doi.org/10.1007/s12010-013-0647-7>.
- [118] B. Kwakye-Awuah, C. Williams, M.A. Kenward, I. Radecka, Antimicrobial action and efficiency of silver-loaded zeolite X, *J. Appl. Microbiol.* 104 (2007) 1516–1524, <https://doi.org/10.1111/j.1365-2672.2007.03673.x>.
- [119] Y. Inoue, M. Kogure, K. Matsumoto, H. Hamashima, M. Tsukada, K. Endo, T. Tanaka, Light irradiation is a factor in the bactericidal activity of silver-loaded zeolite, *Chem. Pharm. Bull. (Tokyo)* 56 (2008) 692–694.
- [120] K. Shameli, M.B. Ahmad, M. Zargar, W.M.Z.W. Yunus, N.A. Ibrahim, Fabrication of silver nanoparticles doped in the zeolite framework and antibacterial activity, *Int. J. Nanomed.* 6 (2011) 331–341, <https://doi.org/10.2147/IJN.S16964>.
- [121] L. Ferreira, A.M. Fonseca, G. Botelho, C.A.- Aguiar, I.C. Neves, Antimicrobial activity of faujasite zeolites doped with silver, *Microporous Mesoporous Mater.* 160 (2012) 126–132, <https://doi.org/10.1016/j.micromeso.2012.05.006>.
- [122] Y. Inoue, H. Hamashima, Effect of silver loaded zeolite on the susceptibility of *Escherichia coli* against antibiotics, *J. Biomater. Nanobiotechnol.* 3 (2012) 114–117.
- [123] L. Ferreira, C. Almeida-Aguiar, P. Parpot, A.M. Fonseca, I.C. Neves, Preparation and assessment of antimicrobial properties of bimetallic materials based on NaY zeolite, *RSC Adv.* 5 (2015) 37188–37195, <https://doi.org/10.1039/C5RA04960A>.
- [124] V.V. Singh, B. Jurado-Sánchez, S. Sattayasamitsathit, J. Orozco, J. Li, M. Galarnyk, Y. Fedorak, J. Wang, Multifunctional silver-exchanged zeolite micromotors for catalytic detoxification of chemical and biological threats, *Adv. Funct. Mater.* 25 (2015) 2147–2155, <https://doi.org/10.1002/adfm.201500033>.
- [125] L. Ferreira, J.F. Guedes, C. Almeida-Aguiar, A.M. Fonseca, I.C. Neves, Microbial growth inhibition caused by Zn/Ag-Y zeolite materials with different amounts of silver, *Colloids Surf. B Biointerfaces* 142 (2016) 141–147, <https://doi.org/10.1016/j.colsurfb.2016.02.042>.
- [126] S.A.M. Hanim, N.A.N.N. Malek, Z. Ibrahim, Amine-functionalized, silver-exchanged zeolite NaY: preparation, characterization and antibacterial activity, *Appl. Surf. Sci.* 360 (2016) 121–130, <https://doi.org/10.1016/j.apsusc.2015.11.010>.
- [127] S. Chen, J. Popovich, N. Iannuzo, S.E. Haydel, D.-K. Seo, Silver-ion-exchanged nanostructured zeolite X as antibacterial agent with superior ion release kinetics and efficacy against methicillin-resistant *Staphylococcus aureus*, *ACS Appl. Mater. Interfaces.* 9 (2017) 39271–39282, <https://doi.org/10.1021/acsmi.7b15001>.
- [128] H.F. Youssef, M.S. Abdel-Aziz, F.K. Fouda, Evaluation of antimicrobial activity of different silver-exchanged nano and micronized zeolites prepared by microwave technique, *J. Porous Mater.* 24 (2017) 947–957, <https://doi.org/10.1007/s10934-016-0334-5>.
- [129] B. Dong, S. Belkhair, M. Zaarour, L. Fisher, J. Verran, L. Tosheva, R. Retoux, J.-P. Gilson, S. Mintova, Silver confined within zeolite EMT nanoparticles: preparation and antibacterial properties, *Nanoscale* 6 (2014) 10859–10864, <https://doi.org/10.1039/c4nr03169e>.
- [130] O.E. Jaime-Acuña, A. Meza-Villezas, M. Vasquez-Peña, O. Raymond-Herrera, H. Villavicencio-García, V. Petranovskii, R. Vazquez-Duhalt, A. Huerta-Saqueró, Synthesis and complete antimicrobial characterization of CEOBACTER, an Ag-based nanocomposite, *PLoS ONE* 11 (2016) 1–18, <https://doi.org/10.1371/journal.pone.0166205>.
- [131] L. Lv, Y. Luo, W.J. Ng, X.S. Zhao, Bactericidal activity of silver nanoparticles supported on microporous titanasilicate ETS-10, *Microporous Mesoporous Mater.* 120 (2009) 304–309, <https://doi.org/10.1016/j.micromeso.2008.11.028>.
- [132] R. Guerra, E. Lima, A. Guzmán, Antimicrobial supported nanoparticles: Gold versus silver for the cases of *Escherichia coli* and *Salmonella typhi*, *Microporous Mesoporous Mater.* 170 (2013) 62–66, <https://doi.org/10.1016/j.micromeso.2012.11.036>.
- [133] P. Lalueza, M. Monzón, M. Arruebo, J. Santamaría, Antibacterial action of Ag-containing MFI zeolite at low Ag loadings, *Chem. Commun.* 47 (2010) 680–682, <https://doi.org/10.1039/C0CC03905E>.
- [134] P. Lalueza, D. Carmona, M. Monzón, M. Arruebo, J. Santamaría, Strong bactericidal synergy between peracetic acid and silver-exchanged zeolites, *Microporous Mesoporous Mater.* 156 (2012) 171–175, <https://doi.org/10.1016/j.micromeso.2012.02.035>.
- [135] M.S.-L. Yee, P.S. Khiew, Y.F. Tan, W.S. Chiu, Y.-Y. Kok, C.-O. Leong, Low temperature, rapid solution growth of antifouling silver-zeolite nanocomposite clusters, *Microporous Mesoporous Mater.* 218 (2015) 69–78, <https://doi.org/10.1016/j.micromeso.2015.07.004>.
- [136] M.J. Sánchez, J.E. Mauricio, A.R. Paredes, P. Gamero, D. Cortés, Antimicrobial properties of ZSM-5 type zeolite functionalized with silver, *Mater. Lett.* 191 (2017) 65–68, <https://doi.org/10.1016/j.matlet.2017.01.039>.
- [137] P. Saint-Cricq, Y. Kamimura, K. Itabashi, A. Sugawara-Narutaki, A. Shimojima, T. Okubo, Antibacterial activity of silver-loaded “green zeolites”, *Eur. J. Inorg. Chem.* 2012 (2012) 3398–3402, <https://doi.org/10.1002/ejic.201200476>.
- [138] L. Tosheva, S. Belkhair, M. Gackowski, S. Malic, N. Al-Shanti, J. Verran, Rapid screening of the antimicrobial efficacy of Ag zeolites, *Colloids Surf. B Biointerfaces* 157 (2017) 254–260, <https://doi.org/10.1016/j.colsurfb.2017.06.001>.
- [139] S. Sabbani, D. Gallego-Perez, A. Nagy, W. James Waldman, D. Hansford, P.K. Dutta, Synthesis of silver-zeolite films on micropatterned porous alumina and its application as an antimicrobial substrate, *Microporous Mesoporous Mater.* 135 (2010) 131–136, <https://doi.org/10.1016/j.micromeso.2010.06.020>.
- [140] Y. Inoue, M. Hoshino, H. Takahashi, T. Noguchi, T. Murata, Y. Kanzaki, H. Hamashima, M. Sasatsu, Bactericidal activity of Ag-zeolite mediated by reactive oxygen species under aerated conditions, *J. Inorg. Biochem.* 92 (2002) 37–42.
- [141] H. Shi, L. Xue, A. Gao, Q. Zhou, Dual layer hollow fiber PVDF ultra-filtration membranes containing Ag nano-particle loaded zeolite with longer term anti-bacterial capacity in salt water, *Water Sci. Technol. J. Int. Assoc. Water Pollut. Res.* 73 (2016) 2159–2167, <https://doi.org/10.2166/wst.2016.062>.
- [142] S.M. Abo El Ola, R. Kotek, M. King, J.H. Kim, R. Monticello, J.A. Reeve, Studies on poly(trimethylene terephthalate) filaments containing silver, *J. Biomater. Sci. Polym. Ed.* 15 (2004) 1545–1559.
- [143] K. Kamsıoğlu, E.A. Aksoy, B. Akata, N. Hasirci, N. Baç, Preparation and characterization of antibacterial zeolite-polyurethane composites, *J. Appl. Polym. Sci.* 110 (2008) 2854–2861, <https://doi.org/10.1002/app.28838>.
- [144] P. Kaali, E. Strömberg, R.E. Aune, G. Czél, D. Momcilovic, S. Karlsson, Antimicrobial properties of Ag⁺ loaded zeolite polyester polyurethane and silicone rubber and long-term properties after exposure to in-vitro ageing, *Polym. Degrad. Stab.* 95 (2010) 1456–1465, <https://doi.org/10.1016/j.polydegdstab.2010.06.024>.
- [145] P. Kaali, M.M. Perez-Madriral, E. Stromberg, R.E. Aune, G. Czél, S. Karlsson, The influence of Ag⁺, Zn²⁺ and Cu²⁺ exchanged zeolite on antimicrobial and long term in vitro stability of medical grade polyether polyurethane, *Express Polym. Lett.* 5 (2011) 1028–1040, <https://doi.org/10.3144/expresspolymlett.2011.101>.

- [146] M.L. Lind, B.-H. Jeong, A. Subramani, X. Huang, E.M.V. Hoek, Effect of mobile cation on zeolite-polyamide thin film nanocomposite membranes, *J. Mater. Res.* 24 (2009) 1624–1631, <https://doi.org/10.1557/jmr.2009.0189>.
- [147] X. Xu, H. Ding, B.K. Wang, Preparation and performance of Ag⁺-Zn²⁺-zeolite antimicrobial and antibacterial plastic, *Adv. Mater. Res.* 96 (2010) 151–154, <https://doi.org/10.4028/www.scientific.net/AMR.96.151>.
- [148] D.L. Boschetto, L. Lerin, R. Cansian, S.B.C. Pergher, M. Di Luccio, Preparation and antimicrobial activity of polyethylene composite films with silver exchanged zeolite-Y, *Chem. Eng. J.* 204–206 (2012) 210–216, <https://doi.org/10.1016/j.cej.2012.07.111>.
- [149] M. Cushen, J. Kerry, M. Morris, M. Cruz-Romero, E. Cummins, Silver migration from nanosilver and a commercially available zeolite filler polyethylene composites to food simulants, *Food Addit. Contam. Part A Chem. Anal. Control Expo. Risk Assess.* 31 (2014) 1132–1140, <https://doi.org/10.1080/19440049.2014.905874>.
- [150] E.M.V. Hoek, A.K. Ghosh, X. Huang, M. Liong, J.I. Zink, Physical–chemical properties, separation performance, and fouling resistance of mixed-matrix ultrafiltration membranes, *Desalination* 283 (2011) 89–99, <https://doi.org/10.1016/j.desal.2011.04.008>.
- [151] D. Zampino, T. Ferreri, C. Puglisi, M. Mancuso, R. Zaccone, R. Scaffaro, D. Bennardo, PVC silver zeolite composites with antimicrobial properties, *J. Mater. Sci.* 46 (2011) 6734, <https://doi.org/10.1007/s10853-011-5629-y>.
- [152] M.J. Kim, T.H. Oh, S.S. Han, S.W. Joo, H.Y. Jeon, D.W. Chang, Preparation of poly(vinyl alcohol)/silver-zeolite composite hydrogels by UV-irradiation, *Fibers Polym.* 15 (2014) 101–107, <https://doi.org/10.1007/s12221-014-0101-7>.
- [153] J. Wu, C. Yu, Q. Li, Novel regenerable antimicrobial nanocomposite membranes: Effect of silver loading and valence state, *J. Membr. Sci.* 531 (2017) 68–76, <https://doi.org/10.1016/j.memsci.2017.02.047>.
- [154] S. Belkhair, M. Kinninmonth, L. Fisher, B. Gasharova, C.M. Liauw, J. Verran, B. Mihailova, L. Tosheva, Silver zeolite-loaded silicone elastomers: a multidisciplinary approach to synthesis and antimicrobial assessment, *RSC Adv.* 5 (2015) 40932–40939, <https://doi.org/10.1039/C5RA03856A>.
- [155] C. Hamciuc, E. Hamciuc, D. Popovici, A.I. Danaila, M. Butnaru, C. Rimbu, C. Carp-Carare, Y. Kalvachev, Biocompatible poly(ether-ether-ketone)/Ag-zeolite L composite films with antimicrobial properties, *Mater. Lett.* 212 (2018) 339–342, <https://doi.org/10.1016/j.matlet.2017.10.120>.
- [156] A. Fernández, E. Soriano, P. Hernández-Muñoz, R. Gavara, Migration of antimicrobial silver from composites of polylactide with silver zeolites, *J. Food Sci.* 75 (2010) E186–E193, <https://doi.org/10.1111/j.1750-3841.2010.01549.x>.
- [157] C. Praprudivongs, N. Sombatsompop, Wood, silver-substituted zeolite and triclosan as biodegradation controllers and antibacterial agents for poly(lactic acid) (PLA) and PLA composites, *J. Thermoplast. Compos. Mater.* 30 (2017) 583–598, <https://doi.org/10.1177/0892705715604683>.
- [158] K. Jai-eau, E. Womolmal, N. Sombatsompop, Cure behavior and antimicrobial performance of sulfur-cured natural rubber vulcanizates containing 2-hydroxypropyl-3-piperazinylquinoxalinecarboxylic acid methacrylate or silver-substituted zeolite, *J. Vinyl Addit. Technol.* 19 (2013) 123–131, <https://doi.org/10.1002/vnl.20330>.
- [159] S. Shankar, L.-F. Wang, J.-W. Rhim, Preparations and characterization of alginate/silver composite films: effect of types of silver particles, *Carbohydr. Polym.* 146 (2016) 208–216, <https://doi.org/10.1016/j.carbpol.2016.03.026>.
- [160] H.M. Lim, J.S. Jung, B.Y. Kim, S.H. Lee, Application of zeolites on cellulose fiber, *Key Eng. Mater.* 317 (2006) 777–780.
- [161] K.A. Rieger, H.J. Cho, H.F. Yeung, W. Fan, J.D. Schiffman, Antimicrobial activity of silver ions released from zeolites immobilized on cellulose nanofiber mats, *ACS Appl. Mater. Interfaces* 8 (2016) 3032–3040, <https://doi.org/10.1021/acsami.5b10130>.
- [162] F.A.P. Scacchetti, E. Pinto, G.M.B. Soares, Thermal and antimicrobial evaluation of cotton functionalized with a chitosan-zeolite composite and microcapsules of phase-change materials, *J. Appl. Polym. Sci.* 135 (2018) 46135, <https://doi.org/10.1002/app.46135>.
- [163] L. Geranio, M. Heuberger, B. Nowack, The behavior of silver nanotextiles during washing, *Environ. Sci. Technol.* 43 (2009) 8113–8118, <https://doi.org/10.1021/es9018332>.
- [164] T.M. Benn, P. Westerhoff, Nanoparticle silver released into water from commercially available sock fabrics, *Environ. Sci. Technol.* 42 (2008) 4133–4139, <https://doi.org/10.1021/es7032718>.
- [165] B. Galeano, E. Korff, W.L. Nicholson, Inactivation of vegetative cells, but not spores, of *Bacillus anthracis*, *B. cereus*, and *B. subtilis* on stainless steel surfaces coated with an antimicrobial silver- and zinc-containing zeolite formulation, *Appl. Environ. Microbiol.* 69 (2003) 4329–4331, <https://doi.org/10.1128/AEM.69.7.4329-4331.2003>.
- [166] M.M. Cowan, K.Z. Abshire, S.L. Houk, S.M. Evans, Antimicrobial efficacy of a silver-zeolite matrix coating on stainless steel, *J. Ind. Microbiol. Biotechnol.* 30 (2003) 102–106, <https://doi.org/10.1007/s10295-002-0022-0>.
- [167] A.M.P. McDonnell, D. Beving, A. Wang, W. Chen, Y. Yan, Hydrophilic and antimicrobial zeolite coatings for gravity-independent water separation, *Adv. Funct. Mater.* 15 (2005) 336–340, <https://doi.org/10.1002/adfm.200400183>.
- [168] R.S. Bedi, R. Cai, C. O'Neill, D.E. Beving, S. Foster, S. Guthrie, W. Chen, Y. Yan, Hydrophilic and antimicrobial Ag-exchanged zeolite coatings: a year-long durability study and preliminary evidence for their general microbiocidal efficacy to bacteria, fungus and yeast, *Microporous Mesoporous Mater.* 151 (2012) 352–357, <https://doi.org/10.1016/j.micromeso.2011.10.012>.
- [169] J. Wang, Z. Wang, S. Guo, J. Zhang, Y. Song, X. Dong, X. Wang, J. Yu, Antibacterial and anti-adhesive zeolite coatings on titanium alloy surface, *Microporous Mesoporous Mater.* 146 (2011) 216–222, <https://doi.org/10.1016/j.micromeso.2011.04.005>.
- [170] N. Padachev, V. Patel, P. Santerre, D. Cvitkovitch, H.P. Lawrence, S. Friedman, Resistance of a novel root canal sealer to bacterial ingress in vitro, *J. Endod.* 26 (2000) 656–659, <https://doi.org/10.1097/00004770-200011000-00006>.
- [171] Y. Abe, M. Ishii, M. Takeuchi, M. Ueshige, S. Tanaka, Y. Akagawa, Effect of saliva on antimicrobial tissue conditioner containing silver-zeolite, *J. Oral Rehabil.* 31 (2004) 568–573, <https://doi.org/10.1111/j.1365-2842.2004.01267.x>.
- [172] L.A. Casemiro, C.H.G. Martins, F. de C.P. Pires-de-Souza, H. Panzeri, Antimicrobial and mechanical properties of acrylic resins with incorporated silver-zinc zeolite – part I, *Gerodontology* 25 (2008) 187–194, <https://doi.org/10.1111/j.1741-2358.2007.00198.x>.
- [173] M.E. Odabaş, C. Cinar, G. Akça, I. Araz, T. Ulusu, H. Yücel, Short-term antimicrobial properties of mineral trioxide aggregate with incorporated silver-zeolite, *Dent. Traumatol.* 27 (2011) 189–194, <https://doi.org/10.1111/j.1600-9657.2011.00986.x>.
- [174] M. Saravanan, V.A. Kumar, T.V. Padmanabhan, F. Banu, Viscoelastic properties and antimicrobial effects of soft liners with silver zeolite in complete dental prosthesis wearers: an in vivo study, *Int. J. Prosthodont.* 28 (2015) 265–269, <https://doi.org/10.11607/ijp.3740>.
- [175] S.B. Ghivari, H. Bhattacharya, K.G. Bhat, M.A. Pujar, Antimicrobial activity of root canal irrigants against biofilm forming pathogens – An in vitro study, *J. Conserv. Dent.* 20 (2017) 147, https://doi.org/10.4103/JCD.JCD_38_16.
- [176] T. Nakane, H. Gomyo, I. Sasaki, Y. Kimoto, N. Hanzawa, Y. Teshima, T. Namba, New anti-axillary odour deodorant made with antimicrobial Ag-zeolite (silver-exchanged zeolite), *Int. J. Cosmet. Sci.* 28 (2006) 299–309, <https://doi.org/10.1111/j.1467-2494.2006.00322.x>.
- [177] R. Rizzetto, A. Mansi, D. Panatto, E. Rizzitelli, C. Tinteri, T. Sasso, R. Gasparini, P. Crovari, Silver zeolite antimicrobial activity in aluminium heating, ventilation and air conditioning system ducts, *J. Prev. Med. Hyg.* 49 (2008) 26–33.
- [178] C. Tinteri, M. Potenza, R. Rizzetto, Antimicrobial efficacy and longevity of silver+zeolite incorporating preinsulated ducts installed in real healthcare settings, *J. Prev. Med. Hyg.* 53 (2012) 177–180.
- [179] B.A. Potter, M. Lob, R. Mercaldo, A. Hetzler, V. Kaistha, H. Khan, N. Kingston, M. Knoll, B. Maloy-Franklin, K. Melvin, P. Ruiz-Pelet, N. Ozsoy, E. Schmitt, L. Wheeler, M. Potter, M.A. Rutter, G. Yahn, D.H. Parente, A long-term study examining the antibacterial effectiveness of Agion silver zeolite technology on door handles within a college campus, *Let. Appl. Microbiol.* 60 (2015) 120–127, <https://doi.org/10.1111/lam.12356>.
- [180] T. Haile, G. Nakhla, E. Allouche, Evaluation of the resistance of mortars coated with silver bearing zeolite to bacterial-induced corrosion, *Corros. Sci.* 50 (2008) 713–720, <https://doi.org/10.1016/j.corsci.2007.08.012>.
- [181] T. Haile, G. Nakhla, The inhibitory effect of antimicrobial zeolite on the biofilm of *Acidithiobacillus thiooxidans*, *Biodegradation* 21 (2010) 123–134, <https://doi.org/10.1007/s10532-009-9287-6>.
- [182] J. Lee, Y.-H. Lee, K. Jones, E. Sharek, M.A. Pascall, Antimicrobial packaging of raw beef, pork and turkey using silver-zeolite incorporated into the material, *Int. J. Food Sci. Technol.* 46 (2011) 2382–2386, <https://doi.org/10.1111/j.1365-2621.2011.02760.x>.
- [183] R.J. Jędrzejczyk, K. Turnau, P.J. Jodłowski, D.K. Chlebda, T. Łojewski, J. Łojewska, Antimicrobial properties of silver cations substituted to faujasite mineral, *Nanomaterials* 7 (2017), <https://doi.org/10.3390/nano7090240>.
- [184] T. Møretro, G.S. Høiby-Petersen, C.K. Halvorsen, S. Langsrud, Antibacterial activity of cutting boards containing silver, *Food Control.* 28 (2012) 118–121, <https://doi.org/10.1016/j.foodcont.2012.05.007>.
- [185] A. Griffith, S. Neethirajan, K. Warriner, Development and evaluation of silver zeolite antifouling coatings on stainless steel for food contact surfaces, *J. Food Saf.* 35 (2015) 345–354, <https://doi.org/10.1111/jfs.12181>.
- [186] Ç. Soysal, H. Bozkurt, E. Dirican, M. Güçlü, E.D. Bozhüyük, A.E. Uslu, S. Kaya, Effect of antimicrobial packaging on physicochemical and microbial quality of chicken drumsticks, *Food Control.* 54 (2015) 294–299, <https://doi.org/10.1016/j.foodcont.2015.02.009>.
- [187] J. Fabrega, S.N. Luoma, C.R. Tyler, T.S. Galloway, J.R. Lead, Silver nanoparticles: behaviour and effects in the aquatic environment, *Environ. Int.* 37 (2011) 517–531, <https://doi.org/10.1016/j.envint.2010.10.012>.
- [188] J. Pulit-Prociak, K. Stokłosa, M. Banach, Nanosilver products and toxicity, *Environ. Chem. Lett.* 13 (2015) 59–68, <https://doi.org/10.1007/s10311-014-0490-2>.
- [189] M.C. Stensberg, Q. Wei, E.S. McLamore, D.M. Porterfield, A. Wei, M.S. Sepúlveda, Toxicological studies on silver nanoparticles: challenges and opportunities in assessment, monitoring and imaging, *Nanomedicine* 6 (2011) 879–898, <https://doi.org/10.2217/nmm.11.78>.
- [190] F. Gottschalk, T. Sonderer, R.W. Scholz, B. Nowack, Modeled environmental concentrations of engineered nanomaterials (TiO₂, ZnO, Ag, CNT, fullerenes) for different regions, *Environ. Sci. Technol.* 43 (2009) 9216–9222, <https://doi.org/10.1021/es9015553>.
- [191] R. Kaegi, B. Sinnet, S. Zuleeg, H. Hagedorfer, E. Mueller, R. Vonbank, M. Boller, M. Burkhardt, Release of silver nanoparticles from outdoor facades, *Environ. Pollut.* 158 (2010) 2900–2905, <https://doi.org/10.1016/j.envpol.2010.06.009>.
- [192] J. Gans, M. Wolinsky, J. Dunbar, Computational improvements reveal great bacterial diversity and high metal toxicity in soil, *Science* 309 (2005) 1387–1390, <https://doi.org/10.1126/science.1112665>.
- [193] C. Gunawan, C.P. Marquis, R. Amal, G.A. Sotiriou, S.A. Rice, E.J. Harry, Widespread and indiscriminate nanosilver use: genuine potential for

- microbial resistance, *ACS Nano* 11 (2017) 3438–3445, <https://doi.org/10.1021/acsnano.7b01166>.
- [194] C. Jelenko, Silver nitrate resistant *E. coli*: report of case, *Ann. Surg.* 170 (1969) 296–299.
- [195] G.L. McHugh, R.C. Moellering, C.C. Hopkins, M.N. Swartz, Salmonella typhimurium resistant to silver nitrate, chloramphenicol, and ampicillin, *Lancet Lond. Engl.* 1 (1975) 235–240.
- [196] C. Gunawan, W.Y. Teoh, C.P. Marquis, R. Amal, Induced adaptation of *Bacillus* sp. to antimicrobial nanosilver, *Small* 9 (2013) 3554–3560, <https://doi.org/10.1002/sml.201300761>.
- [197] J.L. Graves, M. Tajkari, Q. Cunningham, A. Campbell, H. Nonga, S.H. Harrison, J.E. Barrick, Rapid evolution of silver nanoparticle resistance in *Escherichia coli*, *Front. Genet.* 6 (2015) 42, <https://doi.org/10.3389/fgene.2015.00042>.
- [198] A. Petushkov, J. Intra, J.B. Graham, S.C. Larsen, A.K. Salem, Effect of crystal size and surface functionalization on the cytotoxicity of silicalite-1 nanoparticles, *Chem. Res. Toxicol.* 22 (2009) 1359–1368, <https://doi.org/10.1021/tx900153k>.
- [199] A. Petushkov, N. Ndiege, A.K. Salem, S.C. Larsen, Chapter 7 – toxicity of silica nanomaterials: zeolites, mesoporous silica, and amorphous silica nanoparticles, in: J.C. Fishbein (Ed.), *Adv. Mol. Toxicol.*, Elsevier, 2010, pp. 223–266, doi:10.1016/S1872-0854(10)04007-5.
- [200] T. Kihara, Y. Zhang, Y. Hu, Q. Mao, Y. Tang, J. Miyake, Effect of composition, morphology and size of nanozeolite on its in vitro cytotoxicity, *J. Biosci. Bioeng.* 111 (2011) 725–730, <https://doi.org/10.1016/j.jbiosc.2011.01.017>.
- [201] P.D. Bowman, X. Wang, M.A. Meledeo, M.A. Dubick, B.S. Kheirabadi, Toxicity of aluminum silicates used in hemostatic dressings toward human umbilical veins endothelial cells, HeLa cells, and RAW267.4 mouse macrophages, *J. Trauma* 71 (2011) 727–732, <https://doi.org/10.1097/TA.0b013e3182033579>.
- [202] L.C.J. Thomassen, D. Napierska, D. Dinsdale, N. Lievens, J. Jammaer, D. Lison, C. E.A. Kirschhock, P.H. Hoet, J.A. Martens, Investigation of the cytotoxicity of nanozeolites A and Y, *Nanotoxicology* 6 (2012) 472–485, <https://doi.org/10.3109/17435390.2011.587901>.
- [203] K. Bhattacharya, P.C. Naha, I. Naydenova, S. Mintova, H.J. Byrne, Reactive oxygen species mediated DNA damage in human lung alveolar epithelial (A549) cells from exposure to non-cytotoxic MFI-type zeolite nanoparticles, *Toxicol. Lett.* 215 (2012) 151–160, <https://doi.org/10.1016/j.toxlet.2012.10.007>.
- [204] Z. Li, J. Hüve, C. Krampe, G. Luppi, M. Tsotsalas, J. Klingauf, L.D. Cola, K. Riehemann, Internalization pathways of anisotropic disc-shaped zeolite L nanocrystals with different surface properties in HeLa cancer cells, *Small* 9 (2013) 1809–1820, <https://doi.org/10.1002/sml.201201702>.
- [205] S. Laurent, E.-P. Ng, C. Thirifays, L. Lakiss, G.-M. Goupil, S. Mintova, C. Burtea, E. Oveisi, C. Hébert, M. de Vries, M.M. Motazacker, F. Rezaee, M. Mahmoudi, Corona protein composition and cytotoxicity evaluation of ultra-small zeolites synthesized from template free precursor suspensions, *Toxicol. Res.* 2 (2013) 270–279, <https://doi.org/10.1039/C3TX50023C>.
- [206] S. Męczyńska-Wielgosz, A. Piotrowska, A. Majkowska-Piliip, A. Bilewicz, M. Kruzewski, Effect of surface functionalization on the cellular uptake and toxicity of nanozeolite A, *Nanoscale Res. Lett.* 11 (2016) 123, <https://doi.org/10.1186/s11671-016-1334-8>.
- [207] A.R. Elmore, Cosmetic Ingredient Review Expert Panel, Final report on the safety assessment of aluminum silicate, calcium silicate, magnesium aluminum silicate, magnesium silicate, magnesium trisilicate, sodium magnesium silicate, zirconium silicate, attapulgite, bentonite, Fuller's earth, hectorite, kaolin, lithium magnesium silicate, lithium magnesium sodium silicate, montmorillonite, pyrophyllite, and zeolite, *Int. J. Toxicol.* 22 (Suppl 1) (2003) 37–102.
- [208] C. Anfray, B. Dong, S. Komaty, S. Mintova, S. Valable, Acute toxicity of silver free and encapsulated in nanosized zeolite for eukaryotic cells, *ACS Appl. Mater. Interfaces* 9 (2017) 13849–13854, <https://doi.org/10.1021/acsmi.7b00265>.
- [209] S. Asghari, S.A. Johari, J.H. Lee, Y.S. Kim, Y.B. Jeon, H.J. Choi, M.C. Moon, I.J. Yu, Toxicity of various silver nanoparticles compared to silver ions in *Daphnia magna*, *J. Nanobiotechnol.* 10 (2012) 14, <https://doi.org/10.1186/1477-3155-10-14>.
- [210] K. Bilberg, H. Malte, T. Wang, E. Baatrup, Silver nanoparticles and silver nitrate cause respiratory stress in Eurasian perch (*Perca fluviatilis*), *Aquat. Toxicol. Amst. Neth.* 96 (2010) 159–165, <https://doi.org/10.1016/j.aquatox.2009.10.019>.
- [211] A. Massarsky, L. Dupuis, J. Taylor, S. Eisa-Beygi, L. Strek, V.L. Trudeau, T.W. Moon, Assessment of nanosilver toxicity during zebrafish (*Danio rerio*) development, *Chemosphere.* 92 (2013) 59–66, <https://doi.org/10.1016/j.chemosphere.2013.02.060>.
- [212] L.V. Stebounova, A. Adamcakova-Dodd, J.S. Kim, H. Park, P.T. O'Shaughnessy, V.H. Grassian, P.S. Thorne, Nanosilver induces minimal lung toxicity or inflammation in a subacute murine inhalation model, *Part. Fibre Toxicol.* 8 (2011) 5, <https://doi.org/10.1186/1743-8977-8-5>.
- [213] J.S. Kim, J.H. Sung, J.H. Ji, K.S. Song, J.H. Lee, C.S. Kang, I.J. Yu, In vivo genotoxicity of silver nanoparticles after 90-day silver nanoparticle inhalation exposure, *Saf. Health Work* 2 (2011) 34–38, <https://doi.org/10.5491/SHAW.2011.2.1.34>.
- [214] J.H. Sung, J.H. Ji, J.U. Yoon, D.S. Kim, M.Y. Song, J. Jeong, B.S. Han, J.H. Han, Y.H. Chung, J. Kim, T.S. Kim, H.K. Chang, E.J. Lee, J.H. Lee, I.J. Yu, Lung function changes in sprague-dawley rats after prolonged inhalation exposure to silver nanoparticles, *Inhal. Toxicol.* 20 (2008) 567–574, <https://doi.org/10.1080/08958370701874671>.
- [215] J.H. Sung, J.H. Ji, J.D. Park, J.U. Yoon, D.S. Kim, K.S. Jeon, M.Y. Song, J. Jeong, B.S. Han, J.H. Han, Y.H. Chung, H.K. Chang, J.H. Lee, M.H. Cho, B.J. Kelman, I.J. Yu, Subchronic inhalation toxicity of silver nanoparticles, *Toxicol. Sci.* 108 (2009) 452–461, <https://doi.org/10.1093/toxsci/kfn246>.
- [216] J.H. Ji, J.H. Jung, S.S. Kim, J.-U. Yoon, J.D. Park, B.S. Choi, Y.H. Chung, I.H. Kwon, J. Jeong, B.S. Han, J.H. Shin, J.H. Sung, K.S. Song, I.J. Yu, Twenty-eight-day inhalation toxicity study of silver nanoparticles in sprague-dawley rats, *Inhal. Toxicol.* 19 (2007) 857–871, <https://doi.org/10.1080/08958370701432108>.
- [217] J.R. Roberts, W. McKinney, H. Kan, K. Krajnak, D.G. Frazer, T.A. Thomas, S. Waugh, A. Kenyon, R.I. MacCuspie, V.A. Hackley, V. Castranova, Pulmonary and cardiovascular responses of rats to inhalation of silver nanoparticles, *J. Toxicol. Environ. Health A* 76 (2013) 651–668, <https://doi.org/10.1080/15287394.2013.792024>.
- [218] M.F. Rahman, J. Wang, T.A. Patterson, U.T. Saini, B.L. Robinson, G.D. Newport, R.C. Murdock, J.J. Schlager, S.M. Hussain, S.F. Ali, Expression of genes related to oxidative stress in the mouse brain after exposure to silver-25 nanoparticles, *Toxicol. Lett.* 187 (2009) 15–21, <https://doi.org/10.1016/j.toxlet.2009.01.020>.
- [219] Y.S. Kim, J.S. Kim, H.S. Cho, D.S. Rha, J.M. Kim, J.D. Park, B.S. Choi, R. Lim, H.K. Chang, Y.H. Chung, I.H. Kwon, J. Jeong, B.S. Han, I.J. Yu, Twenty-eight-day oral toxicity, genotoxicity, and gender-related tissue distribution of silver nanoparticles in sprague-dawley rats, *Inhal. Toxicol.* 20 (2008) 575–583, <https://doi.org/10.1080/08958370701874663>.
- [220] H.-Y. Lee, Y.-J. Choi, E.-J. Jung, H.-Q. Yin, J.-T. Kwon, J.-E. Kim, H.-T. Im, M.-H. Cho, J.-H. Kim, H.-Y. Kim, B.-H. Lee, Genomics-based screening of differentially expressed genes in the brains of mice exposed to silver nanoparticles via inhalation, *J. Nanoparticle Res.* 12 (2010) 1567–1578, <https://doi.org/10.1007/s11051-009-9666-2>.
- [221] M.E. Samberg, S.J. Oldenburg, N.A. Monteiro-Riviere, Evaluation of silver nanoparticle toxicity in skin in vivo and keratinocytes in vitro, *Environ. Health Perspect.* 118 (2010) 407–413, <https://doi.org/10.1289/ehp.0901398>.
- [222] A. Loghman, S.H. Iraj, D.A. Naghi, M. Pejman, Histopathologic and apoptotic effect of nanosilver in liver of broiler chickens, *Afr. J. Biotechnol.* 11 (2012) 6207–6211, <https://doi.org/10.5897/AJB11.1768>.
- [223] M. Kazem Koohi, M. Hejazy, F. Asadi, P. Asadian, Assessment of dermal exposure and histopathologic changes of different sized nano-silver in healthy adult rabbits, *J. Phys. Conf. Ser.* 304 (2011), <https://doi.org/10.1088/1742-6596/304/1/012028>.
- [224] D. Bandyopadhyay, H. Baruah, B. Gupta, S. Sharma, Silver nano particles prevent platelet adhesion on immobilized fibrinogen, *Indian J. Clin. Biochem.* 27 (2012) 164–170, <https://doi.org/10.1007/s12291-011-0169-4>.
- [225] U. Suriyakalaa, J.J. Antony, S. Suganya, D. Siva, R. Sukirtha, S. Kamalakkannan, P.B.T. Pichiah, S. Achiraman, Hepatocurative activity of biosynthesized silver nanoparticles fabricated using *Andrographis paniculata*, *Colloids Surf. B Biointerfaces* 102 (2013) 189–194, <https://doi.org/10.1016/j.colsurfb.2012.06.039>.
- [226] R.O. Becker, Induced dedifferentiation: a possible alternative to embryonic stem cell transplants, *NeuroRehabilitation* 17 (2002) 23–31.
- [227] R. Klippstein, R. Fernandez-Montesinos, P.M. Castillo, A.P. Zaderenko, D. Pozo, Silver nanoparticles interactions with the immune system: implications for health and disease, *INTECH Open Access Publ.* 16 (2010) 309–324.
- [228] L.J. Rendin, C.L. Gamba, W.M. Johnson, Colloidal oxide of silver in the treatment of peptic ulcer; a nine-day therapy, *Pak. Med. J.* 61 (1958) 612–614.
- [229] M.A. Munger, P. Radwanski, G.C. Hadlock, G. Stoddard, A. Shaaban, J. Falconer, D.W. Grainger, C.E. Deering-Rice, In vivo human time-exposure study of orally dosed commercial silver nanoparticles, *Nanomed. Nanotechnol. Biol. Med.* 10 (2014) 1–9, <https://doi.org/10.1016/j.nano.2013.06.010>.
- [230] V. Baral, A. Dewar, G. Connert, Colloidal silver for lung disease in cystic fibrosis, *J. R. Soc. Med.* 101 (2008) 51–52, <https://doi.org/10.1258/jrsm.2008.s18012>.
- [231] Scientific Committee on Emerging and Newly Identified Health Risks – Nanosilver: safety, health and environmental effects and role in antimicrobial resistance, 2015.
- [232] N. Silvestry-Rodríguez, E.E. Sicairos-Ruelas, C.P. Gerba, K.R. Bright, Silver as a Disinfectant, *Rev. Environ. Contam. Toxicol.*, Springer, New York, NY, 2007, pp. 23–45, https://doi.org/10.1007/978-0-387-69163-3_2.
- [233] E.-J. Park, E. Bae, J. Yi, Y. Kim, K. Choi, S.H. Lee, J. Yoon, B.C. Lee, K. Park, Repeated-dose toxicity and inflammatory responses in mice by oral administration of silver nanoparticles, *Environ. Toxicol. Pharmacol.* 30 (2010) 162–168, <https://doi.org/10.1016/j.etap.2010.05.004>.
- [234] N. Bumbudsanpharoke, J. Choi, S. Ko, Applications of nanomaterials in food packaging, *J. Nanosci. Nanotechnol.* 15 (2015) 6357–6372.